Risk-based Inservice Testing Policy using Multi-Objective Optimization with Robustness

(ロバスト性を有する多目的最適化を用いたリスクベース検査計画)

JUKSANEE VIRULSRI

Abstract

In the maintenance activities of the surveillance test for the standby system in nuclear power plants, the objective usually involves more than one factor regarding, low levels of system unavailability and low costs in maintenance activities. In order to optimize these conflicting objectives, the multi-objective optimization is usually applied. Nevertheless, maintenance activities typically involve significant uncertainties such as those involving downtime and costs of maintenance. Therefore, some regions in the Pareto-optimal solutions may have the properties that are inappropriate due to the large scatter of the solutions. Moreover, in some regions, there are high sensitivities of a variation in one objective value to a variation in the other. Thus, attention should increasingly be focused on a robust solution. Unfortunately, the conventional method for decision-making processes has not sufficiently considered the robustness. Therefore, a methodology for selecting an appropriate solution with acceptable robustness is required.

In this research, new methodologies for assisting in decision-making for a multi-objective optimization framework based on robustness are presented (according to the user's requirement). The robustness considered in this research includes the sensitivity of a variation in one objective value to a variation in the other objective function value, and the uncertainty intrinsic to each parameter.

In the viewpoint of sensitivity, a new index of *Sensitivity index*, (*SI*) is proposed to determine the lowest sensitivity of the variation in one objective value to the variation in the other of the Pareto-optimal solutions. Moreover, in order to evaluate the effect due to the uncertainty of the parameters, we make use of the Monte Carlo method to obtain families of the Pareto optimal solutions. Then, efficient methodology that is

capable of identifying the most promising solution from a multi-objective optimization framework under uncertainty is also proposed. The uncertainty of each choice of the Pareto-optimal solutions is evaluated using the *uncertainty index, UI.* However, the promising solution with the lowest deviation is not necessarily the solution to give the best sensitivity, or vice versa. Therefore, to achieve a good compromise between sensitivity and uncertainty, the *decision index, DI* is then proposed.

Furthermore, since the importance parameter for the surveillance test is the surveillance test interval, therefore the management of the surveillance test interval groups is also significant for improving the efficient of the surveillance test. The risk-based inservice testing provides the prioritization efforts of maintenance activities for the rational safety management. Thus, the risk-based inservice testing can be applied for managing the surveillance test interval groups. However, no work has been reported on the methodology of updating the multi-objective optimization results by risk-based inservice testing.

This paper also proposes a new methodology to determine the robust surveillance test with the most optimal surveillance test interval based on risk based inservice testing. In the proposed methodology, the application of a multi-objective optimization to risk-based inservice testing is performed to determine the most optimal test interval based on risk consideration. And, in order to obtain the robust solution, the proposed decision-making for the multi-objective optimization in the viewpoint of robustness is applied.

The proposed indexes and methodology are examined using a standby system of a simplified high-pressure injection system (HPIS) in a nuclear power plant's pressurized water reactor (PWR) as the application. It is confirmed that the proposed methodology gives the satisfactory results in the viewpoint of risk and robustness.

List of Figures

List of Tables

Table of Contents

Chapter 1

Introduction

1.1 Backgrounds and motivations

The safety systems in the nuclear power plant are usually standby systems. For maintenance of the safety systems, the periodically test of the surveillance test [22,41,58] is performed to discover hidden failures that might occur in standby functions and then to assure that the component is still promptly to operate when the system is needed. The surveillance test is issued by the U.S. Nuclear Regulatory Commission (NRC)[51] through regulations published in Title 10 of the Code of Federal Regulations, Energy Part 50 (10CFR50) [56]. The probability that the component has failed at any point in time between surveillance test increases until the component is reset to zero by each successful test. The surveillance test is important because if the standby system does not function properly when its design function is required, severe damage to the plant may occur.

Because the surveillance test is important, the efficient scheme for improving the surveillance test in the maintenance activities is then required. The optimization is one of the techniques for improving surveillance test. However, the concerned essential quantities for the surveillance test include several factors such as the unavailability, the surveillance test interval (STI), and the maintenance costs. The unavailability [15] is the probability that a system or component is not performing its required function when it is needed. Therefore, the low level of unavailability is required in the maintenance activities. On the other hand, the reduction of the maintenance costs is also required.

So far, single-objective optimization is wildly used in probabilistic risk analysis (PRA) for nuclear power plants [4,14,24,26,50]; unavailability is considered as the objective and cost function is considered an implicit constraint, or vice versa. Nevertheless, an obvious trade-off (conflicting scenarios) exists among these purposes. Clearly, it is difficult to find an optimal solution in maintenance activities with single-objective optimization.

Therefore, a multi-objective optimization [16,23,27] framework is required to solve such trade-offs problems. A set of non-dominated optimal solutions is selected from feasible region and forms a so-called the Pareto-optimal solutions [27]. Moreover, in order to optimize of surveillance test, there are the multi-related parameters [48] as the decision variables. And the problem also consists of the non-linear objective functions based on risk (or unavailability) and the maintenance cost of the standby system. Genetic algorithm (GA) [38,54] is efficient for solving such problems and the multi-objective optimal problems using genetic algorithm is appropriate to optimize the surveillance test. Nowadays, the multi-objective optimization is applied to optimal treatment in various fields, which are summarized as shown in Table1.1.

However, most of these researches have mainly focused only on obtaining the Pareto-optimal solutions, but have not paid attention to robustness of the decision making point for the Pareto-optimal solutions. Thus, one attention should increasingly be focused on a robust solution. In this research, the considered robustness includes the sensitivity of a variation in one objective value to a variation in the other objective function value, and the uncertainty intrinsic to each parameter. Unfortunately, the conventional method [60,61] for selecting an appropriate alterative solution is not sufficient for the treatment of robustness of sensitivity and uncertainty.

Table 1.1. Summary of examples of research on multi-objective optimization in various fields

Field	First objective function	Second objective function	Third objective function
composite aerospace structure[17]	Stiffness	Weight	-
composite aerospace structure[28]	Cost	Weight	-
Design of plant process[12]	Cost	Environmental effect	-
Agricultural policy[29]	Profit	Environmental effect	-
Thermal energy system[11]	Cost	Energy	-
Waste water treatment[1]	Cost	Environmental effect	clean water
Transportation for urban school routing[45]	Cost	Satisfaction of demand of service	Equity

Furthermore, one of the important parameters for the surveillance test is the surveillance test interval. In the surveillance test, the system components have been grouped into different test strategies. All components in the same group are determined as the same surveillance test interval. Therefore, the management of the surveillance test interval groups is also significant for improving the maintenance activities. So, performing the multi-objective optimization without considering the appropriate surveillance test interval groups may not lead to the satisfactory results in the risk management point of view. In order to manage the most satisfactorily surveillance test interval groups in the viewpoint of risk, the optimization including prioritization of maintenance should be treated.

The risk-based maintenance (RBM) [46,63] is the method that provides a maintenance activities program using risk as a basis for prioritizing and managing the efforts of the inspection and maintenance programs. Thus, the RBM can be used for managing the surveillance test interval groups. So far, many researches have shown that the RBM has been efficiently applied in maintenance [18,19,21,25,39] and there are several guidelines that are developed about risk-based maintenance [2,3,5-9]. For components in the standby system such as pumps and valves, RBM for testing is called risk-based inservice testing (RBT) [9,10,30,59], which is developed in the guidelines of the American societies of mechanical engineers (ASME).

Nevertheless, no work has been report on applying the multi-objective optimization to the risk-based inservice testing, although both of these concepts are important. The multi-objective optimization is needed to solve the trade-offs problem and to assist in determining the robust solution. While the risk-based inservice testing is required to make the multi-objective optimization being most efficient based on risk. Therefore, a methodology for assisting in planning the most optimal surveillance test interval that makes the multi-objective optimization results being most optimized based on risk and robustness is required.

1.2 Objective

The main objective of this research is to develop the methodologies for improving the surveillance test in the maintenance activities of a standby safety system in a nuclear power plant from the viewpoint of risk and robustness.

In order to improve the surveillance test, the multi-objective is performed for solving the intrinsic trade-offs in the surveillance test. Then the following researches are proposed in order to achieve the main objective.

1) Propose the new decision-makings for the multi-optimization solutions based on robustness (Chapter 3, 4).

In order to achieve the robust surveillance test, the decision-makings for the multi-optimization solutions based on robustness are proposed. The robustness considered in this research includes the sensitivity of a variation in one objective value to a variation in the other objective function value, and the uncertainty intrinsic to each parameter. Therefore, the new decision-makings for the multi-optimization solutions based on robustness are proposed in the following point of views.

- Propose the decision-makings for the multi-optimization solutions in the viewpoint of robustness of sensitivity. (Chapter 3)

- Propose the decision-makings for the multi-optimization solutions in the viewpoint of robustness of uncertainty. (Chapter 4)

2) Propose the risk-based in-service testing policy using multi-objective optimization with robustness (Chapter 5).

In order to achieve the robust surveillance test with the most optimal surveillance test interval based on risk, the risk-based in-service testing policy using multi-objective optimization with robustness is proposed.

The new proposed methodology is based on risk-based maintenance theory for improving the prioritization in the surveillance test that makes the multi-objective optimization results being most optimized based on risk. The multi-objective optimization is performed in the proposed methodology for solving the trade-offs in the problem. And the proposed decision-makings for the multi-optimization solutions based on robustness is then determined to obtain the robustness surveillance test planning.

1.3 Outlines of research

This thesis contains 6 chapters and the structure of these chapters is presented in Fig.1.1. Each chapter is summarized below.

Chapter 1 shows the background and motivations of this research. Then, all of the problems are discussed and the objectives of this research are proposed. The outlines of this research are summarized in this chapter.

Chapter 2 shows the overall basic theories that are used in this research such as, risk and probabilistic risk analysis in nuclear power plant, genetic algorithms and multi-objective optimization using genetic algorithms, the conventional method for decision-making in the Pareto-optimal solutions and risk-based maintenance.

Chapter 3 proposes the new decision making for the Pareto-optimal solutions in the viewpoint of sensitivity and indicates the problem that may occur in the conventional method. In addition the case study for examining the efficiency of the proposed methodology in this research is presented. The formulation of unavailability and maintenance costs of the standby system are explained. Then, discussions and results and concluding remarked are explained.

Chapter 4 proposes the decision making for the multi-objective optimization framework under uncertainty. Then, the combination of decision-making in the viewpoint of robustness of the solution is also considered together with the uncertainty. Finally, the discussions and conclusions of the results of the case study for the proposed index and methodology in this chapter are explained.

Chapter 5 proposes the risk-based in-service testing policy using multi-objective optimization with robustness in order to optimize the surveillance test interval groups that make the Pareto-optimal solution being most effective based on risk and having robustness. Discuss and conclude the result of the case study for the proposed methodology in this chapter.

Chapter 6 shows the conclusions and the suggestion for the furthering researches.

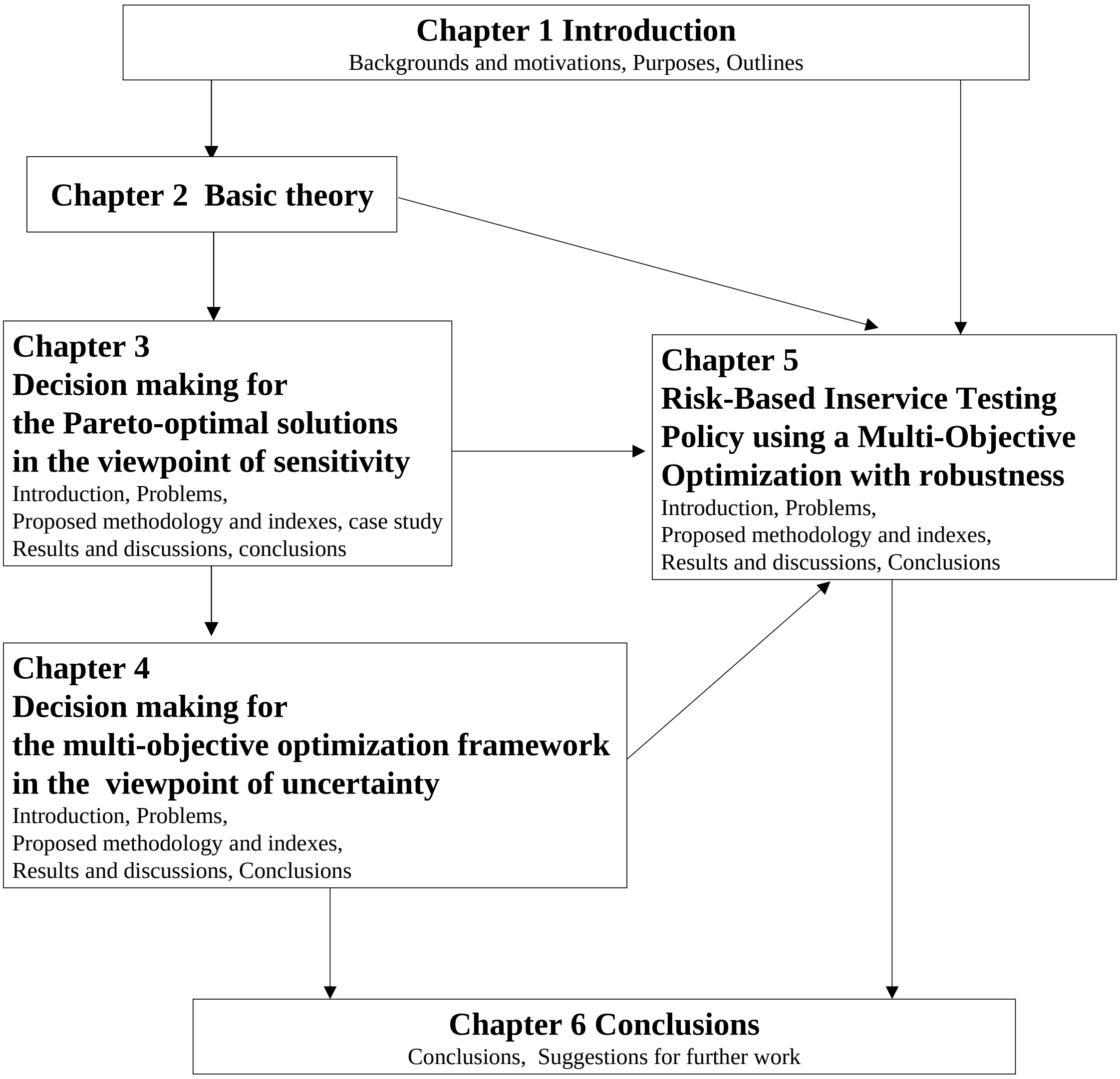

Fig.1.1 Structure of this research

Chapter 2

Basic Theory

This chapter will describe the overall basic theory that is used for development in this research.

2.1 Probabilistic risk analysis (PRA) in nuclear power plant

In October 1975, the U.S. Nuclear Regulatory Commission (NRC) [51] released the Reactor Safety Study, entitled as WASH-1400 [57] (also called the Rasmussen Report according to Professor Norman Rasmussen of MIT) evaluated the probability of a number of accident sequences that might lead to melting of the fuel in the reactor (also referred to as Core Melt). The WASH-1400 study was the first comprehensive risk analysis of a nuclear power plant and represented a step forward in the risk analysis of a complicated engineered system. The WASH-1400 was the most important development in the probabilistic risk analysis.

This risk evaluation methodology was then improved upon. In most countries the method is referred to as probabilistic safety assessment (PSA). In the United States, the method is referred to as probabilistic risk analysis (PRA) [13,36,43,44,55]. They are just different name, but in the same techniques. Probabilistic risk analysis is an analytic method for protecting the safety. The event tree, fault tree methodology were developed and the significant development of the study was the use of event trees to link the system fault trees to the accident initiators and the core damage states. Nowadays, probabilistic risk assessment is also being wildly applied to many fields such as transport, construction and energy etc.

This thesis used probabilistic risk assessment as the tool to assist in optimization of the maintenance activities of the standby system. Fault tree is built to determine accident sequences using initiating events and systems. Initiating events and other failure events that comprise each system can be assigned frequencies or probabilities. Minimal cut sets (MCS) (i.e., a minimally sufficient group of failures that can lead to an undesired outcome) can be generated to quantify fault trees and sequences. The probabilistic risk assessment analysis has mechanisms available to perform a variety of different uncertainty analyses, sensitivity analyses, and importance measures.

The followings are the main system analysis and quantification tools in probabilistic risk assessment that are used in this research.

2.1.1 Fault and event trees analysis

Fault and event trees [40] are modeling tools used as part of a quantitative analysis of a system. The event trees play a central role in connecting the accident initiators to the consequences by providing linking structure for the probabilistic risk assessment. They show how the systems are involved to the initiating event and then model the system responses in the fault tree, for simple example as shown in Fig. 2.1.

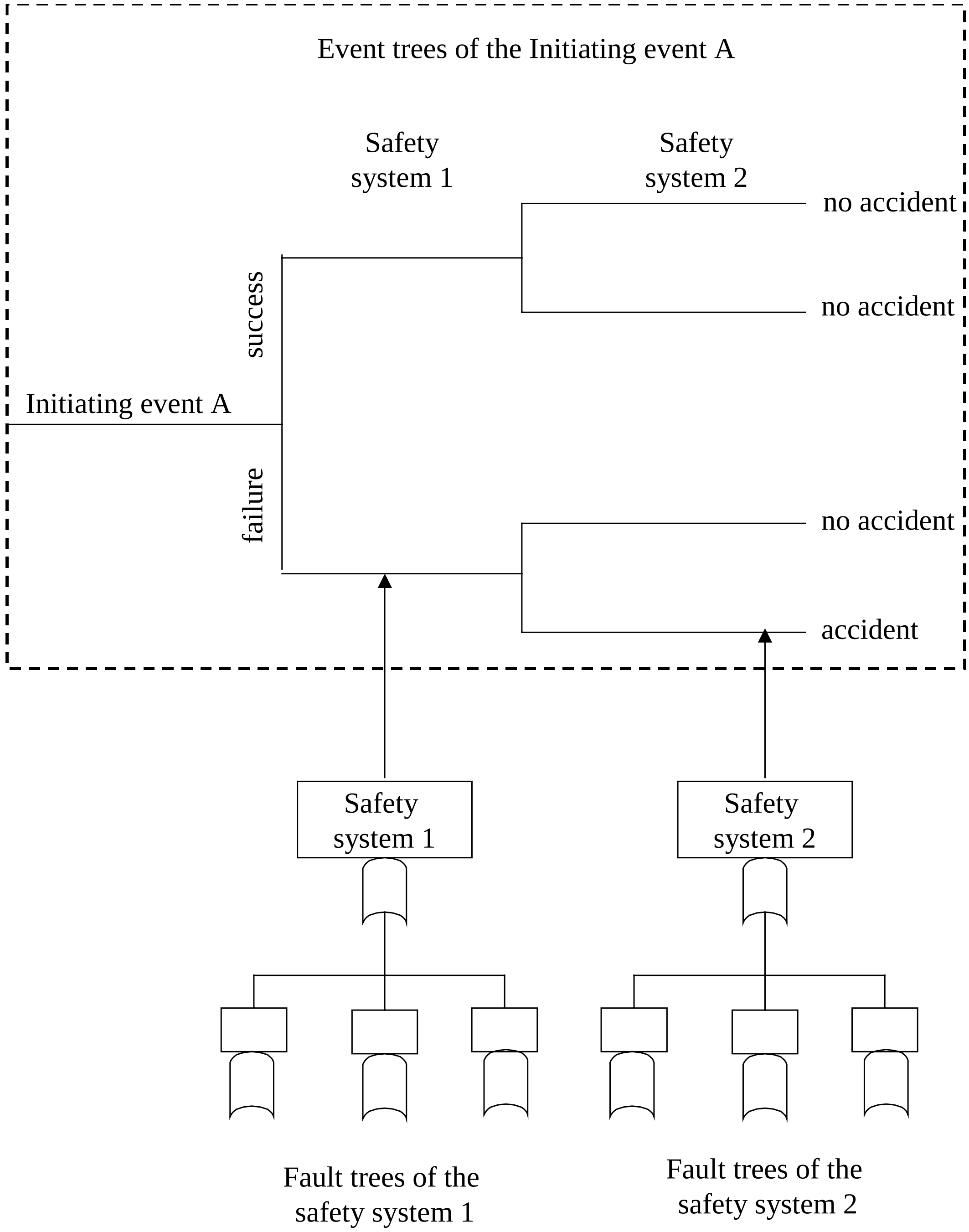

Fig. 2.1 Simple example of event trees that show how fault trees provide the branching of event trees.

The event trees use forward logic. They begin an initiating event that is an abnormal incident. A schematic of event tree is also shown in Fig 2.1. It consists of an initiating event and two safety systems, which are designed to mitigate the initiating event. The line going up shows the success (no failure) and the line going down represents the failure. The branching probability of safety system at a node is then determined by a fault trees analysis as illustrated in Fig. 2.1.

The fault trees work with backward logic starting with the top event. The top event of the fault tree is specified by a particular failure of a system in the event tree. Using the Boolean operations AND, OR one write down which combinations of component faults events which may contribute to the top event in logical sequence to the logical connections. The generally used conventional fault tree symbols are shown in Fig. 2.2.

The symbols shown in Fig. 2.2 can be explained as followings.

AND gate symbol – Output fault if all of the input faults occur.

OR gate symbol – Output fault occur if at least one of the input faults occurs.

Transfer in symbol – indicates that the tree is developed further at the occurrence of the corresponding Transfer out.

Transfer out symbol – indicates that this portion of the tree must be attached to the corresponding Transfer in.

Basic event symbol – failure at the lowest level (no further development necessary).

Intermediate event symbol – a fault event that occurs because of one or more antecedent causes acting through logic gates.

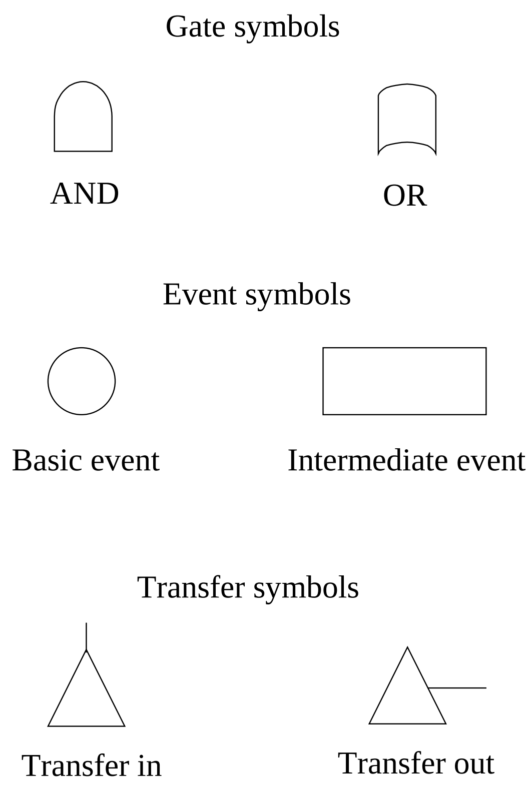

Fig. 2.2. The generally used conventional fault tree symbols.

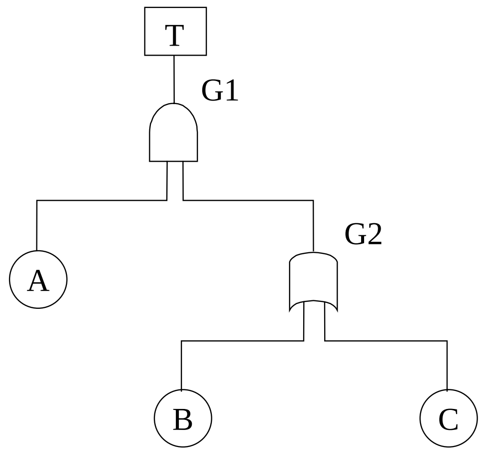

Fig. 2.3. The simple example of a fault tree.

Such an analysis produces a tree-like structure having basic events at its extremities. The basic events are the finest level of detail that cannot be further dissected into more elementary events. The simple example of a fault tree is shown in Fig. 2.3.

2.1.2 Cut sets and Minimal cut set (MCS)

From the fault tree diagram, a cut set is a collection of basic events such that if these events occur together then the top event will certainly occur. The minimal cut set [36,43,44,55] represents the smallest combination of component failures that will result in the top event.

The fault tree is simply represent a Boolean expression. The symbols + and * represent the operation of AND and OR gate respectively. For example as the fault tree from Fig. 2.3, which have a top event, T and three basic event A, B and C with OR gate G1 and AND gate G2. Then the top event is represent by

$$
\begin{aligned}
\text{Top event} &= G1 \\
&= A \ \text{OR} \ G2 \\
&= A + G2 \\
&= A + (B \ \text{AND} \ C) \\
&= A + (B*C)
\end{aligned}
\qquad (2.1)
$$

It is clearly that if every component fails then the top event must occur. Therefore, the cut set of this fault tree is given by {A, B, C}. But from the above top event Eq.(2.1) can explain that top event will occurs when A fails, or B and C fail together. Then consider Eq.(2.1) together with the reduction rules (for example A*B + A = A), the MCSs for this fault tree is {A} and {B,C}.

2.1.3 From probabilistic risk assessment to risk equation

All MCSs could result in large accident. The final results of a probabilistic risk analysis study are then represent in the risk equation. The system unavailability model is usually formulated into the probabilistic risk assessment, which is an upper bound, as follows [20]:

$$U(x) \approx \sum_{j} \prod_{k} u_{jk}(x), \tag{2.2}$$

where j is the index of minimal cut set.

k is the index of each basic event of the corresponding minimal cut set.

$u_{jk}(x)$ is the unavailability associated with the basic event k belonging to minimal cut set number j, which define an unavailability of a safety component that depends on the vector of decision variables x.

2.2 Multi-objective optimization.

The multi-objective optimization method [16,23,27] is performed when there are conflicting objectives in a problem. Since in the multi-objective optimization, the effort is made in finding the set of trade-off optimal solutions by considering all objectives to be important. The multi-objective optimization problem is solved and a number of optimal solutions are selected from the entire feasible region; these are called Pareto-optimal solution [16,23,27]. Among the Pareto-optimal solutions, none can be said to be better or worse than the others. In another words, they are a non-dominated set.

Many classical methods have been used to solve multi-objective optimization problems; these include the Weighted Sum Method [31] and the ε-constraint method[49]. Most of the classical methods start with one random guess solution. From that point, the algorithm is explored to search for a direction to locate a better solution. The process is repeated for a number of times to obtain the best optimum solution. These classical algorithms must be iterated many times to obtain a different solution from the Pareto-optimal solution set. Moreover, some of the classical methods are not efficient in non-differentiable, discontinuous problems or in non-convex Pareto-optimal regions. However, the Multi-objective optimization using genetic algorithms can diminish these problems. Because genetic algorithms work with a population of solutions, it is advantageous to obtain the Pareto-optimal solutions in a single simulation run. GA can be developed to give equal emphasis to all non-dominated solutions in the population and to simultaneously maintain a diverse set of multiple non-dominated solutions.

2.2.1 Genetic algorithms (GA)

In this subsection, we will briefly describe the general concept of genetic algorithms[27,38,54] for single-objective to be the basic for the multi-objective optimization using genetic algorithms that will be explained in next section.

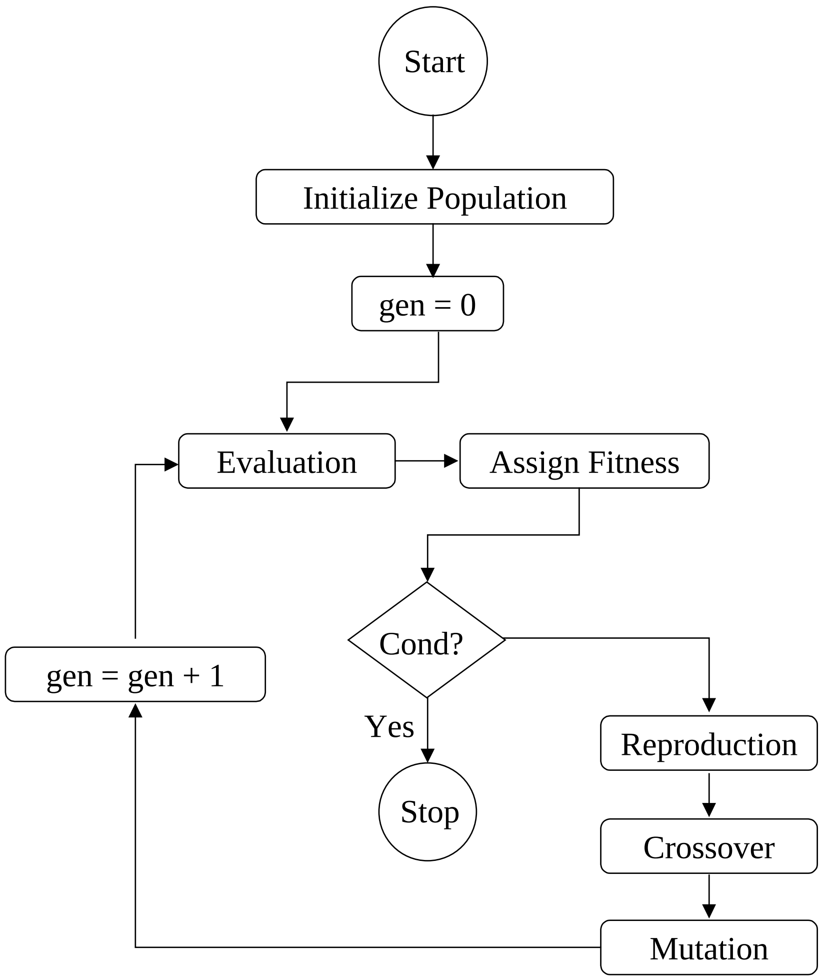

Fig. 2.4. A flowchart of the working principle of a GA [27].

Genetic algorithms are the efficient search and optimization tools. The flowchart of the working principle of GA is illustrated in Fig.2.4. The searching of GA starts with initial a random set of solutions, which are call population. It is different from the classical methods that operating with one solution. Then, a value of the objective function is calculated by considering each of the population as parameter. These calculated values of the objective function are called fitness. After that, the generation number is checked. If it is still not satisfied, three main operators, which are the selection operator, the crossover operator, and the mutation operator, have been performed to modify the population of the solutions to be a new population. This new population is expected to be better than the old population. Accordingly, the one generation GA is completed and the next generation is performed.

For each of the three main operators of genetic algorithm will be described as follows:

(1) Reproduction or Selection Operator

The reproduction operator is mainly purposed to make copies of good solutions and eliminate bad solutions in a population, while keeping the population size constant. The selected better solutions have been copied into the mating pool and the worse solutions have been discarded.

(2) Crossover Operator

With realize that the reproduction operator cannot create any new solutions in the pupation. The crossover and mutation operators have been processed to perform the creation of new solutions. In crossover operation, two solutions are random picked from the mating pool and are blended into two new solutions.

(3) Mutation Operator

The mutation operator is generally used to create a local perturbation that is useful in keeping diversity in the population.

2.2.2 Multi-objective optimization using genetic algorithms [27]

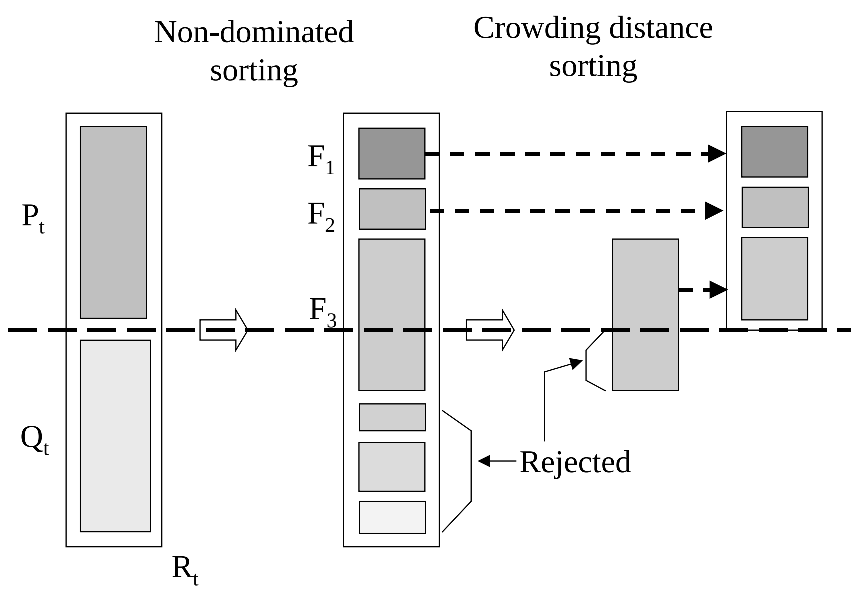

Fig. 2.5. The NSGA-II procedure [27]

In this research, the Elitist Non-Dominated Sorting Genetic Algorithm or NSGA-II by Deb et al. [27] has been chosen. NSGA-II is a multi-objective GA, which has the advantage of a crowding comparison procedure acting as an explicit diversity–preserving mechanism. The procedure is illustrated in Fig. 2.5.

In NSGA-II, the parent population P_t first creates the offspring population Q_t by GA, as described in section 2.2.1. The two populations are then combined to form R_t of size 2N. Next, non-dominated sorting is used to rank R_t into various fronts as shown in

Fig.2.6. To select the new population, the best non-dominated front (f_1 front) is chosen, followed by the f_2 front and continuing with the next non-dominated front. Because the original population size is N, the entire population from R_t cannot be selected to be the new population.

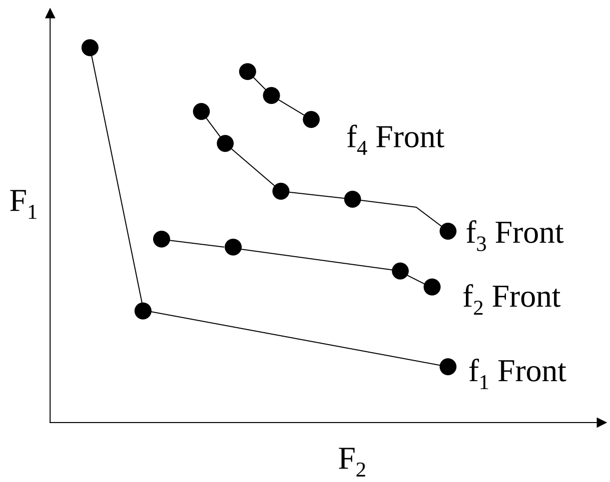

Fig. 2.6 Example of non-dominated sorting into fi front for problem of minimizing of objectives f1 and f2

As seen from Fig. 2.5, the last selected front, which causes the mating pool to exceed N in population size, has been considered, while other worse non-dominated fronts can be deleted. The niching strategy of a crowding tournament selection operator is used to choose the members of the last front for the purpose of maintaining diversity in the solutions. After that, another offspring population is created from the selected new population by a GA process such as selection, crossover and mutation operations. The generation is then completed, and the generation counter is increased.

2.3 Decision making in the Pareto-optimal solutions

Once a set of non-dominate Pareto-optimal solutions is obtained, some higher-level decision-making considerations are used to choose a solution as a schematic shown in Fig.2.7.

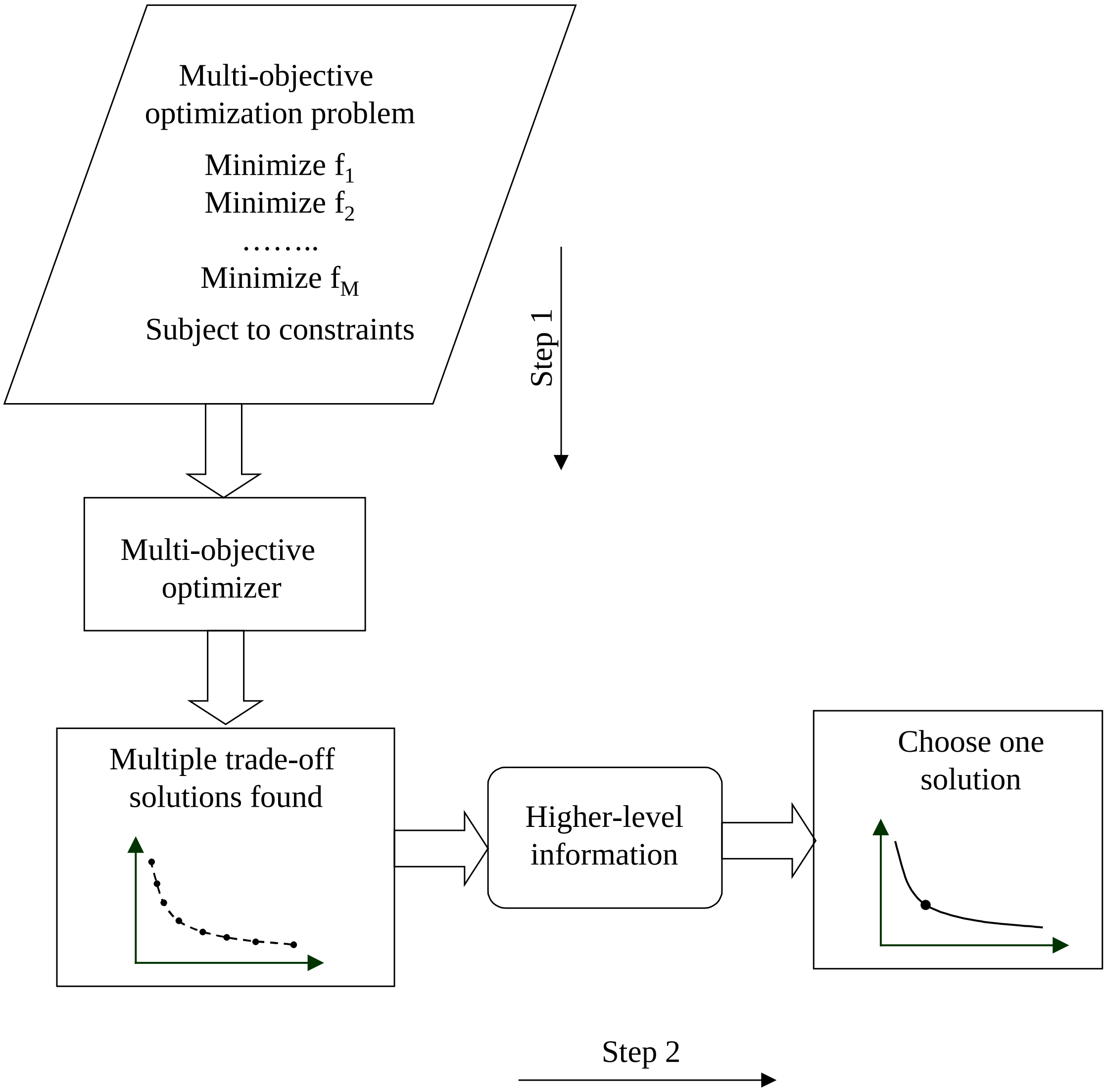

Fig.2.7. Schematic of a multi-objective optimization procedure [27].

Figure.2.7 shows schematically the principles in the multi-objective optimization procedure. In step1, multiple trade-off solutions are found. Thereafter, in step2, which is the concept of the decision-making in the Pareto-optimal solutions presented in this subsection, higher-level information is used to choose one of the trade-off solutions.

The generally used conventional method of identifying the promising point within the Pareto-optimal solution, called the global criteria method [27], gives a solution as the closest position to the ideal point [60,61]. An example of the ideal point is represented as Z^* in Fig. 2.8.

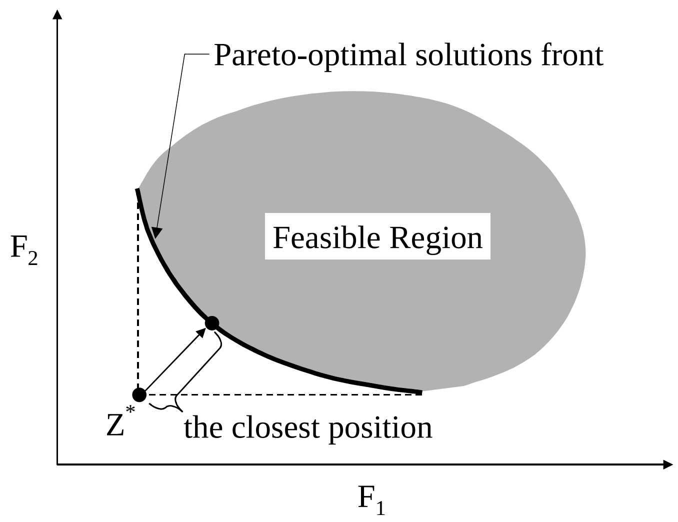

Fig. 2.8. The method of global criteria

The ideal point, which is not located in the feasible region shown by the gray area, is defined as the point of the lower bound of all objective functions. In the concept of the conventional method, the solution that is minimally located from this point is considered to be appropriate. Using the Euclidean distance, the method of global criteria is shown as

$$\text{Minimize} \quad \left(\sum_{i=1}^{n} \left| f_i(x) - z_i^* \right|^2 \right)^{\frac{1}{2}}, \qquad (2.3)$$

where z_i* is the i[th] coordinate of the ideal point, and n is the number of objective functions.

Because each objective function value has a different dimension, the values of the objective function should be normalized before calculating the distance from each point on the Pareto-optimal solutions to the ideal point. The normalized term is shown as follow

$$f_{in}(x) = \frac{f_i(x) - f_{i\min}}{f_{i\max} - f_{i\min}}, \qquad (2.4)$$

Where $f_{in}(x)$ is the normalized value of the objective function value $f_i(x)$.

f_{imax} and f_{imin} are the maximum and minimum values of the objective function f_i respectively.

Henceforth, the distance from the point on the Pareto-optimal solutions normalized by Eq.(2.4) to the ideal point will be called the normalized distance in this research. The normalized distance values varies within the range of 0～1.

However, the concept of the decision-making for the Pareto-optimal solutions by the conventional method does not determine the robustness. Therefore, the obtained decision point may not have enough robustness. This research then proposed the decision-making for the Pareto-optimal solutions in the viewpoint of robustness in chapter3 and chapter4.

2.4 Risk-based maintenance

Risk-based maintenance (RBM) [46,62,63] is an approach to improving maintenance management systems, programs, and practices. The advantage of RBM over normal maintenance approaches is that RBM provide a maintenance activities program using risk as a basis for prioritizing and managing the efforts of the inspection and maintenance programs. Risk Based approaches is used to rearrange inspection and maintenance resources to increase attention, such as frequency of inspection or maintenance, on high-risk items and reduce it in lower risk equipment. Therefore, RBM make more effective use of resources while maintaining a high level of safety.

2.4.1 The definition of risk.

Risk [55] is the product of 'likelihood of an unwanted event P' and the 'consequences C of that unwanted event', or in mathematical form given as,

$$R = P \cdot C \tag{2.5}$$

Then risk simultaneous accounts for both likelihood and consequence of an event. The event probability P is such as component failure rates. In the standby system, the unavailability of the system is a very important parameter. Therefore the unavailability is usually considered to be an equivalent parameter for the likelihood of event.

2.4.2 Risk matrix

In order to illustrate risk, the likelihood and consequence is displayed on an X-Y plot as shown in Fig. 2.9.

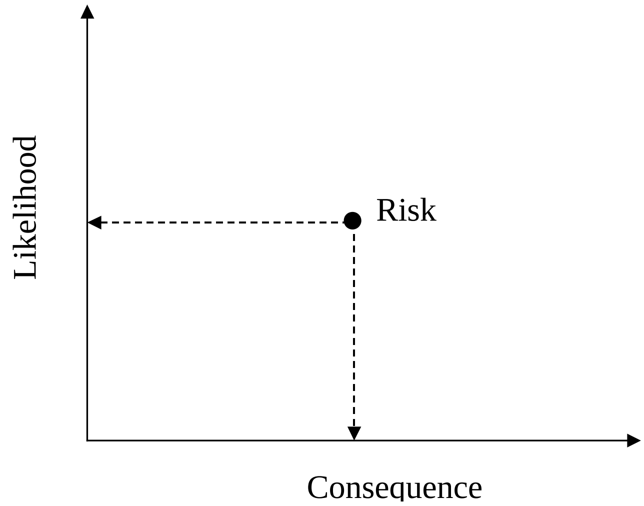

Fig. 2.9 Likelihood and consequence X-Y plot.

From the X-Y plot of likelihood and consequence, in order to categorize the risk, the qualitatively or quantitatively risk is determined. For the qualitatively risk, the likelihood and consequence of event are determined as high or low category. While for the quantitatively risk, the likelihood and consequence of event are determined as magnitude. In this research, we apply the qualitatively risk analysis and the X-Y plot of likelihood and consequence in qualitatively risk analysis can be determined as the risk matrix as shown in Fig.2.10.

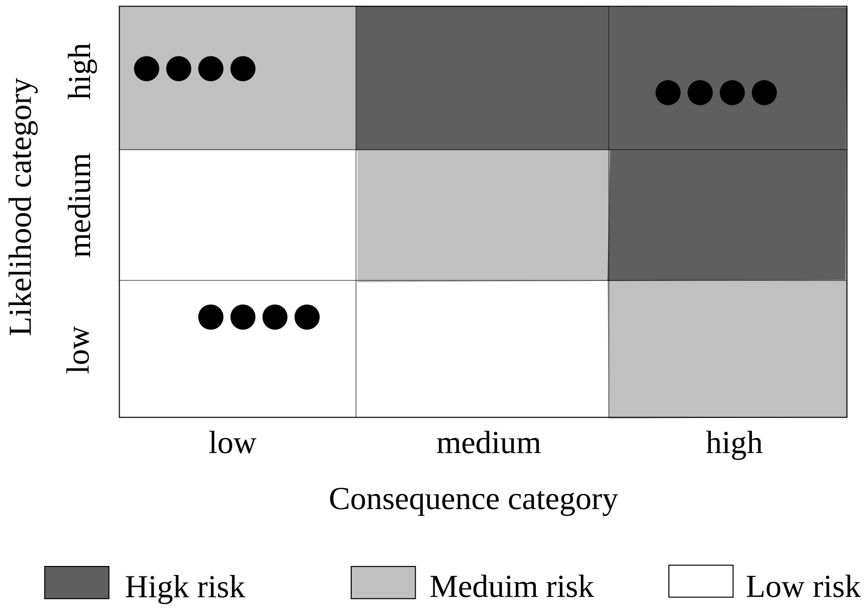

Fig. 2.10. Qualitative risk matrix.

Thereafter, the concept of risk-based decision-making is determined by focusing in the area of high, medium and low risk to prioritize the components for maintenance corresponding to their risk-significance as described above.

2.4.3 Risk-based inservice testing by ASME

For the risk based maintenance of components in the standby system such as pumps and valves, the American societies of mechanical engineers (ASME) have developed guidelines for Risk-based maintenance for testing or so called risk-based inservice testing (RBT) [9,10,30,59].

The relative ranking of the standby components developed by ASME requires the importance measures [35,37,52], which are the Fussel-Vesely (FV) and the Risk Achievement Worth (RAW), as a quantitative decision criteria. The details of the importance measures are shown in section 2.4.4. FV and RAW used as a measure of risk importance and safety importance, respectively. Component important ranking by ASME is determined by the combination of FV and RAW matrix.

For the purpose of dividing the plot of FV-RAW matrix into four quadrants, FV indicating level of 0.001 (0.1%) and RAW indicating level of 2 have been defined by the ASME. Figure 2.11 illustrates an example of a plot of FV-RAW matrix.

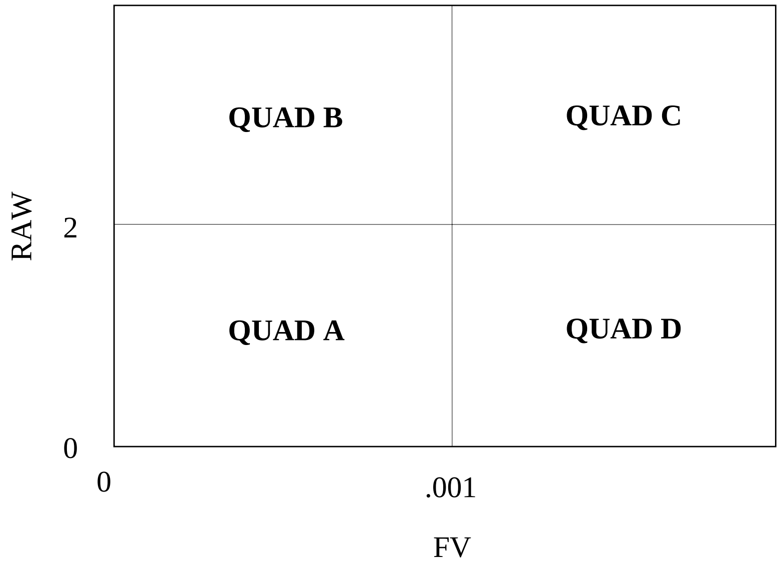

Fig. 2.11 RAW/FV quadrant graph of risk by ASME[9]

From Fig.2.11, components in quadrant **A** may be candidates for no or relaxed testing. Components in quadrant **C** should have focused for effective testing. While, infrequent test are considered for components in quadrant **B** and **D**.

However, by this ASME method, the risk significance of the components may locate in the same quadrant, although there are extreme differences in their values. Therefore, fixing the values of FV and RAW for creating the risk matrix by ASME is not flexible enough. Moreover, the ASME method has not clearly presented the method to revise risk-ranking process. Therefore, the ASME method may not clearly give the most optimal surveillance test interval groups for the surveillance test based on risk consideration. Moreover, the method by ASME does not consider the multi-objective optimization and robustness for the surveillance test. Therefore, in chapter 5 of this research, the risk-based in-service testing policy using multi-objective optimization with robustness is proposed. The proposed methodology in chapter 5 is for determining the robust surveillance test with the most optimal surveillance test interval based on risk consideration. The processes in the proposed methodology have the idea of risk ranking and revising risk matrix and the proposed risk matrix that is more flexible for each system and situation.

2.4.4 Risk Importance Measure

Risk importance measures [35,37,52] have been defined for the interpretation of probabilistic risk analysis (PRA) and for their use in the prioritization of operation and safety improvements.

Table 2.1 The importance measures used in the RBT by ASME

Importance Measure	Abbreviation	Principle
Fussell-Vesely	FV	$\frac{R(\text{base}) - R(x_i = 0)}{R(\text{base})}$
Risk achievement worth	RAW	$\frac{R(x_i = 1)}{R(\text{base})}$

Table 2.1 shows the risk importance measures that are used in the risk based inservice testing defined by ASME. In Table 2.1 the following definitions are used.

$R(x_i = 1)$, the increased risk level without basic event x_i or with basic event x_i assumed failed,

$R(x_i = 0)$, the decreased risk level with the basic event optimized or assumed to be perfectly reliable,

R(base), the present risk level,

x_i(base), present risk of component i

Chapter 3

Decision making for the Pareto-optimal solutions in the viewpoint of sensitivity

3.1 Introduction

In the maintenance activities of a nuclear power plant, the objective usually involves more than one factor regarding, including low levels of system unavailability and low costs in maintenance activities. Therefore, the problem should be considered as a simultaneous multi-objective optimization. A multi-objective optimization problem is solved and the Pareto-optimal solutions are then obtained. After a set of non-dominated Pareto-optimal solutions is obtained, some higher levels of decision-making are required to choose an appropriate solution. One of the conventional methods for selecting the appropriate solution from the alternatives in the Pareto-optimal solutions is the global criteria method. However, there are high sensitivities of a variation in one objective value to a variation in the other in some regions of the Pareto-optimal solutions. Nevertheless, the conventional method does not consider this robustness of sensitivity. Therefore, in this chapter, new sensitivity index is proposed for decision-making when the robustness of sensitivity is part of the intention.

3.1.1 Problems in the conventional method

The conventional method called global criteria [27], which is explained in chapter 2, is widely used for the decision-making on the Pareto-optimal solutions. With this method, the one solution among the Pareto-optimal solutions that is closest to an ideal point is selected.

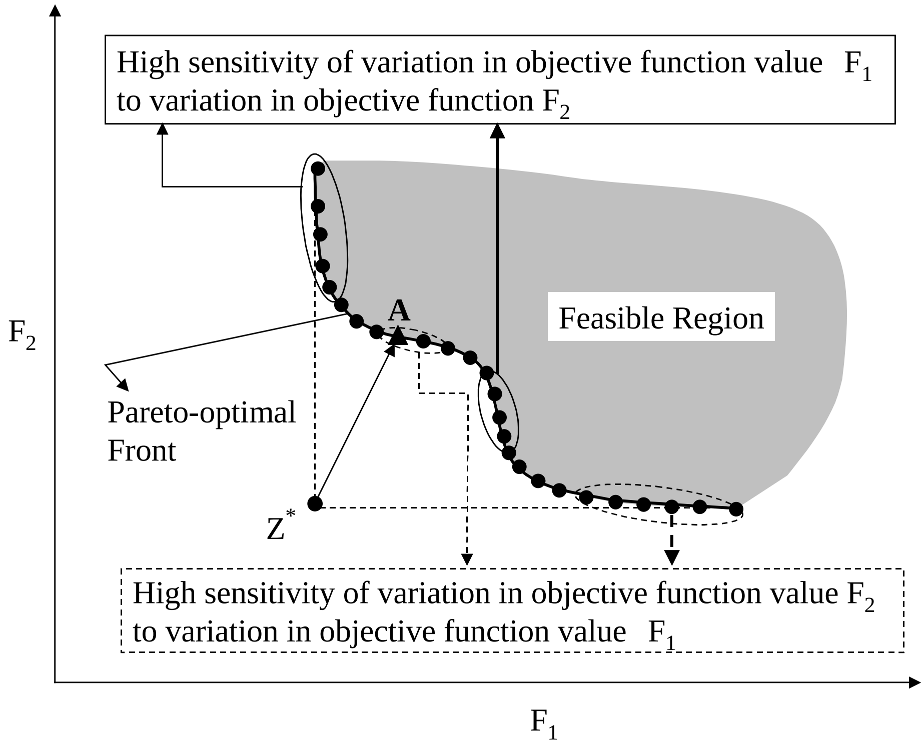

Fig 3.1. The typical Pareto-optimal solutions in minimization of objective functions F_1 and F_2.

Although there is no problem for selecting a decision point by the conventional method for Fig.2.8 in Chapter 2, however, in the case of Fig.3.1, a problem does occur. Fig.3.1 shows some regions in the Pareto-optimal front in which a variation in one objective value has high sensitivity to a variation in the other objective function value. This means that the solution has no robustness in operation. Since, the conventional method does not consider this sensitivity, it is possible that the obtained solution may be located in high sensitivity zones.

For example, the point A in Fig.3.1 is the solution that is minimally located from the given ideal point (Z^*). Nevertheless, this solution is located in a high sensitivity zone; here, objective function value F_2 is highly sensitive to variations in objective function F_1 values. In this case, the decision made by the conventional method does not have the robustness. If not only the robustness but also the distance from an ideal point is considered, an appropriate index is required along with the Pareto-optimal solutions. In this chapter, this new sensitivity index is proposed.

3.2. Sensitivity index

The sensitivity of a variation in one objective value to a variation in the other for the solution on the Pareto-optimal curve is expressed by the proposed sensitivity index, defined by the following dimensionless expression:

$$SI = \frac{\Delta F_j / \overline{F_j}}{\Delta F_k / \overline{F_k}}, \tag{3.1}$$

where ΔF_j and ΔF_k are the variation around specified objective function values $\overline{F_j}$ and $\overline{F_k}$ on the Pareto-optimal curve.

The basic idea of this sensitivity index is as follows.

If $SI = 1$, the variation in the objective functions values F_j and F_k are approximately equivalent.

If $SI > 1$ or $SI < 1$, there is more variation in one objective function values than in the other objective function values and SI value shows the degree of that influence.

Therefore, it is possible that the degree of sensitivity can be measured using *SI*. The solution with *SI* = 1 shows that it is robust and have the lowest sensitivity for all of objectives. Moreover, by using *SI* a criterion for sensitivity can be set up. For example, in this paper, we define the range of $1/1.5 \leq RI \leq 1.5$ as robust, i.e. the range in which the variation in one objective is not greater than 1.5 times the variation in the other.

3.3. Procedure to determine the decision-making point in the Pareto-optimal solutions

The decision-making process becomes more rational than before if the *SI* is used combined with the conventional method as follows.

(1) When the point closest to the ideal point is coincide with that of the decision-point at *SI* = 1, the point is appropriate because both conditions are satisfied.

(2) When the distance to the ideal point is more important than the sensitivity, the conventional method is appropriate.

(3) When emphasis is placed on the sensitivity, the sensitivity index is used for evaluation.

(4) When both the distance to the ideal point and the sensitivity are important, the following process is proposed.

1. The graph relation between *SI* values and normalized distances is drawn at first as shown in Fig.3.2(a). The normalized distances are the normalized distances from the

point on the Pareto-optimal solutions as explained in section 2.3 of chapter 2. The normalized term is shown by the normalized termed in Eq.(2.4).

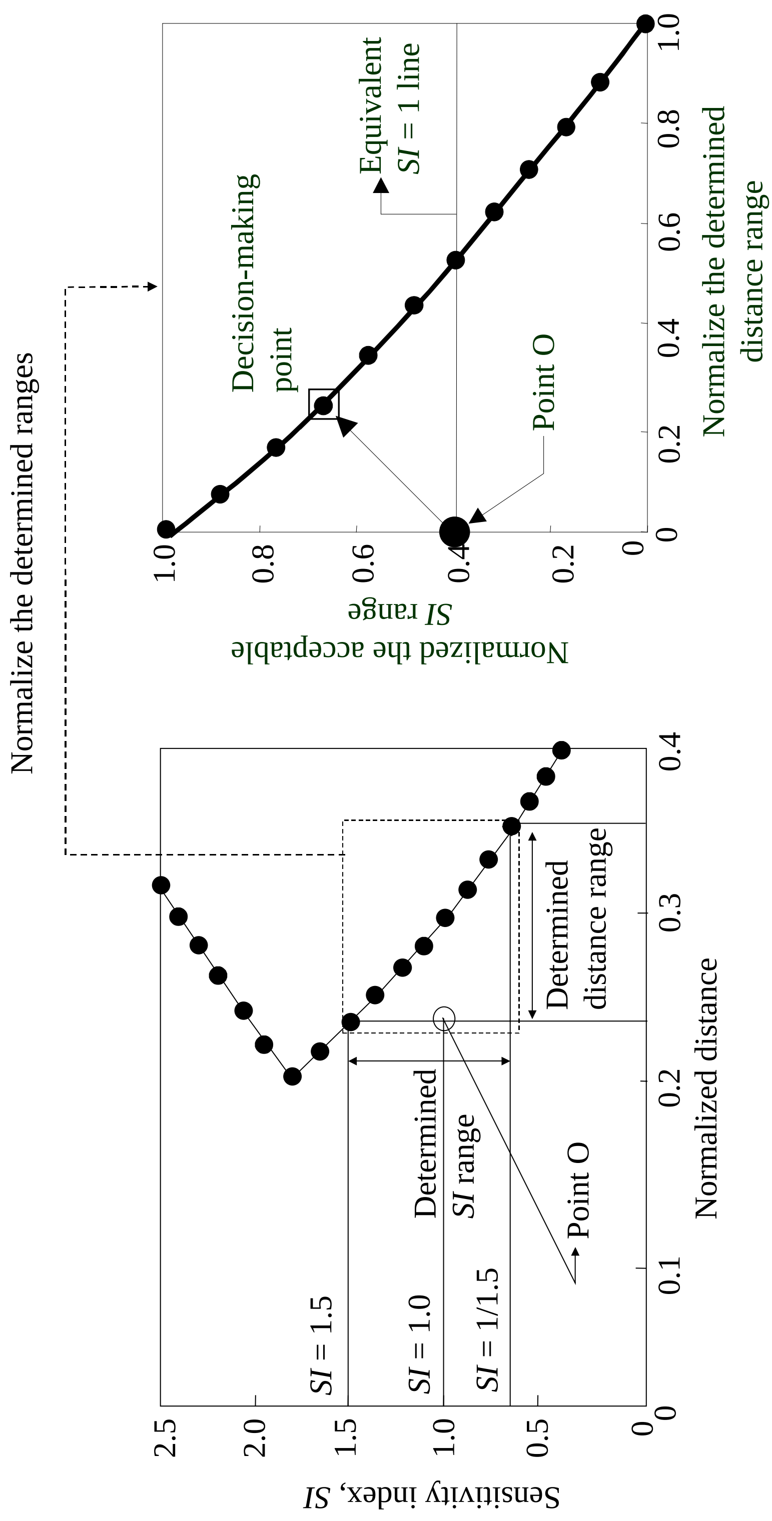

Fig. 3.2 (a)

Fig.3.2(a). Graph between sensitivity analysis and normalized distance with the determined *SI* and distance range

Fig.3.2(b). Graph between the normalized ranges from Fig.3.2(a) and the decision-making point by determining of both method

2. From Fig.3.2(a), the acceptable area shown with a dashed line is extracted. For this extracted area, the vertical axis and the horizontal axis are then normalized by Eq.(1) and then plotted the normalized space of the extracted area as shown in Fig.3.2(b).

3. Because the ideal point for the extracted area can be determined as the point whose *SI* values equals to 1 and normalized distance is minimum, as point O in Fig.3.2(a) and Fig.3.2(b), the minimum distance point from point O in Fig3(b) is considered as decision-making point.

(5) When the Pareto optimum curve have a number of inflection points as shown in Fig 3.1 and Fig.3.3, there might be a number of lowest sensitivity points with *SI* = 1. In this case, it is possible to determine the optimal point from the consideration of both sensitivity and closeness to the ideal solution. And the decision-making point is the point with *SI* = 1 that is closest to the ideal point as illustrated in Fig.3.3.

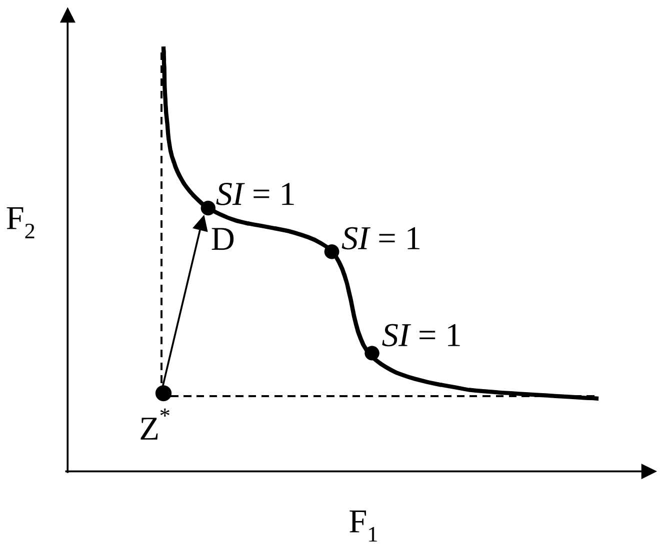

Fig.3.3 The decision making point when the Pareto optimum curve have a number of inflection points.

Moreover, in some conditions, the multi-objective optimizations are the constrained problems. Typically, a constrained multi-objective optimization problem can be subject to the constraint functions such as; $g_j(x) \geq 0$, $j = 1,2,\ldots,k$, where x is the decision variables. Constraints divide the search space into feasible and infeasible regions. With constraints, a part of the original Pareto-optimal region is not feasible and a new Pareto-optimal region emerges as shown in Fig.3.4.

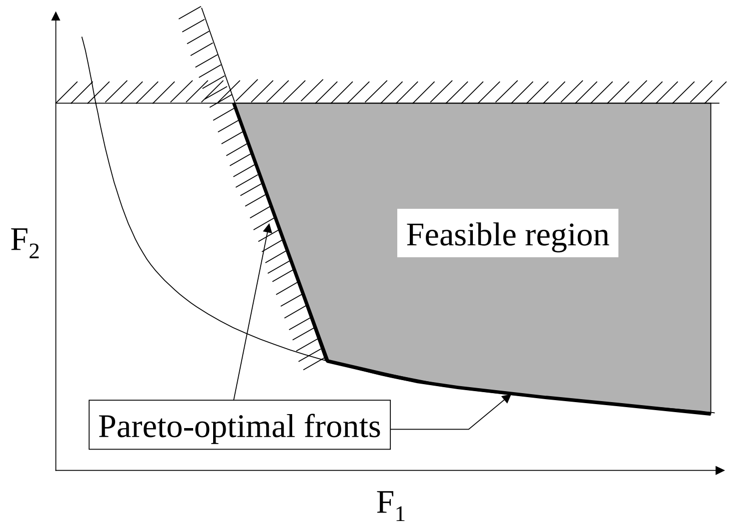

Fig. 3.4 Pareto-optimal fronts for the constrained multi-objective optimization[27]

As illustrated in Fig.3.4, which is reference from the example problem by Deb et al 2001[27], the Pareto-optimal fronts of constrained multi-objective optimization are more complicated. In some regions, the sensitivities of a variation in one objective value to a variation in the other of the Pareto-optimal solutions are almost constant. For such these Pareto-optimal solutions, the procedures to determine the decision-making point are illustrated in following section 3.3(6).

(6) When the Pareto-optimal solutions not have the *SI* = 1 point al all. This condition can be considered into 2 cases as follows.

1. When the feasible Pareto-optimal solutions not have the *SI* = 1 point and there is no point that its *SI* value is suddenly changed. Then, the *SI* values on the Pareto-optimal curve are then gradually changed or not changed. The examples of this case are shown in Fig.3.5-a, Fig.3.5-b

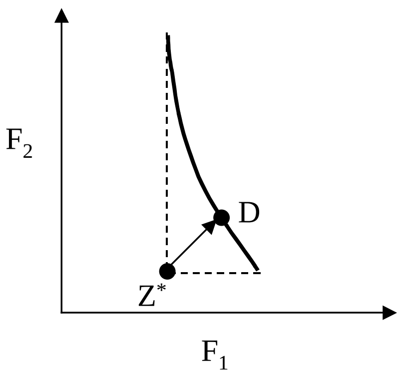

Fig.3.5-a

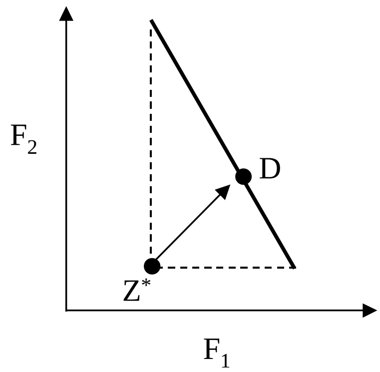

Fig.3.5-b

Fig.3.5 Decision making for the Pareto-optimal solutions that do not have the *SI* = 1 point and do not have the point of suddenly changed of *SI* value.

For these cases, because the degree of robustness for each point on the Pareto-optimal curve is not significantly different, thus the decision making point (point D in Fig. 3.5) should be the point that is closest to the ideal point (point Z^*).

2. When the feasible Pareto-optimal solutions not have the *SI* = 1 point and there is the point whose *SI* value is suddenly changed. The examples of this case are shown in Fig.3.6-a, Fig.3.6-b

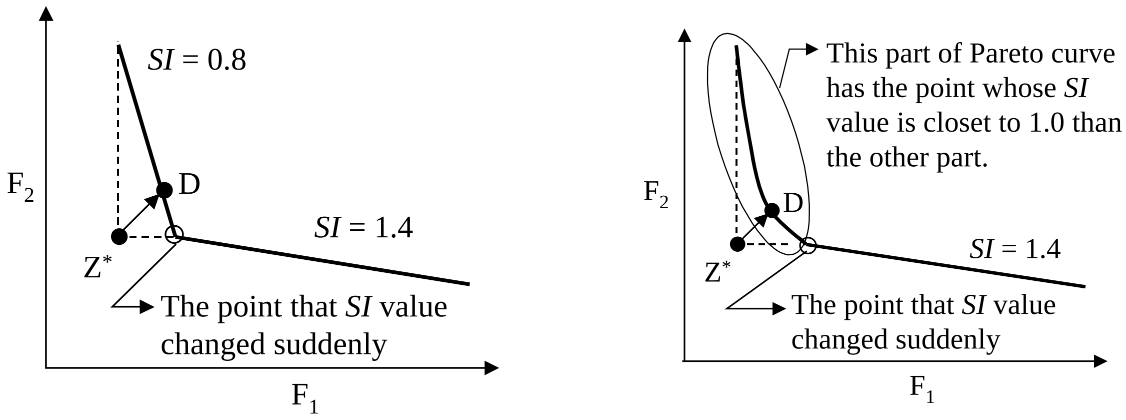

Fig.3.6-a Fig.3.6-b

Fig.3.6 Decision making for the Pareto-optimal solutions that do not have the *SI* = 1 point and there is the point whose *SI* value is suddenly changed.

For these cases, first, the sensitivity index of each solution on the Pareto-optimal solutions is evaluated. After that, determine the point whose *SI* value is suddenly changed, while this point is non-robust and should not be selected. Thereafter, divide the Pareto-optimal curve into many parts at the *SI* point that is suddenly changed. Then, select the part of the Pareto-optimal curve that has the point whose *SI* value is closest to 1.0. For example in Fig.3.6-a, the part of Pareto-optimal curve that has almost constant value of *SI* = 0.8, which is closer to 1.0 than *SI* = 1.4 in the other part, is chosen. The decision-making point is the point whose *SI* value is closest to 1.0. By the way, if this decision-making points by *SI* is located close to the non-robust point whose *SI* value is suddenly changed, the decision-making point should then be the point closest to the ideal point (point Z^* illustrated in Fig.3.6-a, 3.6-b) of the selected part of the Pareto-optimal curve.

3.4 Case study

In this research, to assure the applicability of the proposed methodology and indexes, the standby simplified high-pressure injection system (HPIS) of a nuclear power plant's pressurized water reactor (PWR) that is taken from reference [33] is shown below is examined.

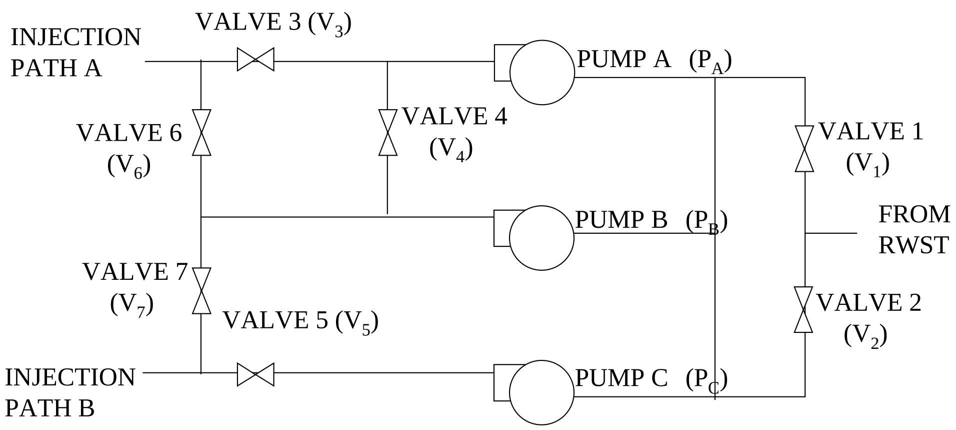

Fig. 3.7 HPIS system [33].

This system is normally in standby mode. Under accidental conditions, the HPIS can be used to remove heat from the reactor in those events in which the steam generators are unavailable.

3.4.1 The fault trees analysis and the minimum cut sets of the case study system

As described in chapter 2, in order to determine the unavailability of the standby HPIS system in Fig. 3.7, the fault trees is built as shown in Fig. 3.8 by considering the top event as the event that there is no flow through the injection path A and B, which means that this system is fail for operating. The symbols using for creating the fault trees in Fig.3.8 are shown in Fig.3.7. The basic events in Fig.3.8 is illustrated as bellows, The basic event V_1 is illustrated as the events that VALVE1 fails.

The basic event V_2 is illustrated as the events that VALVE 2 fails.

The basic event V_3 is illustrated as the events that VALVE 3 fails.

The basic event V_4 is illustrated as the events that VALVE 4 fails.

The basic event V_5 is illustrated as the events that VALVE 5 fails.

The basic event V_6 is illustrated as the events that VALVE 6 fails.

The basic event V_7 is illustrated as the events that VALVE 7 fails.

The basic event P_1 is illustrated as the events that PUMP 1 fails.

The basic event P_2 is illustrated as the events that PUMP 2 fails.

The basic event P_3 is illustrated as the events that PUMP 3 fails.

The fault tree in Fig.3.8 is simply represent by Boolean expression as shown in Eq.(3.2)

$$
\begin{aligned}
\text{Top event} &= G1 \\
&= G2 \cdot G10 \\
&= (G3 \cdot G8) \cdot (G11 \cdot G13) \\
&= [(V_6 + G4) \cdot (V_3 + G6)] \cdot [(V_7 + G12) \cdot (V_5 + G14)] \\
&= [(V_6 + (G5 \cdot G7)) \cdot (V_3 + P_A + (V_1 \cdot V_2))] \cdot \\
&\quad [(V_7 + (P_B + (V_1 \cdot V_2)) \cdot G5) \cdot (V_5 + (P_C + (V_1 \cdot V_2)))] \\
&= [(V_6 + (V_4 + P_A + (V_1 \cdot V_2)) \cdot (P_B + (V_1 \cdot V_2))) \cdot \\
&\quad (V_3 + P_A + (V_1 \cdot V_2))] \cdot [(V_7 + (P_B + (V_1 \cdot V_2)\ ) \cdot \\
&\quad (V_4 + P_A + (V_1 \cdot V_2))) \cdot (V_5 + (P_C + (V_1 \cdot V_2)))]
\end{aligned}
\tag{3.2}
$$

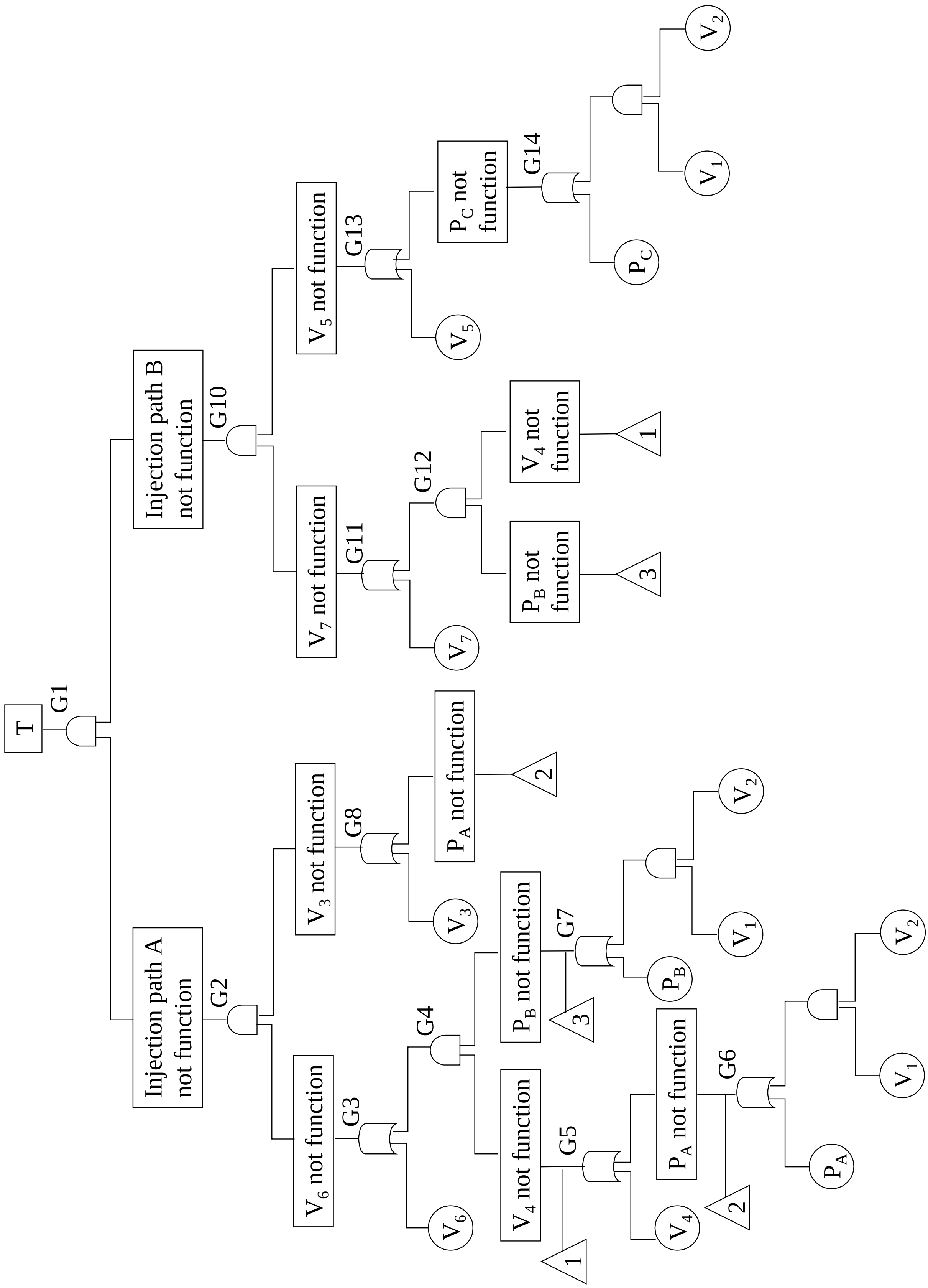

Fig 3.8 The fault tree diagram of HPIS

From the Boolean expression in Eq.(3.2), the minimal cut sets (MCS) can be generated as expressed in Eq.(3.3).

$$\begin{aligned} MCS = & \{P_A \bullet P_B \bullet P_C\} + \{V_1 \bullet V_2\} + \{P_B \bullet P_C \bullet V_3 \bullet V_4\} + \{P_A \bullet P_B \bullet V_5\} + \\ & \{P_B \bullet V_3 \bullet V_4 \bullet V_5\} + \{P_A \bullet P_C \bullet V_6 \bullet V_7\} + \{P_C \bullet V_3 \bullet V_6 \bullet V_7\} + \\ & \{P_A \bullet V_5 \bullet V_6 \bullet V_7\} + \{V_3 \bullet V_5 \bullet V_6 \bullet V_7\} \end{aligned} \tag{3.3}$$

3.5 From probabilistic risk assessment to risk equation.

The nuclear power plants are designed according to the defence-in-depth principle, one single failure of a component or basic event will probably not result in a large accident. A large accident is the result of the combinations of multiple basic events. The probabilistic risk assessment methodology determines all-important cut sets that could result in a large accident. The final results of a probabilistic risk assessment study are then represented in the risk equation.

The purpose of this research is to optimize the effective of surveillance test interval (STI) in the maintenance activities of a standby system by considering both system unavailability and maintenance costs as simultaneous objectives. This subsection will show that STI are represented through appropriated parameters included within the model of system unavailability and maintenance costs, which will be adopted as decision variables for the optimization process. The formulation of the objective functions, which are the unavailability function and cost function, are taken from the model developed by S. Martorell et al [50] and are summarized below. These objective functions are represented by probabilistic risk assessment as described above.

3.5.1 Unavailability function [50]

Unavailability [15] is the probability that a system or component is not performing its required function at a given point in time or over a stated period of time when operated and maintained in a prescribed manner.

The unavailability of a safety function, in turn, depends on the unavailability of the associated safety-related systems, normally on standby and ready to operate on demand. The quantification of the system unavailability is possible using several methods [20,32]. Normally, the fault trees are used to represent the structure function and then the Minimal Cut Sets (MCS) are determined into the probabilistic risk assessment model[4,14,24,26,34,47,50]. The unavailability of the system is defined as the top event while the unavailability of the safety components are defined as the basic events. The Minimal cut set then represents a minimum set of unavailability states of the safety components (or basic events in the probabilistic risk assessment). Correspondingly, as described in section 2.1.3 of chapter 2, the system unavailability model is usually formulated into the probabilistic risk assessment, which is an upper bound, as follows [20]:

$$U(x) \approx \sum_{j} \prod_{k} u_{jk}(x), \qquad (3.4)$$

where j is the index of minimal cut set.

k is the index of each basic event of the corresponding minimal cut set.

$u_{jk}(x)$ is the unavailability associated with the basic event k belonging to minimal cut set number j, which define an unavailability of a safety component that depends on the vector of decision variables x.

Consequently, using the model in Eq.(3.4), the component unavailability is needed to derive the system unavailability. From the literature reviews of ref. [50] unavailability contributions of a component normally in standby can be divided into two main categories as:

1) Unavailability due to random failures called the reliability effect.

2) Unavailability due to testing and maintenance downtimes called the downtimes effect.

Considering unavailability from reliability effect, time dependent unavailability due to random failures at time interval T of the surveillance test interval (STI) and the average unavailability due to random failures can be expressed respectively as,

$$u_r(x,T) \approx \rho + \lambda \cdot T, \tag{3.5}$$

$$u_r(x) \approx \rho + \frac{1}{2}\lambda \cdot T, \tag{3.6}$$

where ρ is a per-demand failure probability.

λ is the standby failure rate.

The unavailability due to downtime effect, which are shown in the following expressions, are commonly used and determined for applied in this research.

$$u_t(x) = f_t(x) \cdot t \cdot q_o^t, \qquad (3.7)$$

$$u_c(x) = f_c(x) \cdot d, \qquad (3.8)$$

where u_t (x) is the unavailability due to testing

$u_c(x)$ is the unavailability due to corrective maintenance.

For Eq.(3.7) and Eq.(3.8), the following notation has been used:

$f_t(x) = 1/T$ is the rate of testing events.

t = mean downtime due to testing.

q_o^t = fraction of the total downtime t with the component unavailable [0,1]. The parameter q_o^t is usually set equal to one with considering that t, which is defined now by the mean down time, represents the time the component is really unavailable for the surveillance test.

$f_c(x)$ is the rate of corrective maintenance events.

d = mean downtime due to corrective maintenance.

While for the component normally in standby which undertakes surveillance test interval T, $f_c(x)$ can be expressed as the following equation

$$f_c(x) = 1/T \cdot u_r(x,T) \qquad (3.9)$$

From Eqs.(3.5)-(3.9), each component unavailability model of $u_{jk}(x)$ in Eq.(3.4) can be expressed as,

$$u(x) = u_r(x) + u_t(x) + u_c(x). \qquad (3.10)$$

3.5.2 Cost function [50]

The maintenance cost model of the standby safety system expresses the relation to surveillance test intervals. The model involves the contributions to the component cost model can be represented as following,

$$C(x) = \sum_i c_i(x), \tag{3.11}$$

where i is the index of each component.

$c_i(x)$ is the maintenance cost model of the component i.

The cost model of each component can be expressed as,

$$c(x) = c_t(x) + c_c(x), \tag{3.12}$$

where $c_t(x)$ is the yearly cost contribution as a consequence of the number of tests being performed over a year period.

$c_c(x)$ is the yearly cost contribution as consequence of performing corrective maintenance.

Consider a component normally in standby, which carries out the surveillance test interval T, the basic cost contributions can be adopt as follows

$$c_t(x) = \frac{t}{T} \cdot c_{ht} \tag{3.13}$$

$$c_c(x) = f_c(x) \cdot d \cdot c_{hc} \tag{3.14}$$

where c_{ht} represents the hourly costs for testing.

c_{hc} is the hourly costs of corrective maintenance.

While $f_c(x)$ can be obtained using Eq.(3.9).

3.6 Objective functions data.

In order to derive the objective functions of the unavailability function and cost function as described in the section 3.5, the related component unavailability and cost data of the HPIS system are summarized from ref.[33] and are shown in Table3.1.

Table 3.1. Component unavailability and cost parameters [33].

Unit	λ (10^{-6}/h)	ρ (10^{-3})	t (h)	d (h)	c_{ht} (\$/h)	c_{hc}(\$/h)
Valves(V)	5.83	1.82	0.75	2.6	20	15
Pumps(P)	3.89	0.53	4	24	20	15

3.7 Multi-objective optimization parameters

After formulating the simultaneous objective functions of the unavailability function and cost function, the multi-objective optimization is performed by NSGA-II method. The parameters shown in Table 3.2 are then used for multi-objective optimization.

Table 3.2. Parameters used in the multi-objective optimization

Parameters	Values
Encoding mechanism	Real-parameter
Population size	500
Generation numbers	20
Crossover probability	0.6
Mutation probability	0.01

3.8 Results and Discussions

In order to assure the effectiveness of the proposed methodology and indexes, the case study of HPIS explained in section 3.4 is applied.

Then, in order to optimize the surveillance test program in the maintenance activities of this HPIS system, the system components have been classified into three surveillance test interval groups; each group will be tested in the same interval, as shown in Table3.3. The symbols in Table 3.3 are shown in Fig. 3.7.

Table 3.3. Groups of test intervals.

T^1	V_1, V_2
T^2	P_A, P_B, P_C, V_3, V_5
T^3	V_4, V_6, V_7

Test intervals for each group are constrained as the follows:

$$T^1 \leq 8760\ h$$

$$T^2 = k_1 \cdot T^1 \quad while \quad 1 \leq k_1 \leq 10$$

$$T^3 = k_2 \cdot T^2 \quad while \quad 1 \leq k_2 \leq 10$$

Consequently, the maintenance activities optimization of this system has decision variables set, x, as shown in Eq.(3.15)

$$x = \{T^1, k_1, k_2\} \tag{3.15}$$

3.8.1 Results and Discussions

After the objective functions of the unavailability function and cost function are derived as explained in the section 3.5 by using the related component unavailability and cost data of maintaining the system are shown in Table 3.1, the multi-objective optimization is applied by using the parameters shown in Table 3.2. The result of Pareto-optimal solutions for minimizing both unavailability and maintenance cost are shown in Fig.3.9.

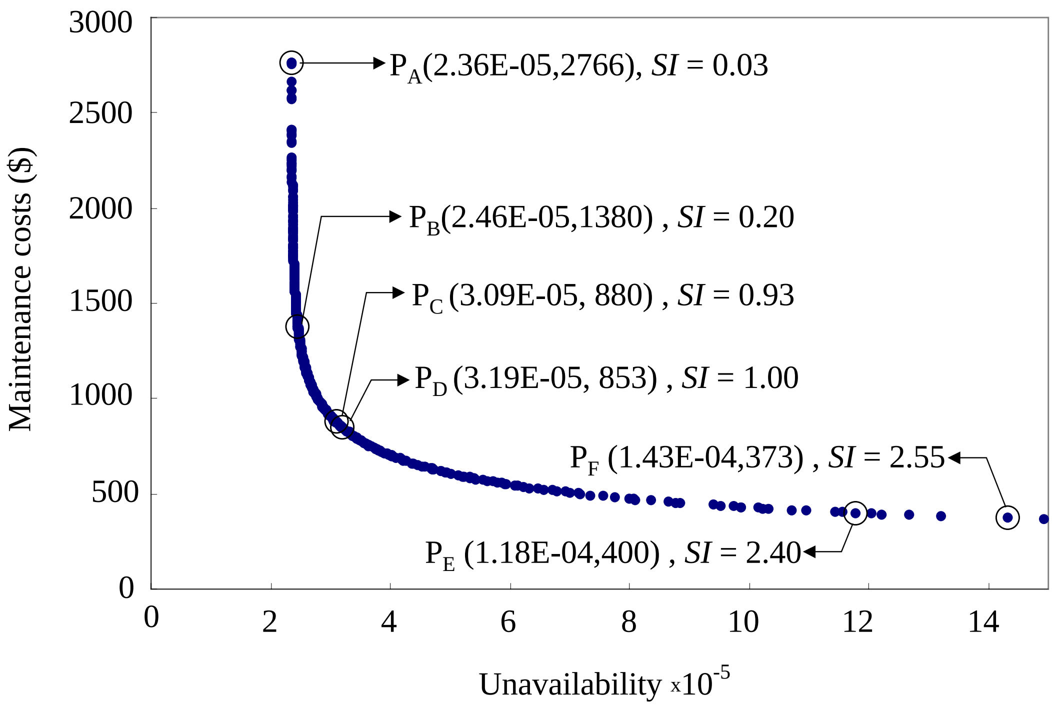

Fig 3.9. The Pareto-optimal solutions for minimization of unavailability and maintenance cost.

From the result of Pareto-optimal solutions in Fig.3.9, it can be shown that Pareto-optimal solutions provide more information than single-objective optimization. However, there are some Pareto-optimal solutions that are not appropriate because of their high sensitivities of a variation in one objective value to a variation in the other. If the single objective optimization is performed in these high sensitivity areas, the optimization result may not robust enough.

For example of the point P_A in Fig.3.9, if a single-objective optimization in which unavailability is set at the constraint value of 2.36E-5; in such a case, the one objective cost optimal solution will be $2766. But if unavailability at point P_B is set as a constraint value of 2.46E-5, the cost optimal value will be $1380. This means that around 2.46E-5, a mere difference in the unavailability constraint value of only 1.E-6, causes the maintenance cost optimization value to have a difference of $1386, or in practical terms, to nearly double. It can be explained that there are high sensitivities of unavailability value to cost value in this region.

On the other hand, at point P_E, the optimal unavailability value is $1.18x10^{-4}$ and the optimal cost value is $400. At point P_F, the optimal unavailability value is $1.43x10^{-4}$ and the optimal value of cost is $373. This indicates that around these points, a slight variation (only $400-$373 = $27) in the maintenance costs causes the variation in unavailability optimization value up to $2.5x10^{-5}$. This means cost has high sensitivities of maintenance cost value to unavailability value in this zone.

However, about the point P_C and P_D, around unavailability value of 3.19E-5, a small difference in the unavailability constraint value of only 1.E-6 causes the maintenance cost optimization value to have a small difference of only \$880-\$853 = \$27. Thus, in this zone, there are low sensitivities for all of objectives.

From the above discussion, if the constraint is not chosen appropriately in a single-objective optimization, the optimization result may fall in the region of high sensitivity. When the maintenance activities are performed in these high sensitivity areas, it is possible that only little variation of the parameters may make the expected objective function values changed with lacking of robustness. Therefore, the sensitivity analysis with the Pareto optimum solution is very important.

The sensitivity index for the Pareto-optimal solutions is introduced as proposed in section 3.2. From the *SI* values for points P_A to P_F in Fig.3.9 show that the *SI* values are far apart from the value of 1.0 in the high sensitivity zones. And *SI* is equal to 1.0 at point P_D, which is described above that this P_D point has low sensitivity for all objective functions. Therefore, it is shown that the proposed sensitivity index is appropriate to find out the robust solution.

In addition, the relation of the calculated sensitivity index values plotted with unavailability is shown in Fig.3.10.

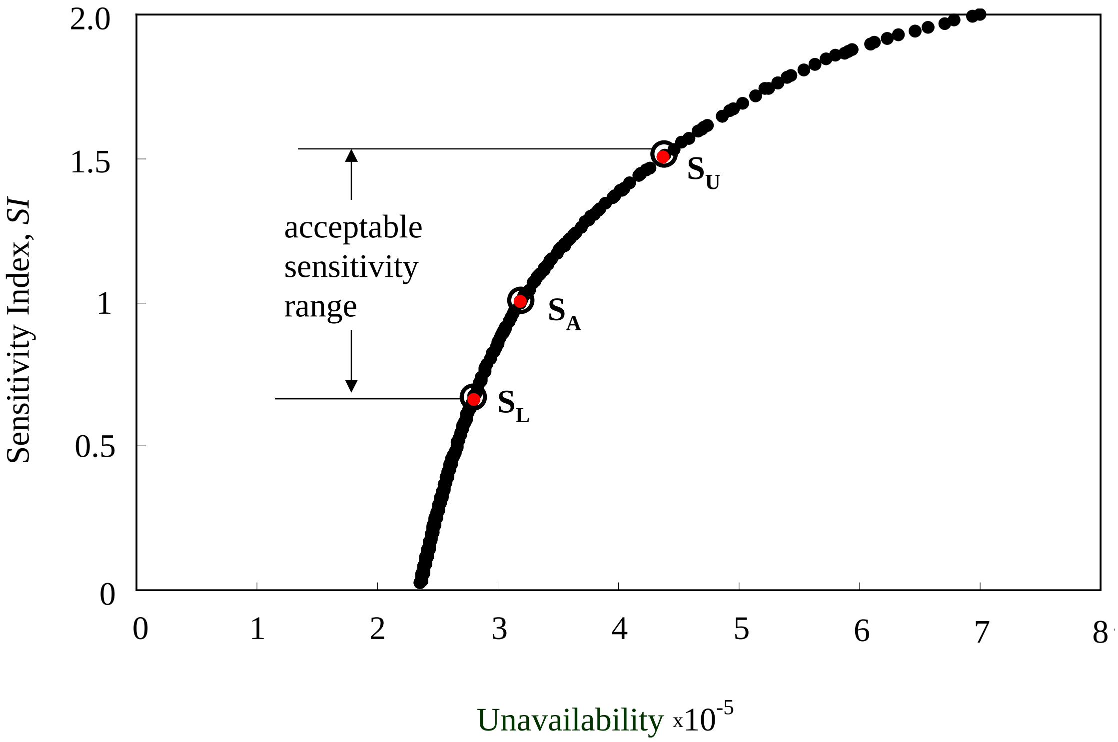

Fig 3.10. The sensitivity index values plot with unavailability.

Because the degree of sensitivity can be represented by the sensitivity index, the acceptable robust range for the decision-making can be quantitatively specified. Therefore, it is possible to make the decision-making flexibly. For example, in this paper the acceptable range of $1/1.5 \leq SI \leq 1.5$ is defined. This means that the variation in one objective is not greater than 1.5 times the variation in the other.

As seen from Fig.3.10, the solutions from point S_L to S_U are the acceptable range of solutions that are robust. The *SI* value of point S_A equals to 1. This point S_A then has the lowest sensitivity for all objectives. When both objectives are equally important, this point is suggested as the best decision-making point. If the maintenance cost is more important than the unavailability, the results in the range $1 < SI \leq 1.5$ can be selected. On the other hand, if the unavailability is more important than the maintenance cost, the best results are found in the range $1/1.5 \leq SI < 1$.

The decision making point obtained by the proposed sensitivity index was also compared with that obtained using the conventional method. As described in chapter2, the decision point by the concept of conventional method is a solution that is minimally distant from a given ideal point. Table 3.4 compares the normalized distance suggested by each method. And, those decision-making points by each method are shown in Fig. 3.10.

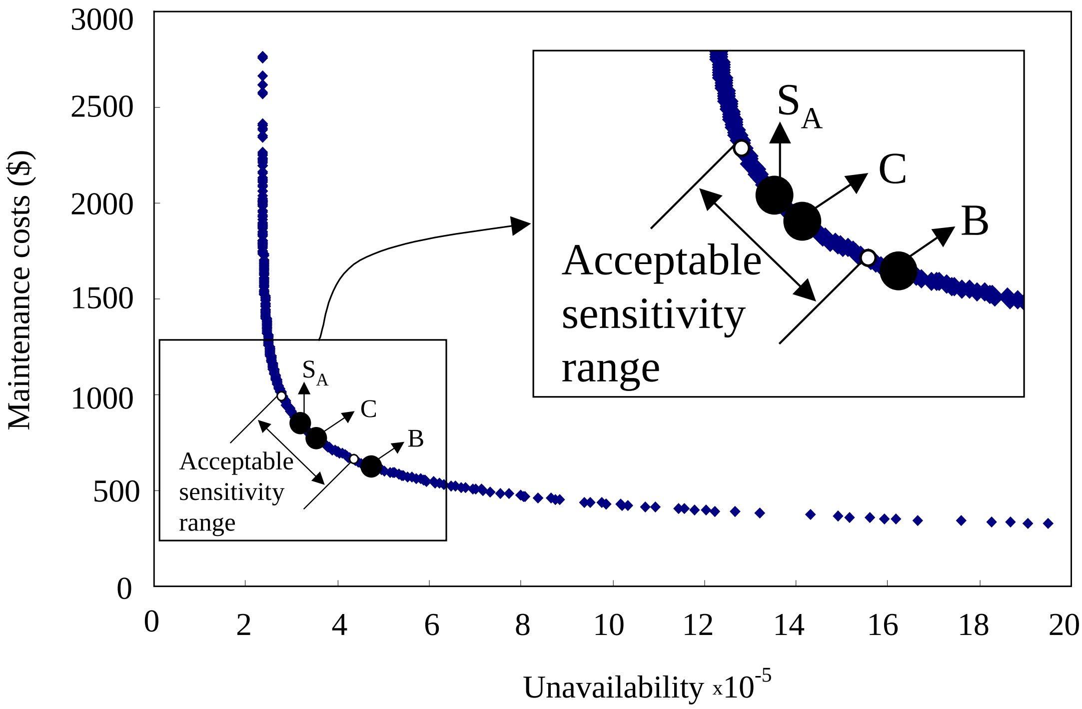

Fig 3.11. The Pareto-optimal solutions with decision points suggested by the proposed index and the conventional.

Table 3.4. The distance after normalized objective values from the suggested decision point to the ideal point by each method represent with their corresponding *SI* value.

Method	Decision point (unavailability, cost)	Normalized distance	*SI*
Sensitivity index	S_A(3.19E-5, 853)	0.286	1.00
Conventional method	B(4.73E-5, 627)	0.209	1.61
By considering Of both method	C(3.55E-5, 770)	0.249	1.20

From Table 3.4, it is shown that the normalized distance of the decision-making point S_A by the proposed index is only a small value further than the decision-making point B by the conventional method. But the point S_A provides less sensitivity and higher in robustness than the point B. If the distance to the ideal point is more paid attention than the robustness, the conventional method is appropriate. Nevertheless, the proposed index is recommended because it provides the solution that has the smallest sensitivity and its result is also very close enough to the ideal solution. Moreover, the Fig.3.11 also shows that the decision point B by the conventional method is located out of the range of the acceptable sensitivity. So, this point B may not be sufficiently robust.

In addition, the good compromise decision-making point between the proposed index and the conventional method is determined according to the section 3.3(4). At first, as seen from Fig.3.12, the relation between *SI* and normalized distance is plotted. The area, which exists in the acceptable range of robustness $1/1.5 \le SI \le 1.5$, is then specified. Thereafter, the specified area in Fig.3.12 is extracted and the values of both horizontal and vertical axis are normalized as shown in Fig.3.13.

From Fig.3.13, the point C that is located minimally to the ideal point O of this extracted area is the compromise decision-making point. The compromise decision-making point C is shown in Table 3.4, and also illustrated in Fig 3.11. If we pay attention to both the normalized distance and *SI* value, both of these values can be satisfied with only point C among the mentioned methods above. Therefore, it is considered that the point C is appropriate as the compromise decision-making point.

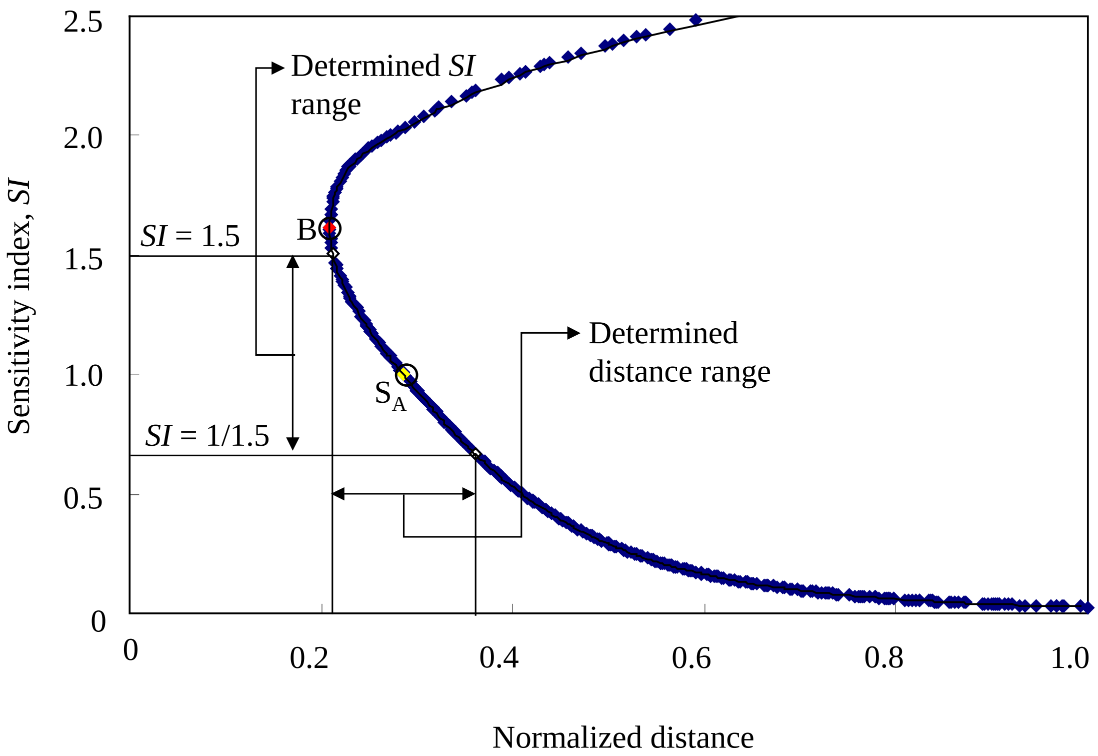

Fig 3.12. The sensitivity index values plot with the normalized distance. The determined ranges are also illustrated.

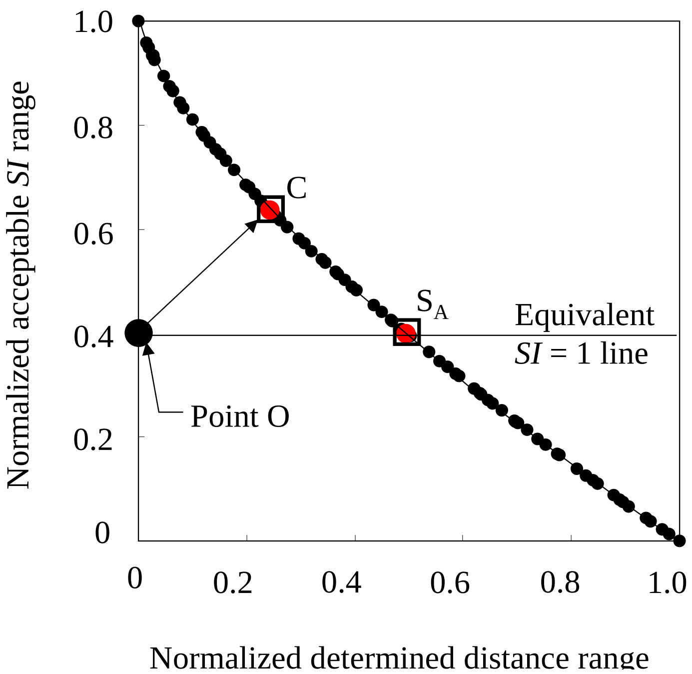

Fig 3.13. Normalized acceptable *SI* range plot with normalized determined distance range and decision-making point by considering by both methods.

3.8.2 Sensitivity studies of the decision variables to the Pareto-optimal values

In addition, the sensitivities of variation of each decision variables also have the effect on both objective function values. Therefore, in this section, the sensitivities of each decision variables to both objective function values are determined.

First, the results of decision variables T^1, T^2(k1·T^1) and T^3 (k1·k2·T^1) plotting with the first objective function values, which is the system unavailability, are shown in Fig.3.14 - Fig.3.16.

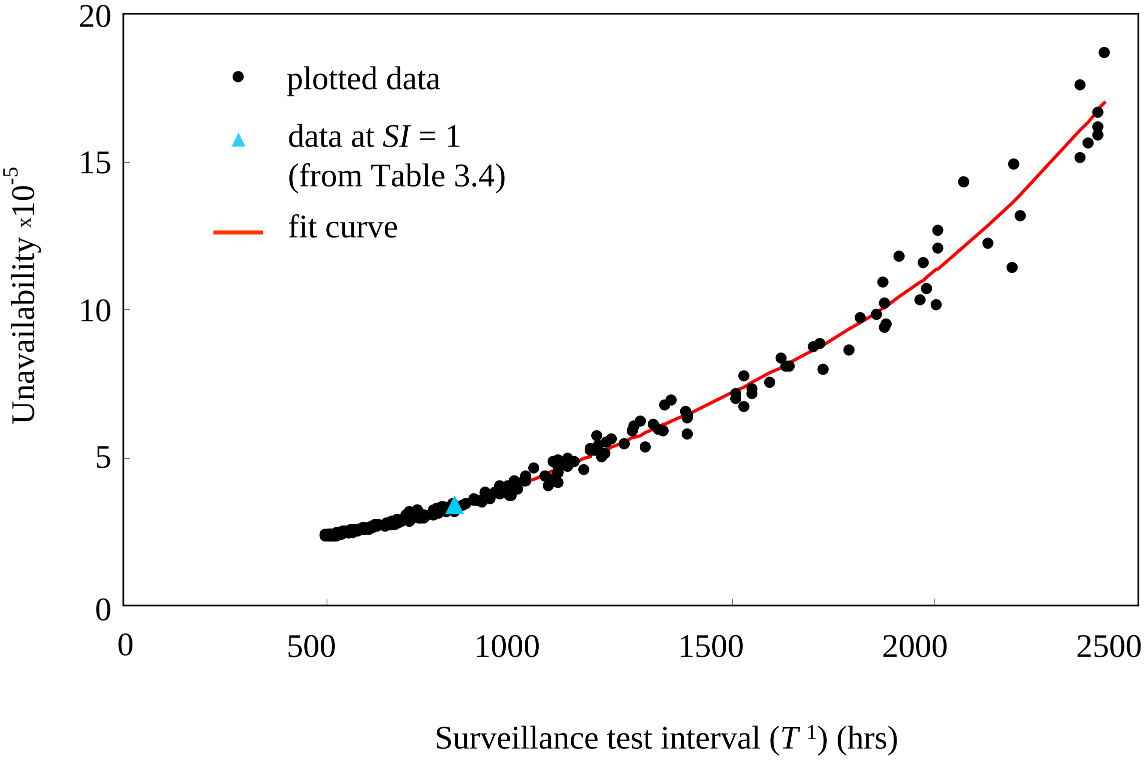

Fig 3.14. Optimal unavailability-T^1 plot

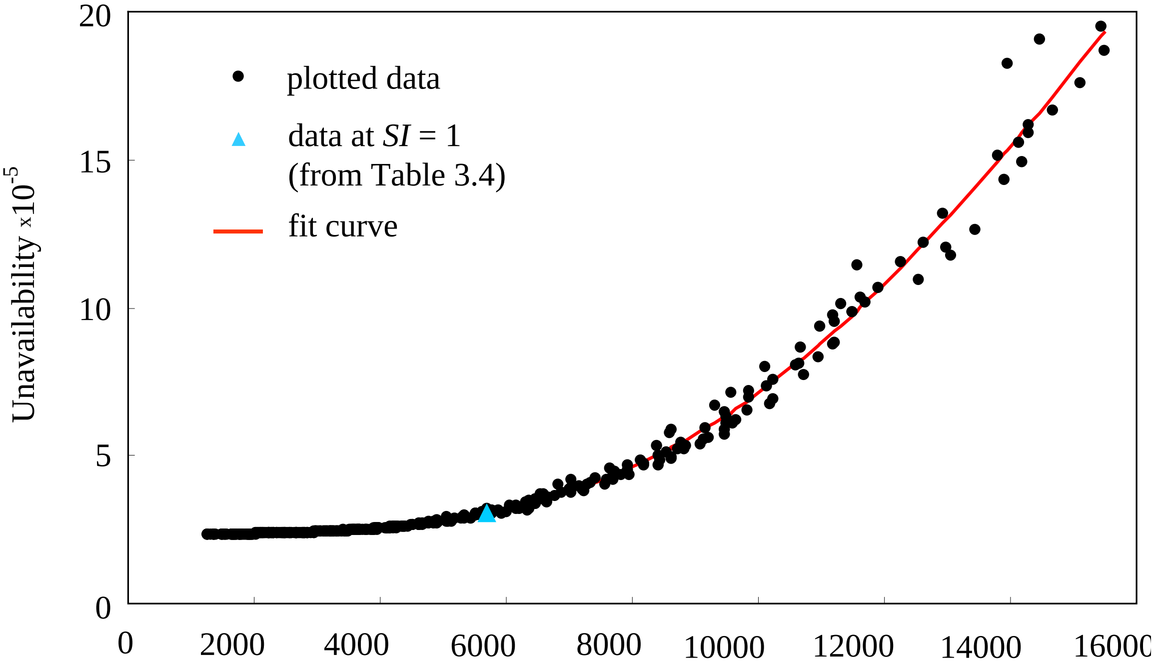

Fig 3.15. Optimal unavailability-T^2 plot

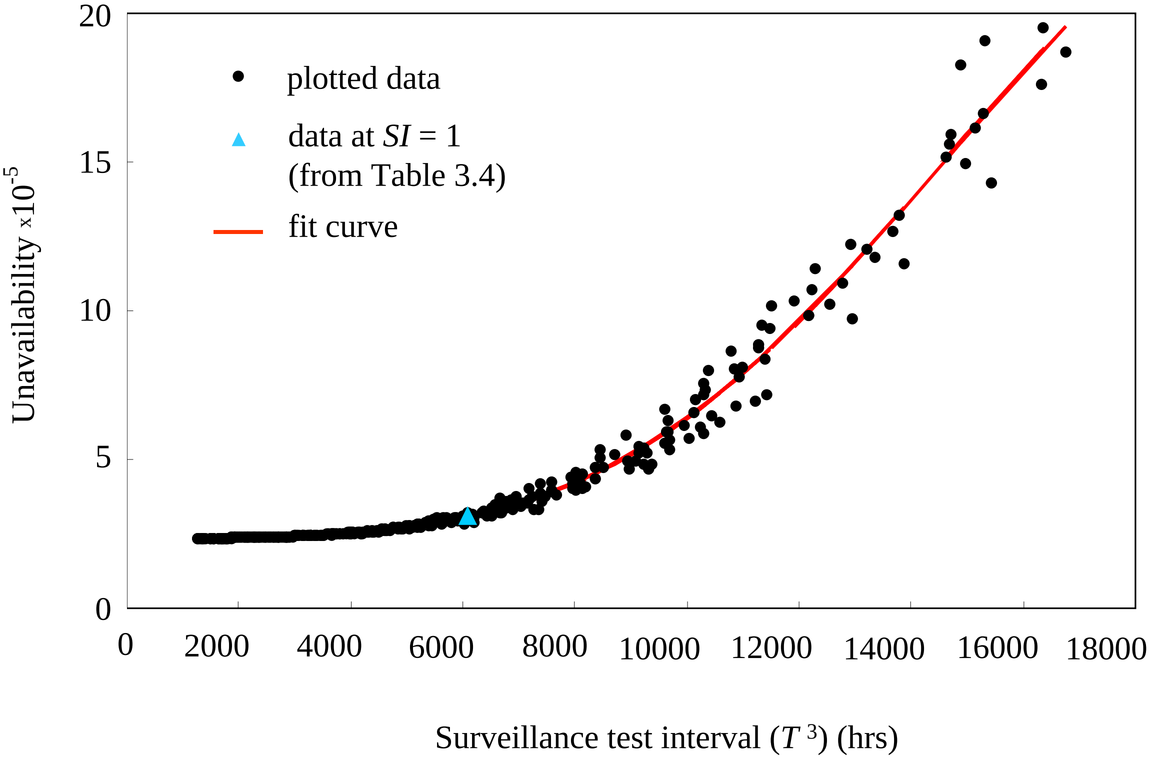

Fig 3.16. Optimal unavailability-T^3 plot

Thereafter, Fig.3.17 - Fig.3.19 show the results of decision variables T^1, T^2 and T^3 plotting with the second objective function that is of system maintenance costs.

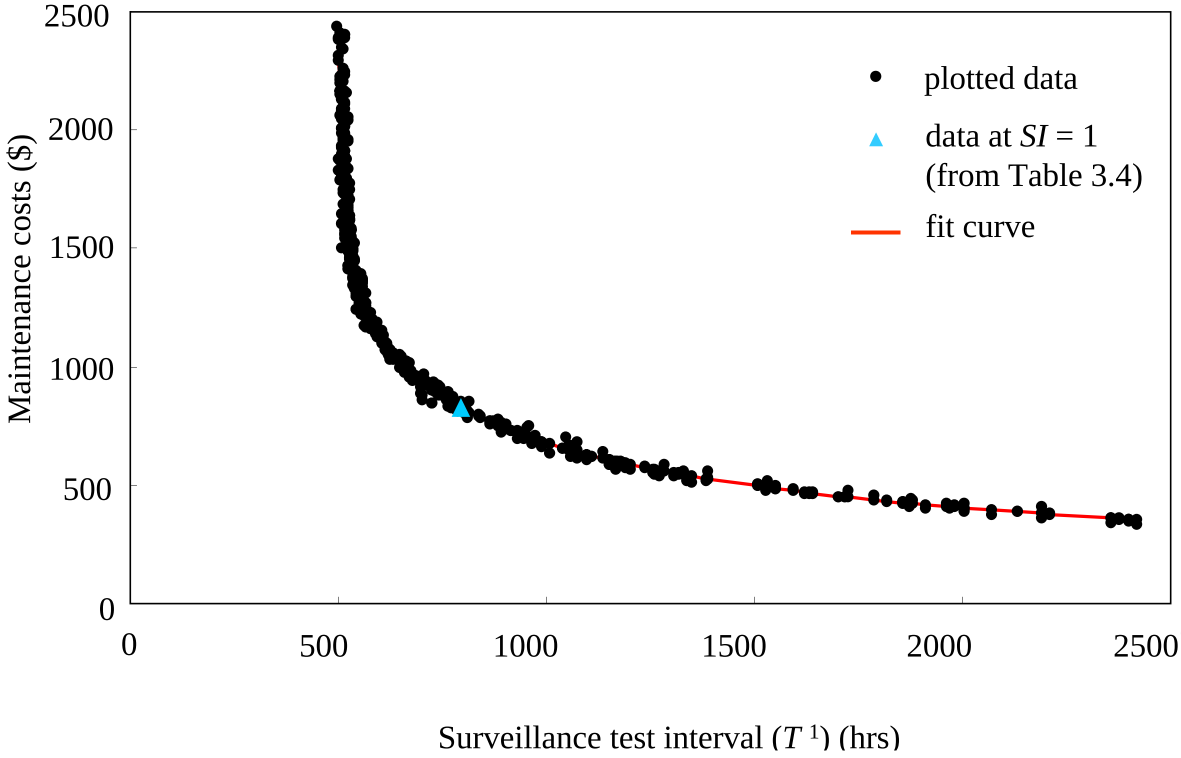

Fig 3.17. Optimal maintenance costs-T^1 plot

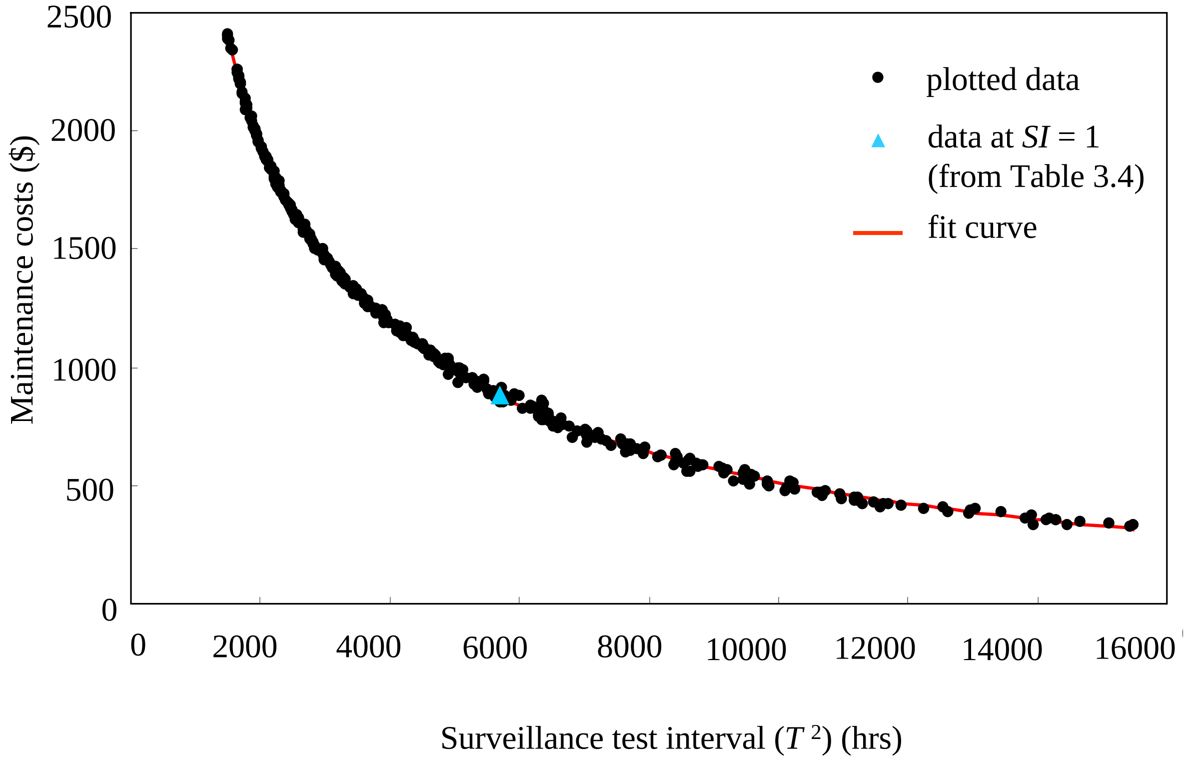

Fig 3.18. Optimal maintenance costs-T^2 plot

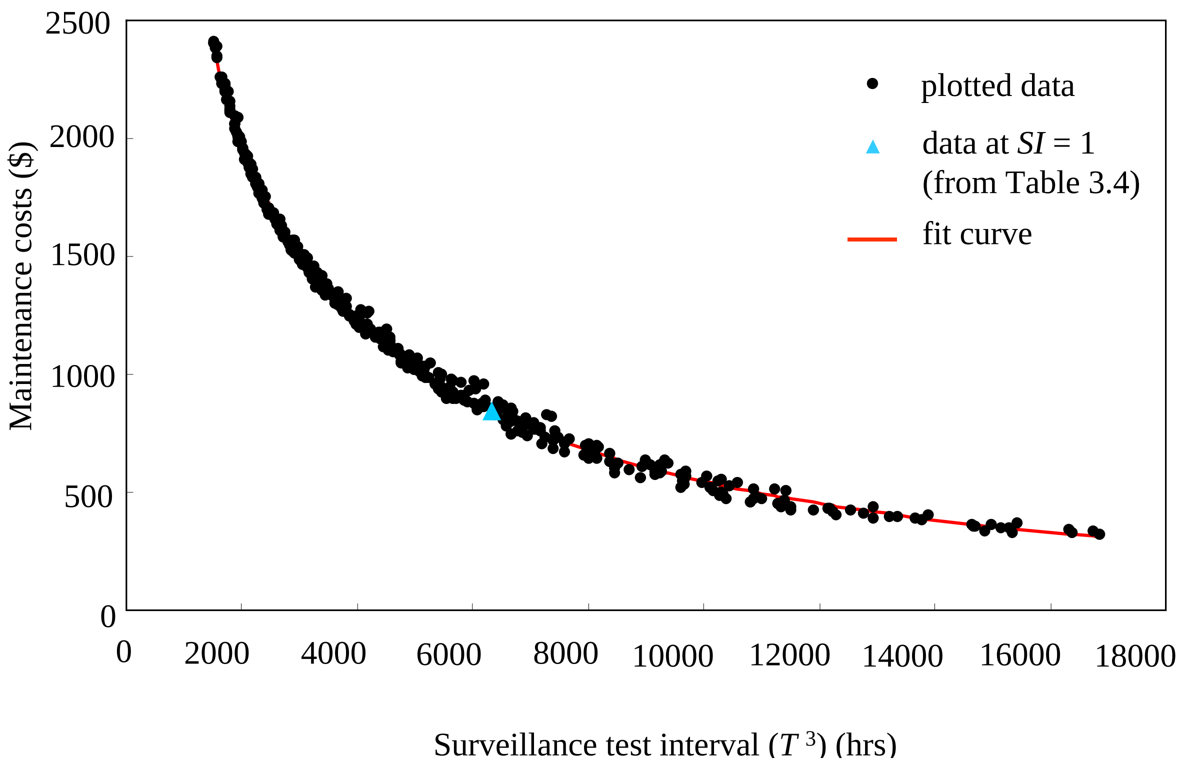

Fig 3.19. Optimal maintenance costs-T^3 plot

The result of decision-making point in the viewpoint of robustness of sensitivity at $SI = 1$ from Table 3.4 (sensitivity variation in one objective value to a variation in the other objective function value) is also shown in Fig. 3.13 - Fig. 3.18. From Fig. 3.13 - Fig. 3.18, by observation with the naked eyes, they are shown that at the decision making point at $SI = 1$ form Table 3.4 are in the zone that the sensitivity of variation in the decision variable values (T^1, T^2 and T^3) to both objective functions values (unavailability, maintenance costs) are low.

In order to determine the sensitivity of variation in the decision variable values to both objective functions values quantitatively, the proposed sensitivity index, which is explained by Eq.(3.1) of section 3.2, is capable to be applied by considering F_j and F_k in Eq.(3.1) as objective function and decision variable, respectively.

When using the sensitivity index to determine the sensitivities of the variation in decision variable to the objective function, the solutions with little values of SI are preferred. From the basic idea of the sensitivity index, the solutions at sensitivity index value = 1 is considered that the variation in the decision variable values and the objective function values are approximately equivalent. When the sensitivity index > 1, there are the tendency to be high in sensitivities because the variation in the objective function values are greater than the variation in the decision variable values.

The results of sensitivity index for decision variables T^1, T^2 and T^3 to the first objective function, which is the system unavailability, are shown in Fig.3.20-Fig.3.22

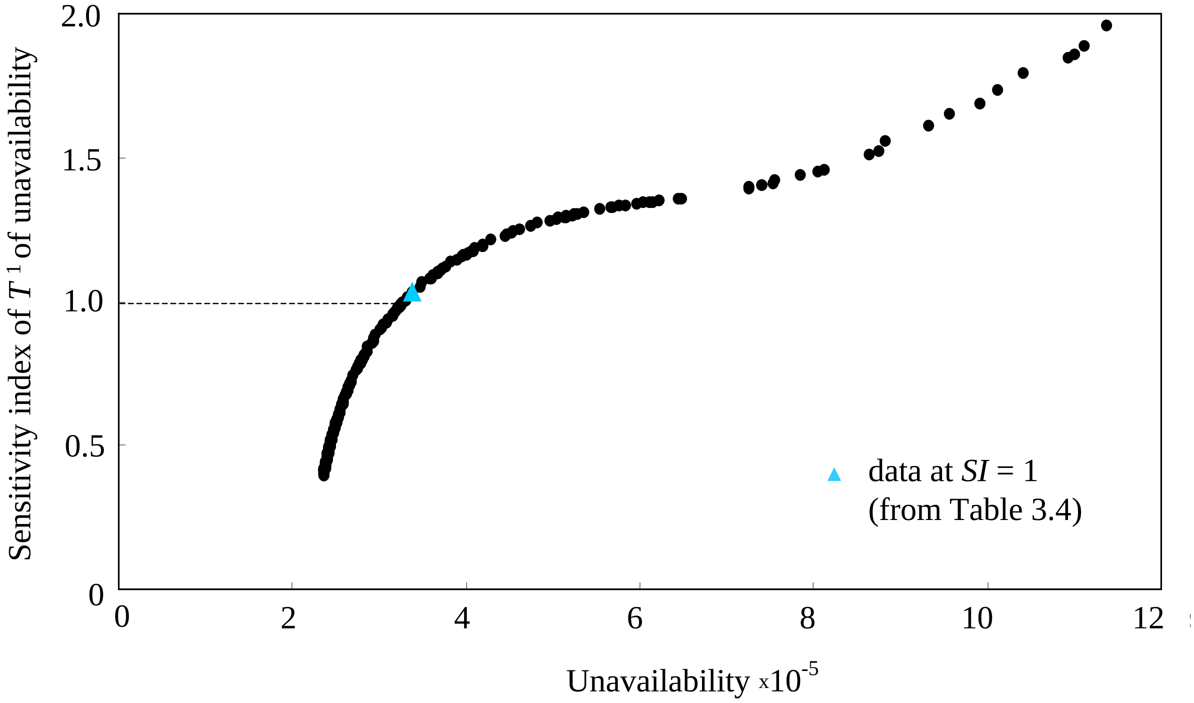

Fig 3.20. Sensitivity index for T^1 to unavailability – unavailability plot

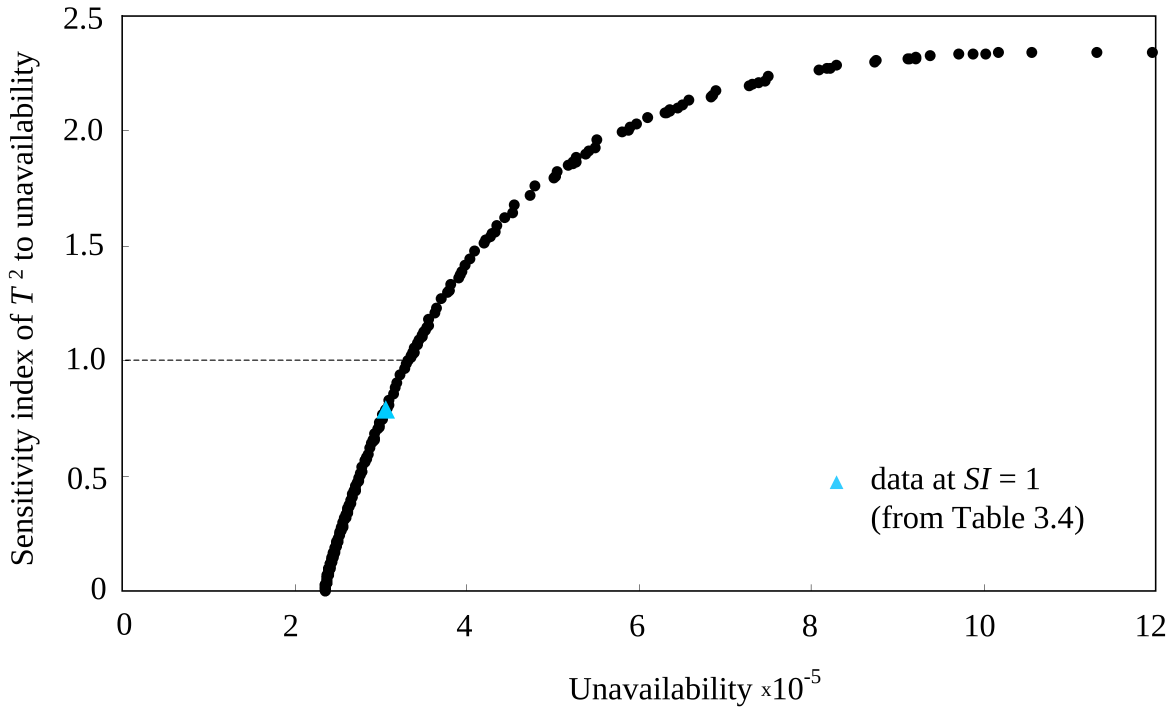

Fig 3.21. Sensitivity index for T^2 to unavailability – unavailability plot

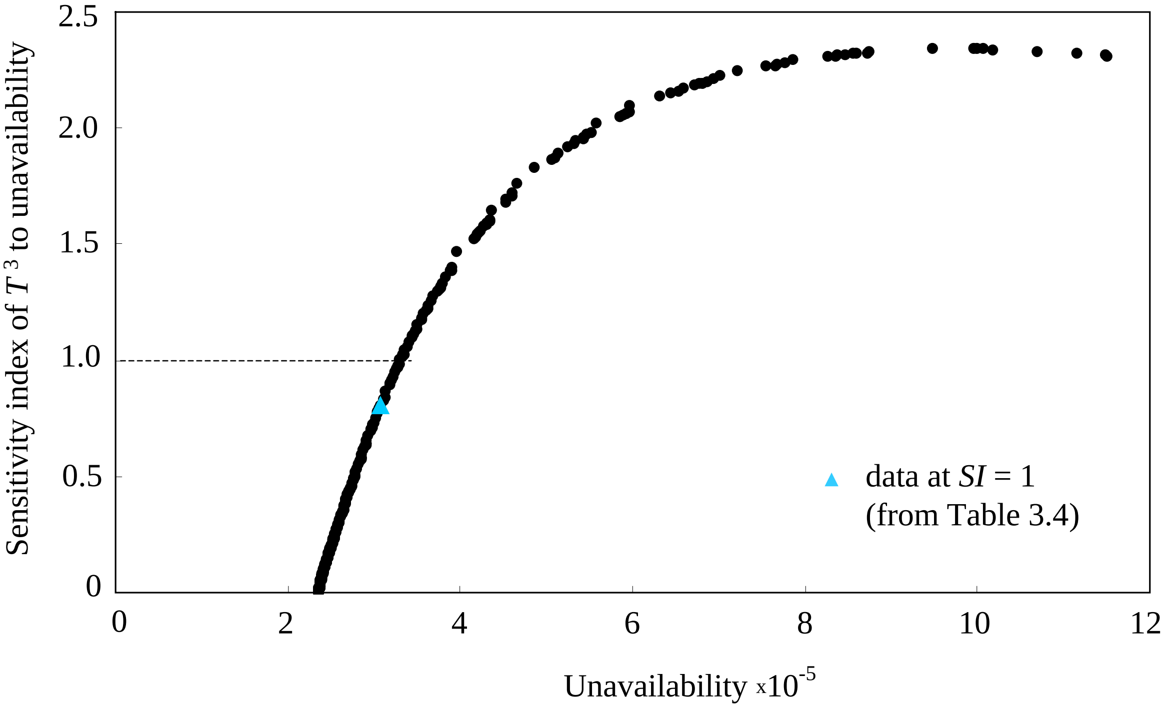

Fig 3.22. Sensitivity index for T^3 to unavailability – unavailability plot

The results of sensitivity index for decision variables T^1, T^2 and T^3 to the second objective function , which is the maintenance costs, are shown in Fig.3.23-Fig.3.25

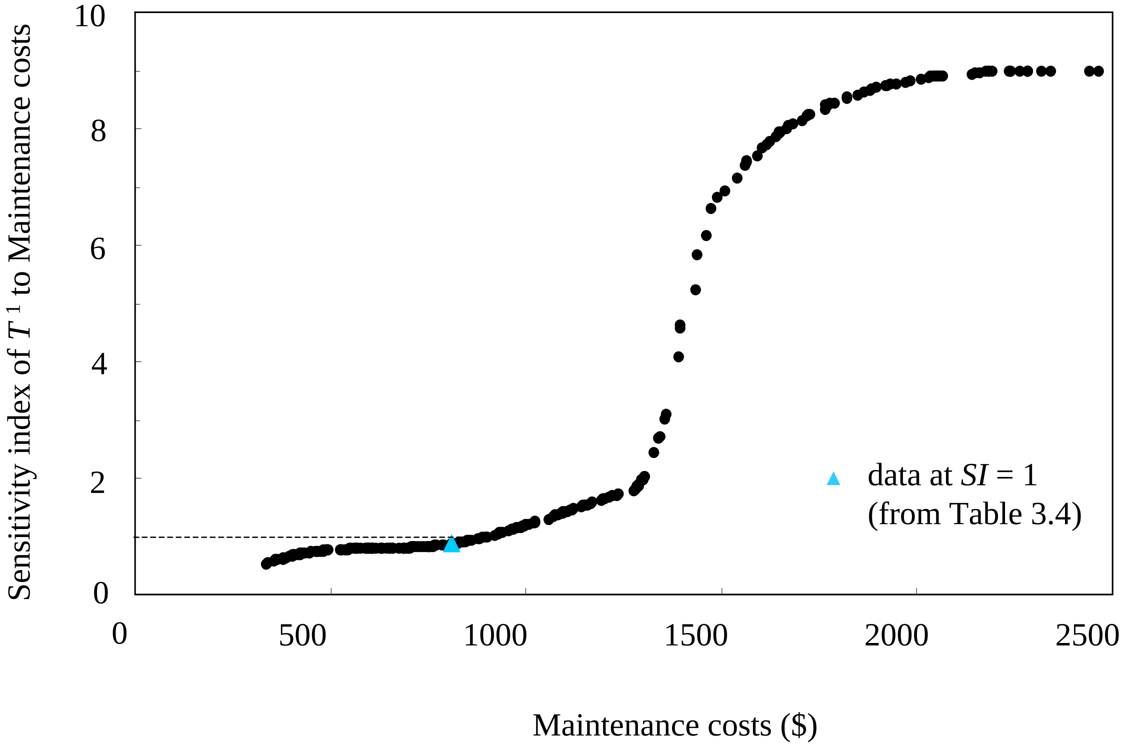

Fig 3.23. Sensitivity index for T^1 to maintenance costs – maintenance costs plot

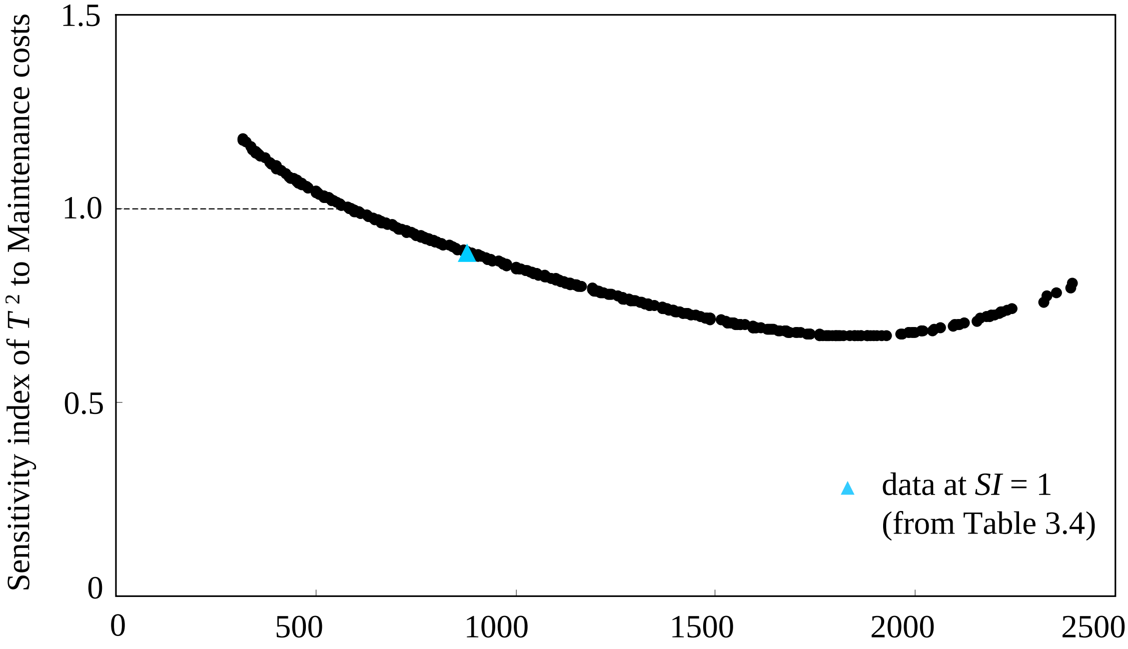

Fig 3.24. Sensitivity index for T^2 to maintenance costs – maintenance costs plot

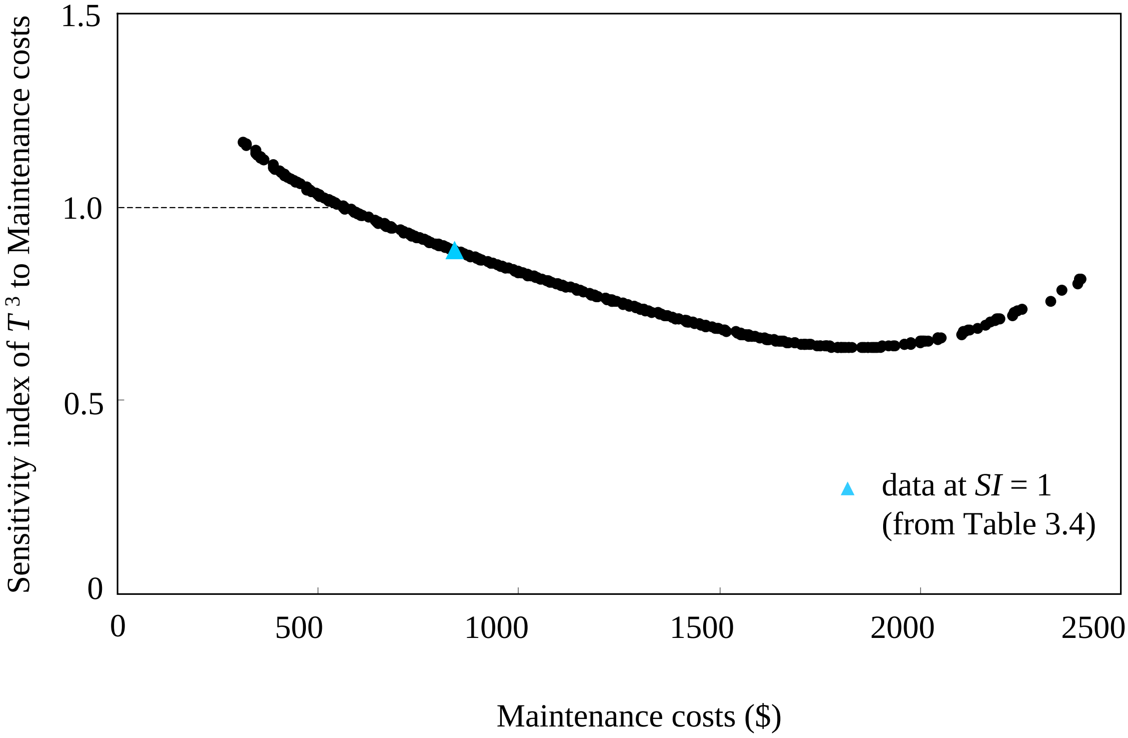

Fig 3.25. Sensitivity index for T^3 to maintenance costs – maintenance costs plot

The results from Fig.3.20-Fig.3.25 show that the decision-making point at SI = 1 from Table 3.4 (sensitivity variation in one objective value to a variation in the other objective function value) also shows the low values in sensitivity for decision variables to the objective function values. Because it has the sensitivity index values < 1 (sensitivity index of decision variables to the objective function values) for almost of all.

However, when considering the sensitivity of each decision variable to each objective function, the results of Fig.3.20 - Fig.3.22 show that it is generally the same for the effect of sensitivity of each decision variable to unavailability (because the sensitivity values for all decision variables are around order of 0-2.5). But, the results of Fig.3.23 - Fig.3.25 show that the effect of sensitivity of T^1 to maintenance costs is greater than T^2 and T^3 (because the sensitivity values for T^1 are around order of 0-10, while the sensitivity values for T^2 and T^3 are around order of only 0-1.5).

When considering the solutions from the perspective of all decision variables, in the part of Pareto-optimal curve that is high in sensitivity of decision variables to the determined objective function, that determined objective function values are also rapidly changed. Therefore, in that part, there is the tendency for the graph plotted between objective functions (Graph unavailability-maintenance costs plot) to have the high sensitivity of the other objective to that determined objective. And, there is the tendency that the part of Pareto-optimal solutions that is low in sensitivity for both objective functions is also low in sensitivity of decision variables to all objective functions, this idea is shown in Fig.3.26.

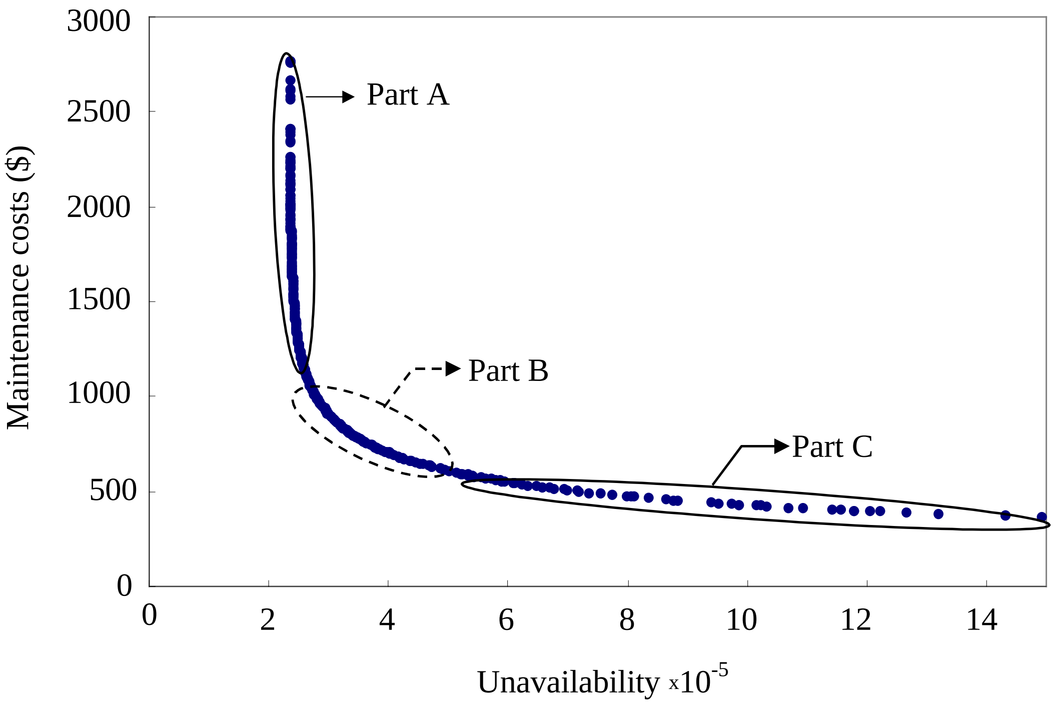

Fig 3.26. Part of sensitivity of decision variables to the objective functions

From Fig.3.26, if consider the sensitivity of variation in one objective function values to the other, part A and part C is high in sensitivity of variation of either objective to the other. While, part B is low in sensitivity for both objectives.

For part A in Fig.3.26, if consider the sensitivity of decision variables to objective function, the effect of sensitivity of decision variables to maintenance costs is higher than the sensitivity of decision variables to unavailability. The sensitivity of decision variables to maintenance costs is decreased from part A to part C. For part C, it is contrast that the effect of sensitivity of decision variables to unavailability is higher than the sensitivity of decision variables to maintenance costs. Consequently, the Pareto-optimal solutions in part B are low in sensitivity of decision variables to both objective functions.

Therefore, from the above discussions, the determination of the sensitivity of variation in one objective value to a variation in the other objective function value, as described in section 3.2, shows that it is sufficiently to represent the sensitivity in the viewpoint of robustness of sensitivity.

3.9 Concluding remarks

In this chapter, the multi-optimization method has been performed to optimize maintenance activities in a nuclear power plant's HPIS in order to solve the trade-off problem between unavailability and maintenance cost.

After considering of the problems that may occur in the global criteria method for the Pareto-optimal solution, the new index of sensitivity index with consideration of the robustness of sensitivity is proposed. The general methodology for compromising decision-making point between the *SI* and the conventional method is shown according to the user's requirement. The promising solution obtained using the proposed methodology was compared with that obtained by the conventional method, and it was confirmed that the proposed methodology defines an optimal solution with low sensitivity.

The sensitivity index for determination of the sensitivity of variation in one objective value to a variation in the other objective function value is shown that it is appropriate for expressing the robustness of the solution in the viewpoint of robustness of sensitivity, because the sensitivity of decision variable to the objective values at the obtained decision-making point is also confirmed sufficiently robust.

Chapter 4

Decision making for the multi-objective optimization framework in the viewpoint of uncertainty

4.1 Introduction and problems in the conventional method

In the maintenance activities of a nuclear power plant, the objective usually involves more than one factor regarding, including low levels of system unavailability and low costs in maintenance activities. In order to optimize these conflicting objectives, the multi-objective optimization is usually applied. Nevertheless, maintenance activities typically involve significant uncertainties such as those involving downtime and costs of maintenance. Therefore, some regions in the Pareto-optimal solutions may have the properties that are inappropriate due to the large scatter of the solutions or due to the lack of robustness of sensitivity. Thus, attention should increasingly be focused on a robust solution.

Unfortunately, the concept of the conventional method [27] for determining the most promising solution from the Pareto-optimal solutions that was explained in chapter 2 might show insufficient robustness. Therefore, a methodology for selecting an appropriate solution with acceptable robustness is required.

In this chapter, new indexes and methodology for the decision-making process in the multi-objective optimization framework under uncertainty are proposed according to user's requirement. In considering robustness, evaluation of the scattering of solutions and a sensitivity analysis are also important. Thus, the robustness considered in the research includes the sensitivity of a variation in one objective value to a variation in the other objective function value, and the uncertainty intrinsic to each parameter.

For considering the sensitivity of one objective value in relation to another objective value, the sensitivity index (*SI*), which has already been proposed in Chapter 3, is used. In addition, for considering the uncertainty intrinsic to each parameter, the decision-making process using a newly developed uncertainty index (*UI*) and decision index (*DI*) is formulated in this Chapter.

4.2 The proposed methodology

The proposed methodology to assist in decision-making so as to determine the most promising solution from the multi-objective optimization framework under uncertainty is illustrated in Fig. 4.1.

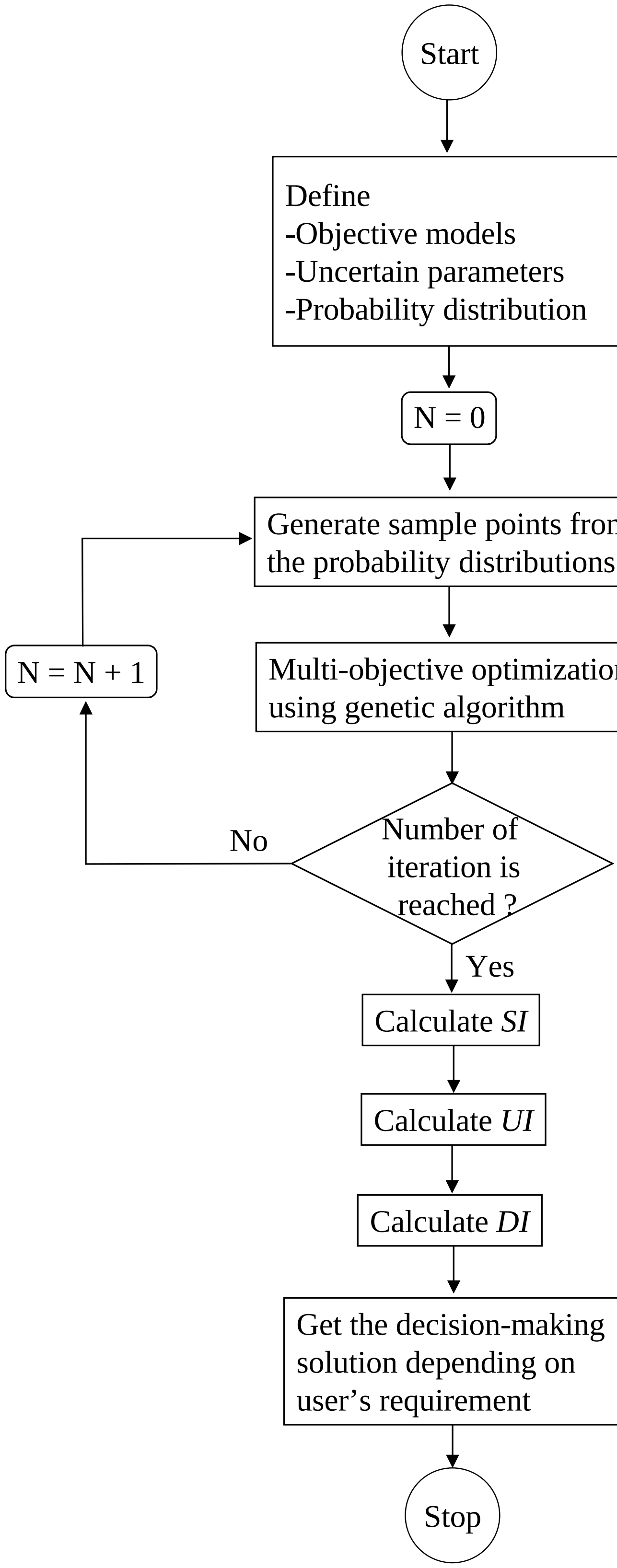

Fig. 4.1. Process of the proposed methodology

The process starts with defining the multi-objective optimization functions and uncertain parameters, and specifying the probability distribution. The simultaneous objectives that are considered in this research are the system unavailability and maintenance costs. In this problem, it is assumed that down time and maintenance costs have uncertainties. These parameters are expressed in terms of probability distribution functions. The distribution type of each uncertain parameter is assumed to follow a normal distribution. The Monte-Carlo [42,53] sampling technique is then utilized to generate sample points from the probability distributions, and the multi-objective optimization is performed in each iteration. After the specified number of Monte-Carlo iterations is reached, a variety of non-dominated sets are obtained.

Thereafter, the robustness is investigated from three viewpoints as follows.

(1) When the main target is to diminish the sensitivity of one objective with respect to another objective, the sensitivity index(*SI*), which is described in chapter 3, is effective.

(2) If the target is to diminish the deviation around the mean value for both objective values, the uncertainty index (*UI*) is more appropriate than *SI*.

(3) Finally, if diminishing not only the sensitivity but also the deviation is to be considered, the decision index (*DI*) is appropriate.

Detailed definitions of these indexes are given in the next subsection.

4.3 Definition of indexes

4.3.1 Uncertainty index (*UI*)

The uncertainty index (*UI*) is defined by the following equation,

$$UI = \left[(\%\text{COV } of \ F_k)^2 + (\%\text{COV } of \ F_j)^2 \right]^{1/2}, \tag{4.1}$$

where %COV is the percentage of the coefficient of variation [53] = $\sigma/\mu \cdot 100$.
While σ is standard deviation and μ is the mean value.

The uncertainty will be minimized when the %COV of objective function F_k and the %COV of the objective function F_j are in close proximity to the origin of the graph of relation between the %COV of each objective. Therefore, the closest position from the origin will be the point with the lowest uncertainty, as illustrated in Fig. 4.2. *UI* calculated by Eq.(4.1) shows the distance from the origin. Thus, the minimum value of *UI* gives the solution with the lowest uncertainty for all objectives.

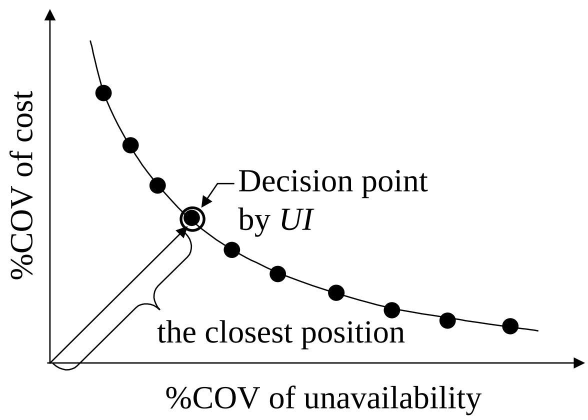

Fig. 4.2. The idea of the uncertainty index (*UI*)

4.3.2 Decision index (*DI*)

The Decision index (*DI*) is defined as

$$DI = \left[(\text{Normalized}\, UI)^2 + (\text{Normalized}\, |SI - 1|)^2 \right]^{1/2}. \quad (4.2)$$

The general idea of *DI* is to consider together both the robustness of sensitivity and the robustness of uncertainty, the parameters of *UI* and *SI* (*SI* is described in chapter 3) are then considered simultaneously. The concept of *DI* is that in view of robustness, the ideal point (*UI*, |*SI*-1|) is (0.0, 0.0). If (*UI*, |*SI*-1|) is mapped into the normalized space, the closest position from the origin will be the point with the most robustness.

In order to make both *UI* and |*SI*-1| carry equal weight, both index values should be normalized such that they fall in the range of 0~1. The region to be normalized will then be the intersection of the acceptable ranges of *UI* and *SI*. The acceptable ranges of *SI* and *UI* are flexible according to the demand of the user. The normalization is performed as

$$I_{in}(x) = \frac{I_i(x) - I_i(x)_{\min}}{I_i(x)_{\max} - I_i(x)_{\min}}, \quad (4.3)$$

$I_{in}(x)$ in Eq.(4.3) is the normalized value for each index. I_i(x) is the index value to be normalized. $I_i(x)_{\min}$ and $I_i(x)_{\max}$ are the minimum and maximum values of $I_i(x)$ in the acceptable range, respectively.

After normalizing *UI* and |*SI*-1| using Eq.(4.3), the distance from the origin of each normalized index value is given by *DI*, as shown in Fig. 4.3. Therefore, the minimum value of *DI* gives the most appropriate solution with a positive compromise regarding both sensitivity and uncertainty.

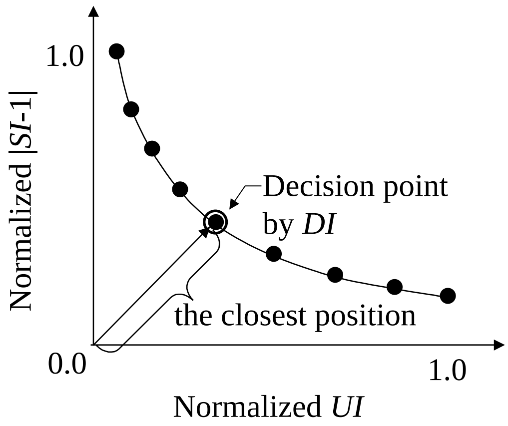

Fig. 4.3. The idea of the decision index (*DI*)

4.4 Procedure to determine the decision-making point in some conditions.

As discuss in section 3.3(6) of chapter 3, in some conditions, the multi-objective optimizations are the constrained problems. With constraints, a part of the original Pareto-optimal region is not feasible and a new Pareto-optimal region emerges as shown in Fig.3.4 of chapter 3. The Pareto-optimal fronts of constrained multi-objective optimization are more complicated. Moreover, in some regions, the sensitivities of a variation in one objective value to a variation in the other of the Pareto-optimal solutions are almost constant.

The following conditions are the conditions that may be occurred in the constrained multi-objective optimizations. The procedures for decision-making proposed in this chapter for applying to these cases are determined as follows.

(1) When entirely of the feasible Pareto-optimal solutions have the almost constant *SI* and *UI* value. The example of this case is shown in Fig.4.4. For this case, because significant of sensitivity and uncertainty for each point on the Pareto-optimal curve are

almost same, thus the decision making point (point D in Fig. 4.4) should be the point that is closest to the ideal point (point Z^*). And *DI* for this case is not necessary evaluated.

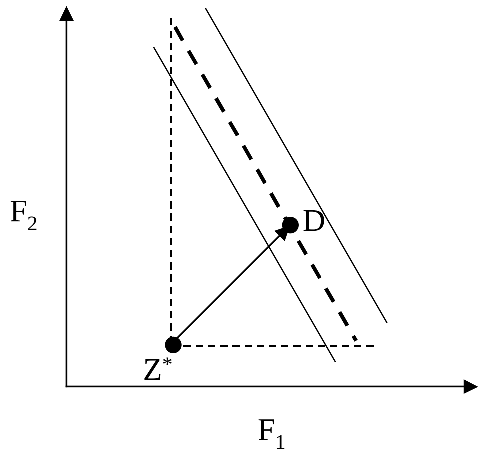

Fig.4.4 Decision making for the Pareto-optimal solutions that *SI* and *UI* values are almost constant.

(2) When *SI* values of entirely of the feasible Pareto-optimal solutions are almost constant, but *UI* values are rather changed, such as shown in Fig. 4.5, the decision making point (point D) should be determined by *UI* method. And *DI* for this case is also not necessary evaluated.

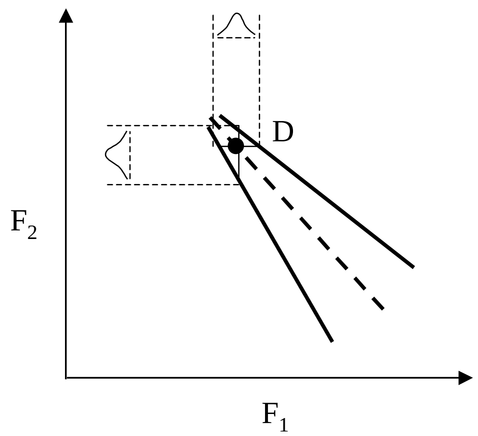

Fig.4.5 When *SI* values of entirely of the feasible Pareto-optimal solutions are almost constant, but *UI* values are rather changed

(3) When entirely of the feasible Pareto-optimal solutions not have the *SI* = 1 point, such as shown in Fig. 4.6, the decision making point should be determined by *UI* method.

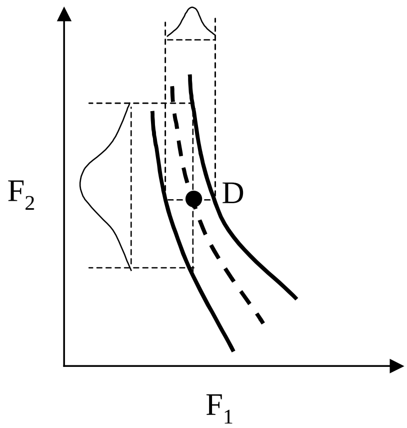

Fig.4.6 Decision making when the Pareto-optimal solutions not have the *SI* = 1 point.

(4) When there is the point whose *SI* value is suddenly changed on the feasible Pareto-optimal curve. The examples of this case are shown in Fig.4.7-a, Fig.4.7-b

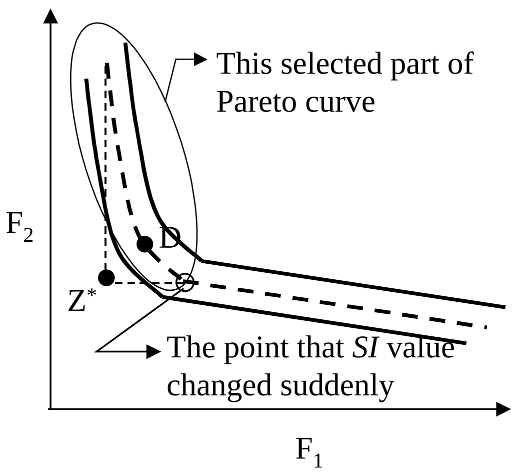

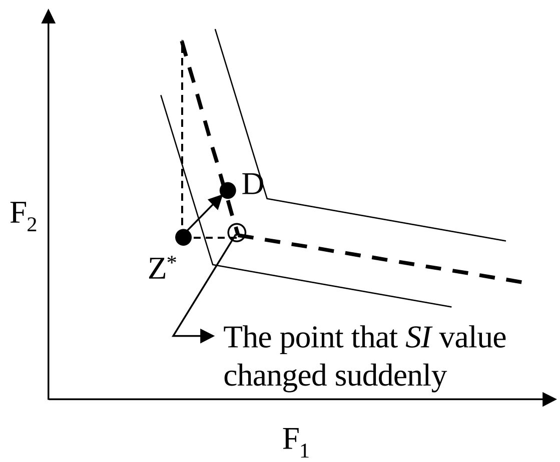

Fig.4.7-a Fig.4.7-b

Fig.4.7 Decision making for the Pareto-optimal solutions when there is the point whose *SI* value is suddenly changed.

For these cases, first, the *UI* and *SI* of each solution on the Pareto-optimal solutions are evaluated. After that, determine the point whose *SI* value is suddenly changed, while this point is non-robust and should not be selected. Thereafter, divide the Pareto-optimal curve into many parts from the *SI* point that is suddenly changed.

After that, select the part of the Pareto-optimal curve for determining the decision-making point. If the sensitivity is considered more important, the select the part of the Pareto-optimal curve is the part that has the point whose *SI* value is closest to 1.0. The decision-making point is the point whose *SI* value is closest to 1.0, or the point that has the smallest *DI* value. By the way, if these decision-making points by *SI* or *DI* are located close to the non-robust point whose *SI* value is suddenly changed, the decision-making point should then be the point closest to the ideal point (point Z^* illustrated in Fig.4.7-a) of the selected part of the Pareto-optimal curve.

If the uncertainty is considered more important, the select the part of the Pareto-optimal curve is the part that has the smallest value of *UI*. The point of smallest *UI* or *DI* is determined to be the decision-making point depending on user's requirement. Nevertheless, the point whose *SI* value is suddenly changed is non-robust and should not be selected. Therefore, in the case that the decision-making point by *UI* is located close to this non-robust point, the decision-making point should be the decision-making point by *DI*. However, if the decision-making point by *DI* is also located close to this non-robust point, the decision-making point should be the point closest to the ideal point (point Z^* illustrated in Fig.4.7-a) of the selected part of the Pareto-optimal curve.

However, for the case in Fig.4.7-b, which the *UI* and *SI* values are almost constant in the select part, the decision-making point is then the point closest to the ideal point (point Z^* illustrated in Fig.4.7-b) of the selected part of the Pareto-optimal curve. And, the *DI* in the case of Fig.4.7-b is also not necessary evaluated.

4.5 Results and Discussions

In order to assure the effectiveness of the proposed methodology and indexes of decision making for the multi-objective optimization framework under uncertainty in this chapter, the case study of HPIS explained in section 3.4 of chapter 3 is applied. The HPIS is shown again here as the Fig. 4.8 for the sake of simplicity.

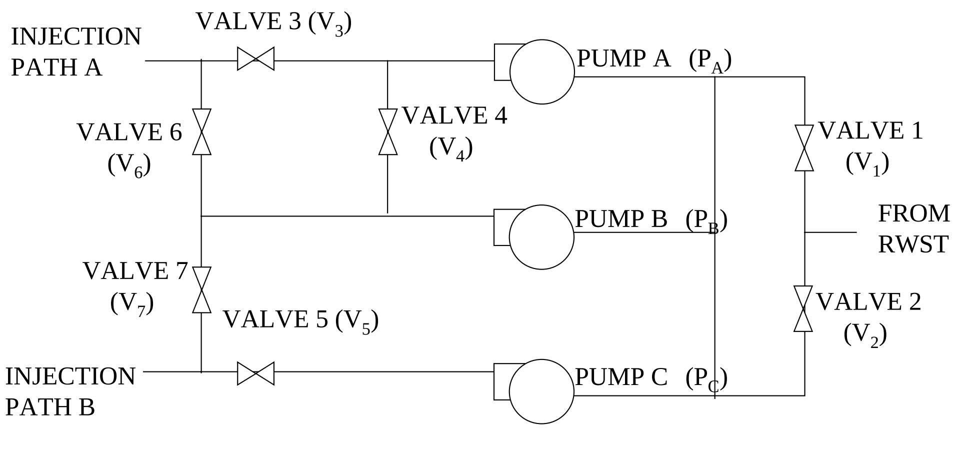

Fig. 4.8 HPIS system [33].

The process of the proposed methodology of decision making for the multi-objective optimization framework under uncertainty starts with defining the multi-objective optimization functions and uncertain parameters, and specifying the probability distribution.

The considered objective functions of this study are the system unavailability and maintenance cost. The component unavailability and cost parameters shown in Table 3.1 of chapter 3 are used in the derivation of the objective functions. In this problem, it is assumed that down time and maintenance costs have uncertainties. These parameters are expressed in terms of probability distribution functions. The distribution type of each uncertain parameter is assumed to follow a normal distribution. Then, the downtime parameters t and d and the maintenance cost parameters C_{ht} and C_{hc} in Table 3.1 of chapter 3 are the mean values.

To investigate the effectiveness of the methodology, the three cases of uncertainty shown in Table 4.1 are examined.

Table 4.1. The investigated cases.

Case	Maintenance cost parameters (C_{ht}, C_{hc})	Unavailability parameters (t, d)
	% COV	% COV
Case1	10%	1%
Case2	1%	10%
Case3	10%	10%

Then, in order to optimize the surveillance test program in the maintenance activities of this HPIS system, we assume that the system components have been classified into two surveillance test interval groups; each group will be tested in the same interval, as shown in Table 4.2. The symbols in Table 4.2 are shown in Fig. 4.8.

Table 4.2. Groups of test intervals.

T^1	V_1, V_2, P_A, P_B, P_C
T^2	V_3, V_4 , V_5, V_6, V_7

Test intervals for each group are constrained as the follows:

$T^1 \leq 8760\ h$

$T^2 = k_1 \cdot T^1 \quad while \quad 1 \leq k_1 \leq 10$

Consequently, the maintenance activities optimization of this system has decision variables set, x, as shown in Eq.(4.4)

$$x = \{T^1, k_1\} \tag{4.4}$$

After the objective functions of the unavailability function and cost function are derived as explained in the chapter 3 by using the related component unavailability and cost data of maintaining the system that are shown in table 3.1 of chapter 3, the multi-objective optimization is applied by using the parameters shown in table 4.3 with Monte-Carlo iteration of 5000 times to get the non-dominated sets of Pareto-optimal solutions.

Table 4.3. Parameters used in the multi-objective optimization

Parameters	Values
Encoding mechanism	Real-parameter
Population size	200
Generation numbers	20
Crossover probability	0.6
Mutation probability	0.01
Monte-Carlo iteration number	5,000

The results of the variety of non-dominated sets of Pareto-optimal solutions for case 1 to case 3 for minimizing both unavailability and maintenance costs are shown in Fig. 4.9-a, Fig. 4.10-a and Fig 4.11-a respectively. Thereafter, the graph of % COV of costs and % COV of unavailability plotted for each point of mean value of the Pareto-optimal solutions for case 1 to case 3 is shown in Fig.4.9-b, Fig.4.10-b and Fig.4.11-b respectively.

The following points shown in Fig.4.9-4.11 are defined as follows.

Point B represents the decision making point by *UI* method.

Point C represents the decision making point by *DI* method.

Point D represents the decision making point by *SI* method.

Point E represents the decision making point by conventional method.

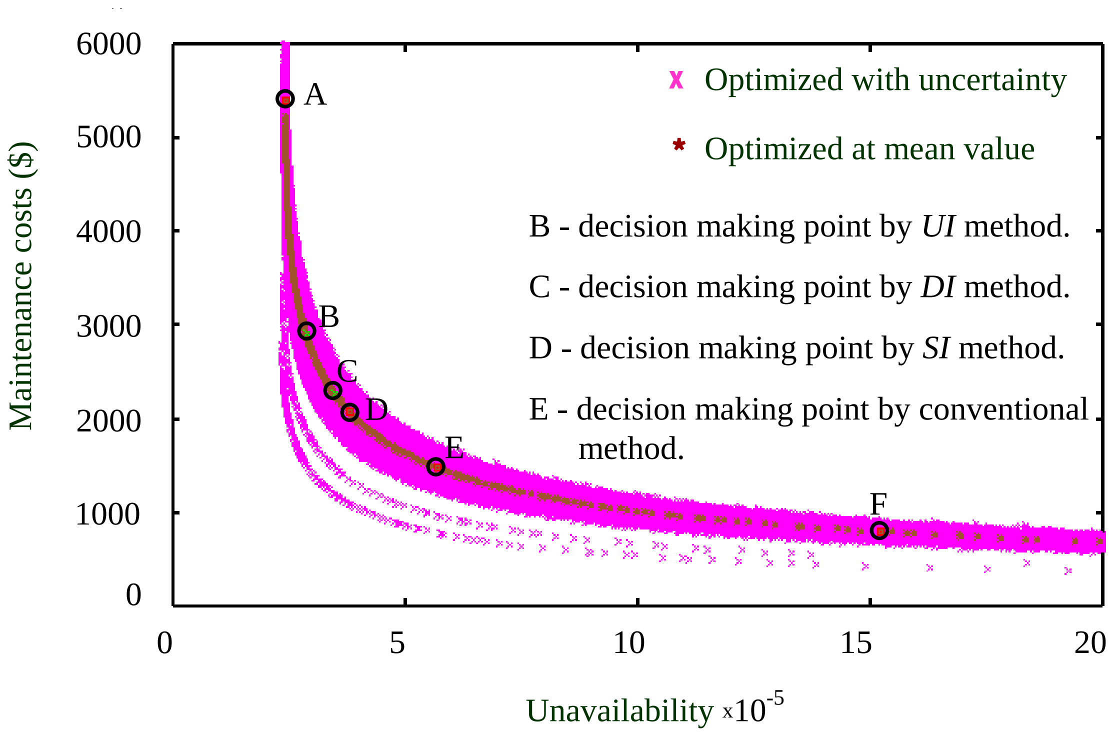

Fig.4.9-a. The variety of non-dominated sets of Pareto-optimal solutions for the investigated case 1.

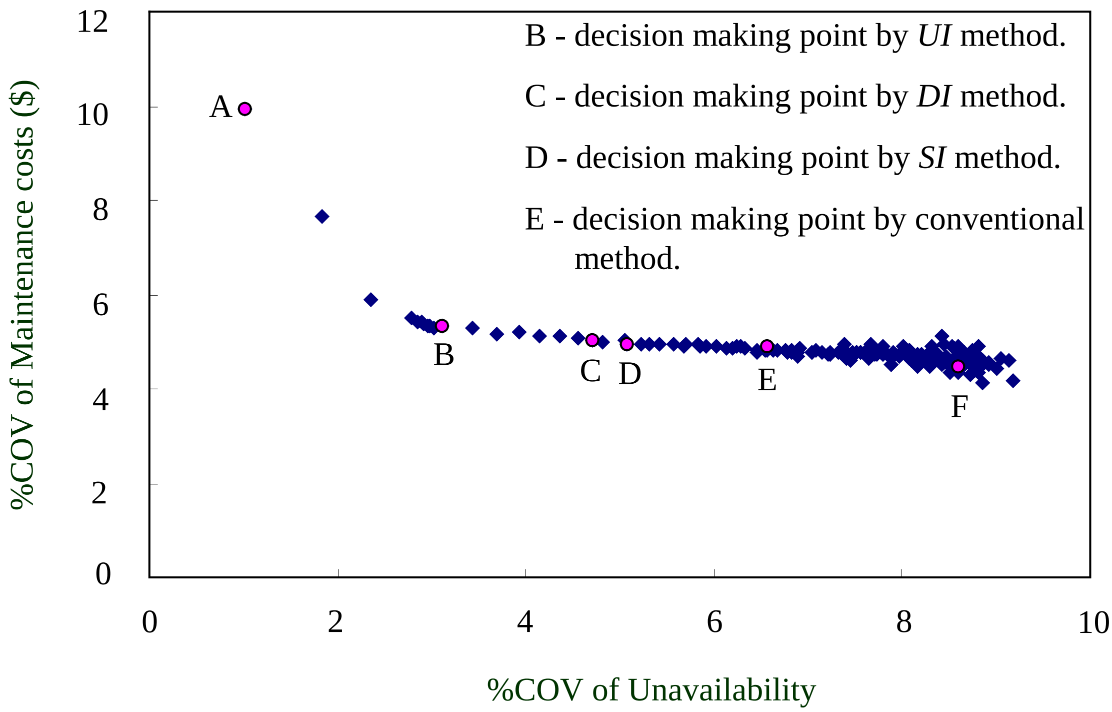

Fig.4.9-b. % COV of maintenance costs - % COV of unavailability plot for each point of the Pareto-optimal solutions for the investigated case 1.

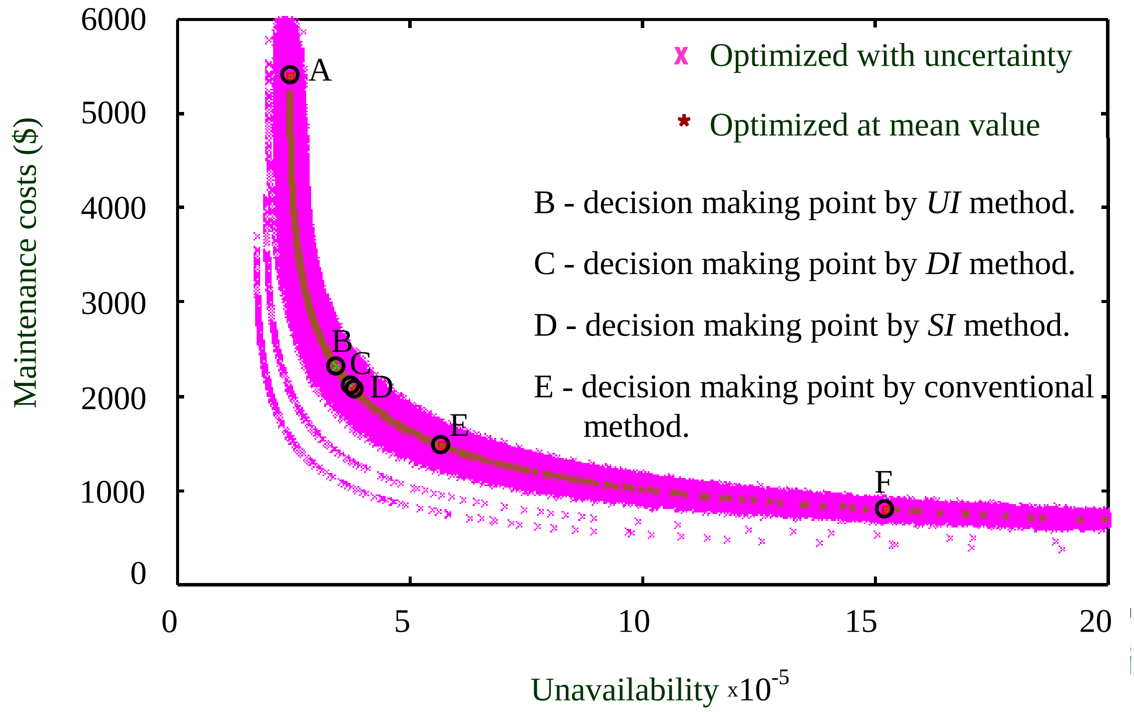

Fig. 4.10-a. The variety of non-dominated sets of Pareto-optimal solutions for the investigated case 2.

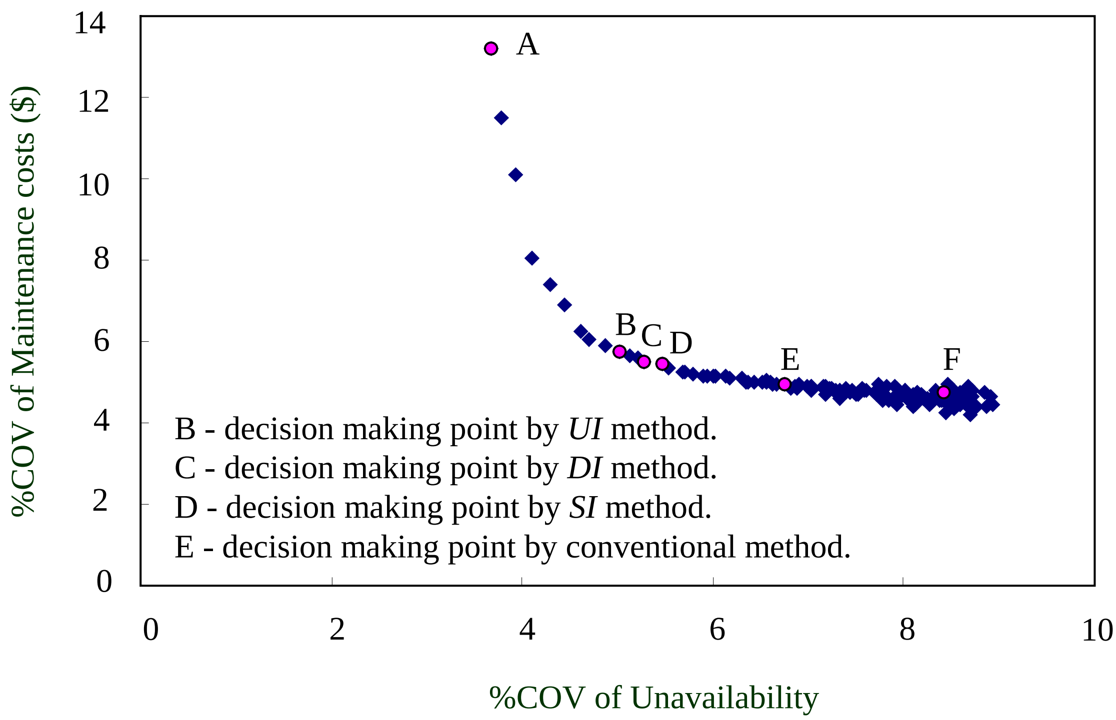

Fig.4.10-b. % COV of maintenance costs - % COV of unavailability plot for each point of the Pareto-optimal solutions for the investigated case 2.

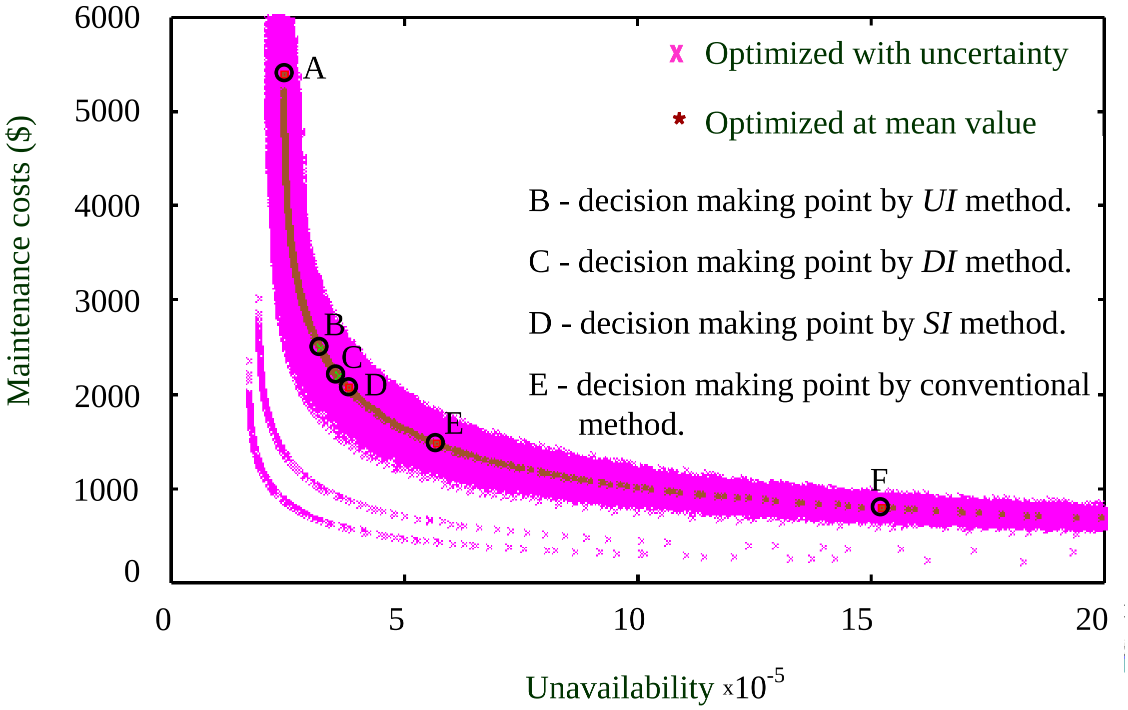

Fig. 4.11-a. The variety of non-dominated sets of Pareto-optimal solutions for the investigated case 3.

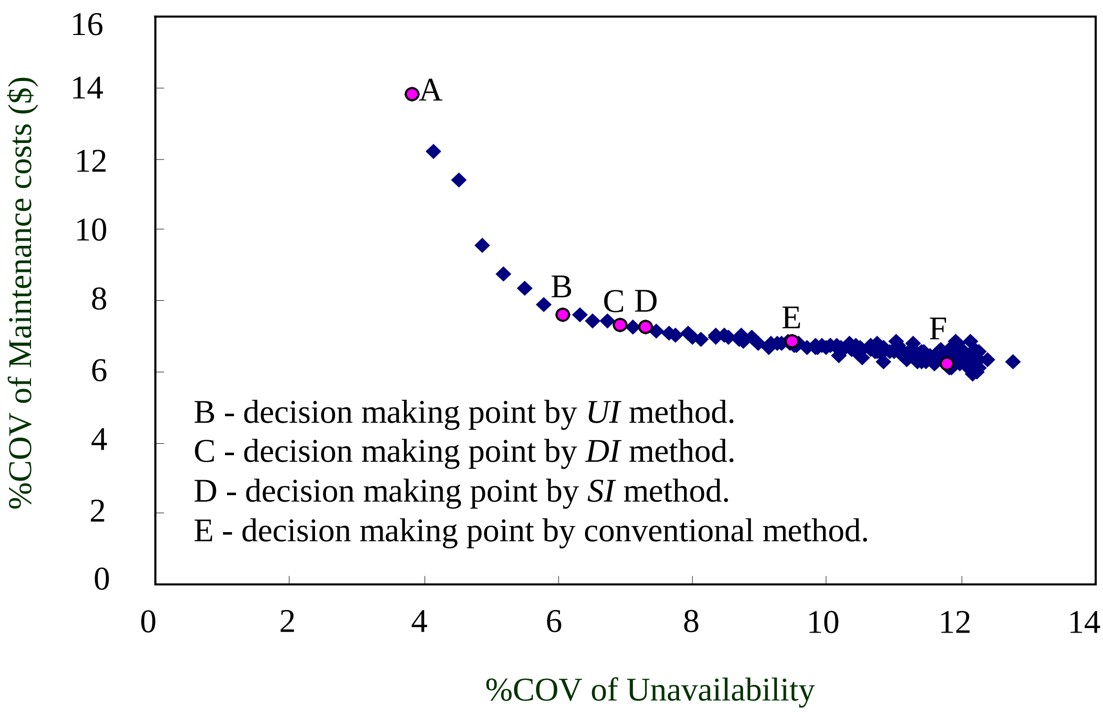

Fig.4.11-b. % COV of maintenance costs - % COV of unavailability plot for each point of the Pareto-optimal solutions for the investigated case 3.

The solutions in Fig. 4.9-4.11 suggest that the solutions around points A and F are not appropriate for carrying out the maintenance activities because there are high sensitivities of variation in one objective function value in relation to variation in the other. Moreover, there are high uncertainties in either objective around these points. To clarify the characteristics of robustness around these points by numerical values, the results data around points A, D, and F are summarized in Table 4.4.

Table 4.4. The objective mean values of the Pareto-optimal solutions with the corresponding %COV of each objective around points A, D, and F

Sol$^{\underline{n}}$ around point	Objective mean values		Case1		Case2		Case3	
	Unavail-ability	Cost	%COV of unavail-ability	%COV of cost	%COV of unavail-ability	%COV of cost	%COV of unavail-ability	%COV of cost
A	2.43E-5	5408	2.47	7.56	3.44	16.14	4.03	15.33
	2.53E-5	3862	2.74	7.13	3.65	13.27	4.38	13.46
D	3.79E-5	2082	5.06	5.04	5.46	5.43	7.31	7.25
	3.89E-5	2027	5.09	5.02	5.52	5.31	7.40	7.17
F	1.52E-4	799	8.51	4.63	8.44	4.60	11.81	6.42
	1.73E-4	744	8.67	4.56	8.57	4.55	12.03	6.36

Let us consider the characteristic of robustness. First, the robustness of sensitivity is determined around each point from Table 4.4 as follows.

Around point A: Around the unavailability value of 2.43E-5, the small difference in the unavailability value of only 1.E-6 causes the maintenance cost optimization value to have a large variation of $1546 ($5408-$3862). Thus, there are high sensitivities of unavailability value in relation to cost value around this point. In contrast, there are low sensitivities of cost value in relation to unavailability value around this point.

On the other hand, around point F: A slight variation of only $55 ($799-$744) in the maintenance costs causes the large difference in unavailability optimization value up to 2.1×10^{-5} (1.73E-4-1.52E-4). This means that there are high sensitivities of cost value in relation to unavailability value around this point. Nevertheless, there are low sensitivities of unavailability value in relation to cost value around this point.

However, around point D: Around the unavailability values of 3.79E-5, a small difference in the unavailability value of only 1.E-6 causes the maintenance cost optimization value to have a small variation of only $55 ($2082-$2027). Thus, in this zone, there are low sensitivities for all of objectives.

Additionally, data in Table 4.4 and Fig.4.9-4.11 also show the high %COV of costs around the point A. And there is a high %COV of unavailability around the point F. Thus, there are high uncertainties for either objective at these points. The point B in Fig.4.9-b, Fig.4.10-b and Fig.4.11-b show the point that is closest to origin of the graph of % COV of costs and % COV of unavailability plotted (at each point of the mean value of the Pareto-optimal solutions). Therefore, the point B is the points that have the lowest uncertainty for all objectives (this is the idea of the *UI* that is described in section 4.3.1).

From Figs.4.9-4.11, we can also see that the robustness in view of sensitivity and uncertainty vary in each region of the Pareto-optimal solutions and are depend on each case. Therefore, considering the decision-making solutions by using only the data at mean values of the Pareto-optimal solutions, such as the conventional method or using the sensitivity index, may not sufficient for being determined in the viewpoint of robustness of uncertainty.

Thus, a methodology for selecting an appropriate most promising solution from the multi-objective optimization framework under uncertainty is extremely important to the robustness of the system. Therefore we propose such a methodology in section 4.2.

To verify the suitability of the solutions by the proposed methodology, promising solutions for all cases obtained by the method of each proposed index (*UI*, *SI*, *DI*), the corresponding index value, and the %COV of each objective are shown in Table 4.5.

Table 4.5. The promising solutions obtained by each proposed index, the corresponding index value, and the %COV of each objective

Case	Solution by	Mean unavail-ability	Mean cost ($)	*SI* value	*UI* value	*DI* value	standard deviation of unavail-ability	%COV of unavail-ability	standard deviation of cost	%COV of cost
Case 1	*SI* method	3.79E-5	2082	1.00	7.14	0.40	1.92E-6	5.06	105	5.04
	UI method	2.87E-5	2916	0.63	6.10	0.74	8.68E-7	3.02	154	5.30
	DI method	3.49E-5	2267	0.93	6.82	0.31	1.59E-6	4.56	115	5.08
Case 2	Solution by	Mean unavail-ability	Mean cost ($)	*SI* value	*UI* value	*DI* value	standard deviation of unavail-ability	%COV of unavail-ability	standard deviation of cost	%COV of cost
	SI method	3.79E-5	2082	1.00	7.70	0.078	2.07E-6	5.46	113	5.43
	UI method	3.41E-5	2322	0.90	7.61	0.176	1.71E-6	5.01	133	5.73
	DI method	3.71E-5	2127	0.99	7.62	0.008	1.97E-6	5.29	117	5.49
Case 3	Solution by	Mean unavail-ability	Mean cost ($)	*SI* value	*UI* value	*DI* value	standard deviation of unavail-ability	%COV of unavail-ability	standard deviation of cost	%COV of cost
	SI method	3.79E-5	2082	1.00	10.30	0.24	2.77E-6	7.31	151	7.25
	UI method	3.20E-5	2502	0.81	9.74	0.38	1.94E-6	6.07	190	7.61
	DI method	3.59E-5	2205	0.96	10.10	0.15	2.48E-6	6.92	161	7.29

The solution by each method (*SI*, *UI*, and *DI* and method) shown in Table 4.5 is represented as point B (*SI* method), point C (*UI* method), point D (*DI* method) in Fig. 4.9 – Fig. 4.11. The results in Table 4.5 indicate that the proposed method described in section 4.2, represented by *SI*, *UI*, and *DI*, gives the robust solutions according to the analyst's demands.

For the decision-making in the viewpoint of robustness of sensitivity, the promising solution that is determined from *SI* is calculated from the mean values of the Pareto-optimal solutions. The unavailability value at $SI=1.0$ is located around point D of Table 4.4. Thus, it is confirmed that at $SI=1.0$ has low sensitivities for both objectives.

Furthermore, when considering the solutions from the perspective of both objective, the %COV of the promising solutions determined using *UI* for all cases are lower than the promising solutions determined by another index. Nevertheless, the solutions from Table 4.5 also show that the %COV of both objectives at the solutions determined by using *SI* in all cases are rather larger than the %COV values at the promising solutions determined from *UI*. In contrast, *SI* values at the promising solutions determined using *UI* are rather remote from the value of 1.0, particularly in case 1. These results indicate that, in most cases, the promising solution with the lowest deviation is not necessarily the solution to give the best sensitivity, or vice versa. Therefore, to achieve a compromise between sensitivity and uncertainty, the *DI* method is important. The acceptable range to calculate *DI* is the intersection of the acceptable range of *UI* and *SI*. In this paper, the range of $1/1.5 \leq SI \leq 1.5$ is used as the acceptable range for the robustness of sensitivity, i.e. the range in which the variation in one objective is not greater than 1.5 times the variation in the other. For the acceptable range of *UI*, the values are determined such that the %COV values of both objectives are less than 10%. As such, the promising solutions determined from *DI* in Table 4.5 indicate that both *SI* and *UI* values are appropriate for all 3 cases. Therefore, the *DI* method gives the best compromise solution between sensitivity and uncertainty.

Thus, the proposed methodology can be applied to determining the most promising solution from the Pareto-optimal solutions according to the user's requirements. If the robustness of sensitivity is considered to be most important, the sensitivity index is appropriate. In contrast, if the robustness of uncertainty is the most important, the uncertainty index is appropriate. However, if a promising solution with the positive compromise on both sensitivity and uncertainty is required, the decision index is appropriate.

Moreover, the index values at the solutions obtained by the proposed methodology are also compared with those by the conventional method. The promising solutions for all cases obtained by the conventional method, the corresponding index value, and the %COV of each objective are shown in Table 4.6.

The solution obtained by the conventional method in Table 4.6 shows that the *SI* values of this solution are far apart from the value of 1.0. In addition, the *UI* values of this solution are rather large. Therefore, the solution by the conventional method shows insufficient robustness. The proposed methodology can therefore provide more appropriate solutions than the conventional method when the attention is focused on the robustness.

Table 4.6 The promising solutions for all cases obtained by the conventional method, the corresponding index value, and the %COV of each objective

Case	Mean unavail-ability	Mean cost ($)	*SI*	*UI*	*DI*	standard deviation of unavail-ability	%COV of unavail-ability	standard deviation of cost	%COV of cost
Case 1	5.67E-5	1480	1.35	8.20	1.07	3.72E-6	6.56	73	4.92
Case 2	5.67E-5	1480	1.35	8.41	0.97	3.85E-6	6.79	74	4.97
Case 3	5.67E-5	1480	1.35	11.74	1.09	5.39E-6	9.51	102	6.89

4.6 Discussion for using COV in the uncertainty index

In this research, we use the coefficient of variation (COV) to represent the uncertainty of results because the coefficient of variation is non-dimensional. The idea of the uncertainty index in the Eq. (4.1) shows that without using the non-dimensional values, the uncertainty of one objective function may make the more large effect to the uncertainty index because of their large order in values. For example, suppose that we use standard deviation (σ) to represent the uncertainty of results. The order of standard deviation for unavailability is around 10E-5 ~ 10E-7. But the order of standard deviation for maintenance costs is around $10 ~ $1000. Therefore, if these large differences in the order of the standard deviation are applied to the uncertainty index in Eq. (4.1), the effect of uncertainty in unavailability will not have any meaning in the calculation. Therefore, in order to solve this difference in order of the dimensional, the non-dimensional parameter COV is chosen for uncertainty index.

However, because COV = σ/μ, therefore the problem will occur when the mean value (μ) is equal to zero. But, for the optimization of surveillance test in this research, if unavailability = zero this means that the failure will not occur, which is the impossible condition. In addition, it is also impossible that the maintenance costs = zero. Therefore using COV is applicable for the surveillance test optimal problem.

By the way, COV is the measure of relative dispersion from its mean value. If the user pays attention to the dispersion without relation to mean value, another non-dimensional uncertainty values are required. In order to make non-dimensional uncertainty values without relation to mean value, the standard deviation of each objective function is divided by some fixed values for the entirely of the Pareto-optimal solutions. These fixed values for both objective functions should have the same significant of uncertainty. At the solution whose COV values of both objective functions are equal, their significant of uncertainties are assumed approximately equivalent. Therefore, the standard deviations at the point that the COV of both objective functions are equal are determined as the representation of fix value to make uncertainty values being non-dimensional without relation to mean value as the following equations.

$$\text{Non}-\text{dimentional uncertainty for unavailability} = \frac{\sigma_{unavailability}}{\text{Representative of } \sigma_{unavailability}} \qquad (4.5)$$

$$\text{Non}-\text{dimentional uncertainty for costs} = \frac{\sigma_{Costs}}{\text{Representative of } \sigma_{Costs}} \qquad (4.6)$$

While, representative of $\sigma_{unavailability}$ is the standard deviation of unavailability at COV of unavailability equal to COV of costs.

Representative of σ_{costs} is the standard deviation of costs at COV of unavailability equal to COV of costs.

The results of decision-making point for case1 to case3 obtained by the uncertainty indexes (*UI*) using the non-dominated terms in Eq.(4.5) and Eq.(4.6) are shown in Fig.4.12-a, Fig 4.13-a and Fig.4.14-a, respectively. The results of decision-making point obtained by the uncertainty indexes (*UI*) using the COV are also compared in those figures.

Thereafter, the graph of standard deviation of costs and standard deviation of unavailability plotted for each point of the Pareto-optimal solutions for case 1 to case 3 are shown in Fig.4.12-b, Fig.4.13-b and Fig.4.14-c respectively.

The following points shown in Fig.4.12-4.14 are defined as follows.

Point B represents the decision making point by by *UI* method using the non-dominated terms of COV.

Point D represents the decision making point by *SI* method.

Point I represents the decision making point by *UI* method using the non-dominated terms in Eq.(4.5) and Eq.(4.6).

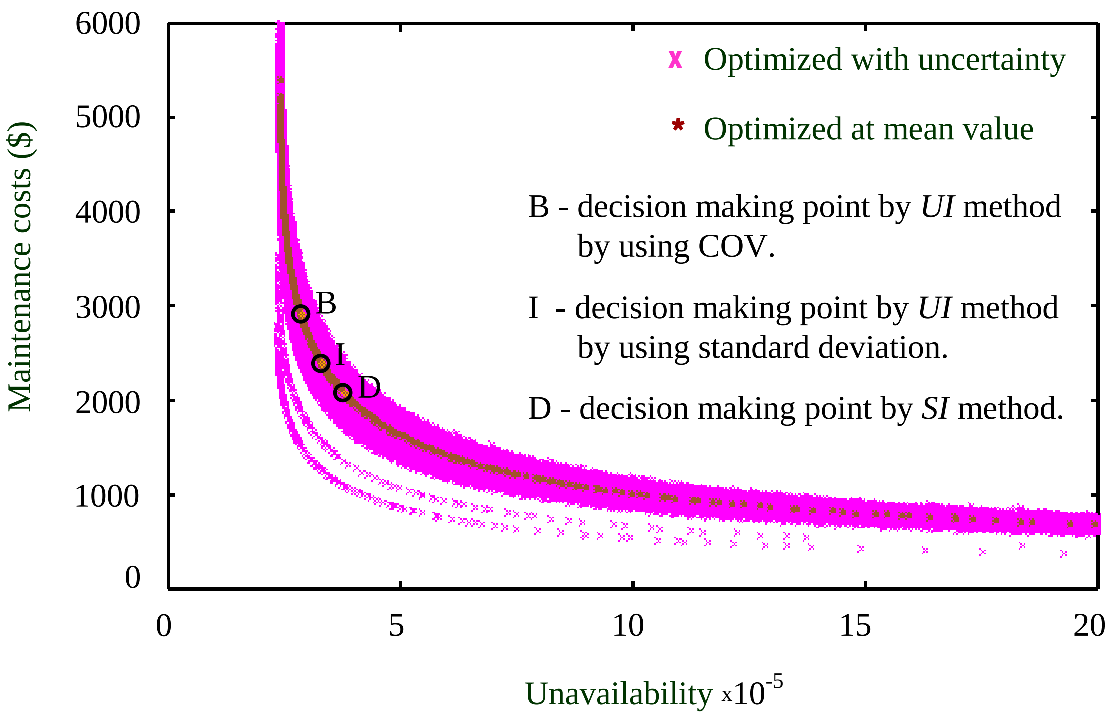

Fig. 4.12-a. The variety of non-dominated sets of Pareto-optimal solutions for the investigated case 1 and the decision making by each method.

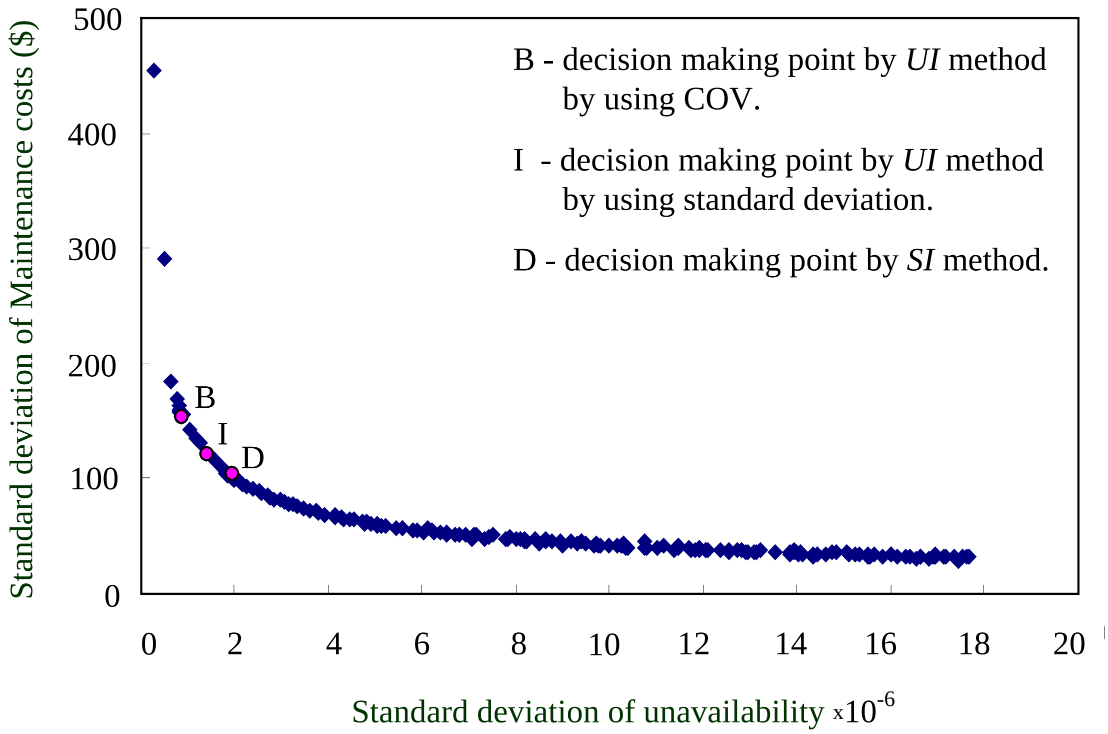

Fig.4.12-b.Standard deviation of maintenance costs-Standard deviation of unavailability plot for each point of the Pareto-optimal solutions for the investigated case 1

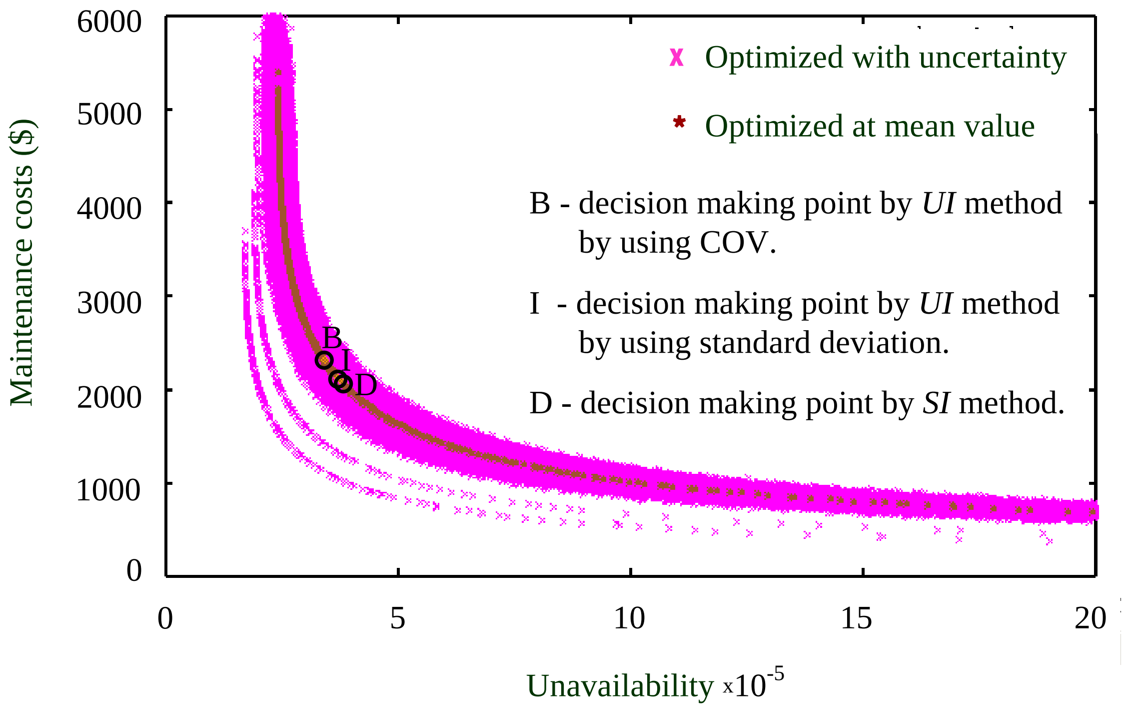

Fig. 4.13-a. The variety of non-dominated sets of Pareto-optimal solutions for the investigated case 2 and the decision making by each method.

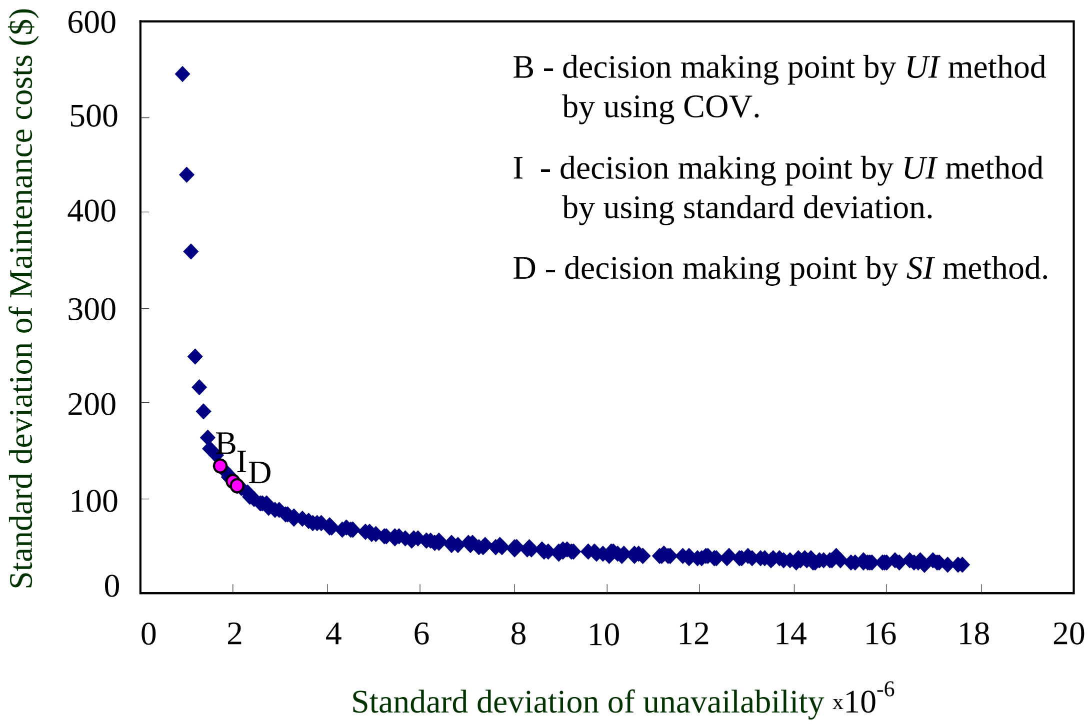

Fig.4.13-b.Standard deviation of maintenance costs-Standard deviation of unavailability plot for each point of the Pareto-optimal solutions for the investigated case 2.

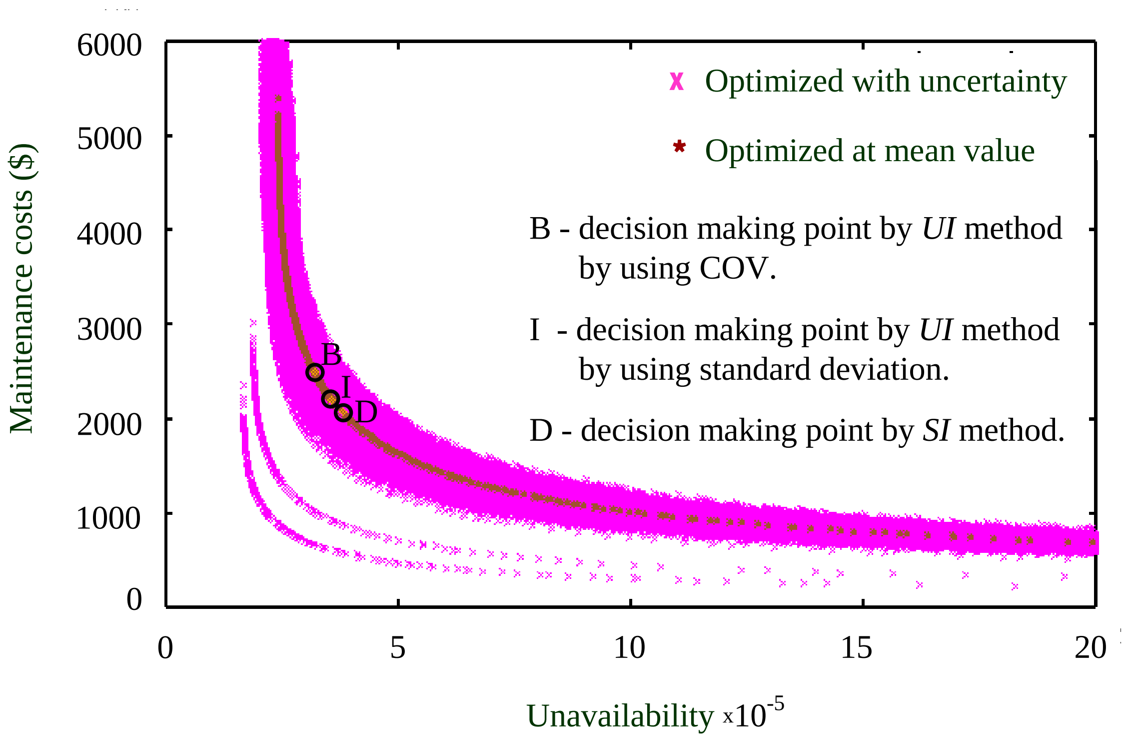

Fig. 4.14-a. The variety of non-dominated sets of Pareto-optimal solutions for the investigated case 3 and the decision making by each method.

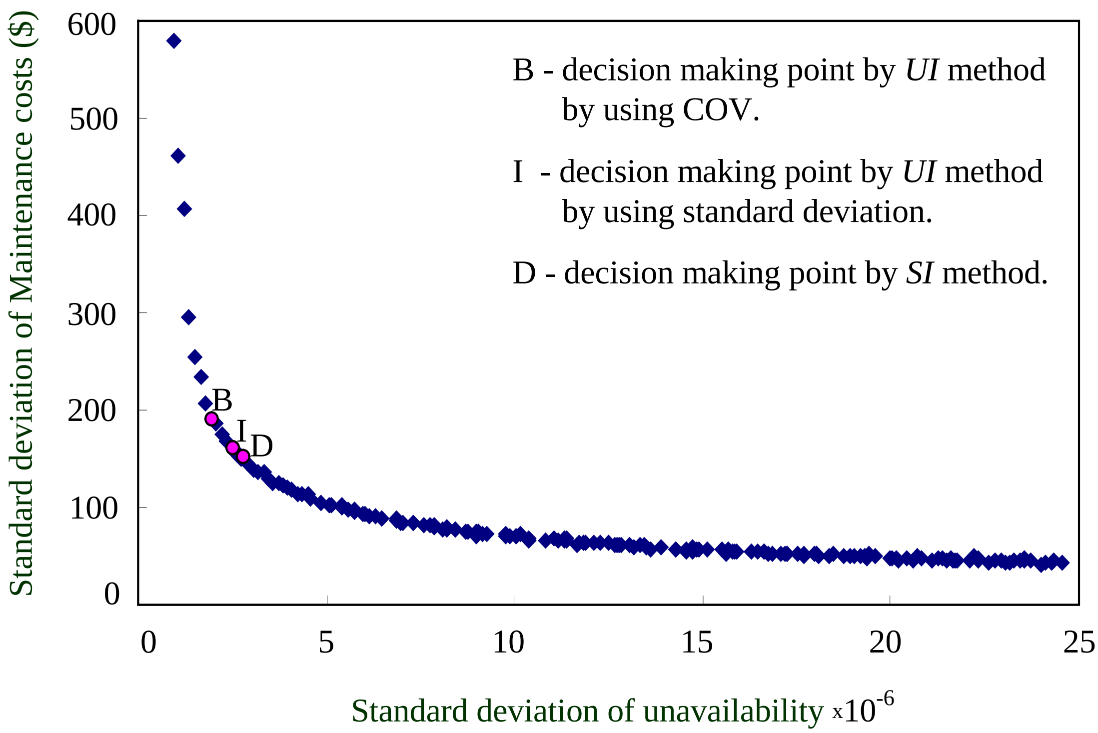

Fig.4.14-b.Standard deviation of maintenance costs-Standard deviation of unavailability plot for each point of the Pareto-optimal solutions for the investigated case 3.

The comparisons of the decision making point shown in Fig.4.12-Fig.4.14 are numerically shown in Table 4.7.

Table 4.7. The decision making point obtained by *UI* method using non-dominated terms in Eq.(4.5)-Eq.(4.6) compare with *UI* method using COV

	Solution by	Mean unavail-ability	Mean cost ($)	*SI* value	standard deviation of unavail-ability	%COV of unavail-ability	standard deviation of cost	%COV of cost
Case 1	*SI* method	3.79E-5	2082	1.00	1.92E-6	5.06	105	5.04
	UI method (using COV)	2.87E-5	2916	0.63	8.68E-7	3.02	154	5.30
	UI method (using standard deviation)	3.31E-5	2402	0.87	1.37E-6	4.15	123	5.12
Case 2	Solution by	Mean unavail-ability	Mean cost ($)	*SI* value	standard deviation of unavail-ability	%COV of unavail-ability	standard deviation of cost	%COV of cost
	SI method	3.79E-5	2082	1.00	2.07E-6	5.46	113	5.43
	UI method (using COV)	3.41E-5	2322	0.90	1.71E-6	5.01	133	5.73
	UI method (using standard deviation)	3.71E-5	2127	0.99	1.97E-6	5.29	117	5.49
Case 3	Solution by	Mean unavail-ability	Mean cost ($)	*SI* value	standard deviation of unavail-ability	%COV of unavail-ability	standard deviation of cost	%COV of cost
	SI method	3.79E-5	2082	1.00	2.77E-6	7.31	151	7.25
	UI method (using COV)	3.20E-5	2502	0.81	1.94E-6	6.07	190	7.61
	UI method (using standard deviation)	3.59E-5	2205	0.96	2.48E-6	6.92	161	7.29

For the results in Fig. 4.12 – Fig.4.14, point I is the decision making point using non-dominated termed in Eq.(4.5)-Eq.(4.6), which are non-dimensional uncertainty values without relation to mean value. And, point B is the decision-making point using COV.

With Recognize that the definition of COV is σ/μ, then there is the effect of the difference in mean values (μ) between each point of the Pareto-optimal solutions. Consequently, the results in Fig. 4.12 – Fig.4.14 and Table 4.7 are shown that the result at point B and point I are not same.

Thus, the non-dominated termed in Eq.(4.5)-Eq.(4.6) are also the another alternative when the user requires the non-dimensional uncertainty values without relation to mean value. However, if the analyst consider that relative dispersion from its mean value is also important, the non-dominated termed using COV in Eq.(4.1) is preferred. The example of the case that there is a significance of relative dispersion from its mean value, such as, the case that there is the same or little change in the standard deviation but the mean value are change rapidly; i.e., there is significant between a point that have $\mu = 1000$, $\sigma = 1$ and a point that have $\mu = 1$, $\sigma = 1$, etc.

4.7 Discussions for the conditions that the proposed methodology is effective.

In section 4.5 and 4.6, the results show that the proposed methodology can be applied to determining the most promising solution from the Pareto-optimal solutions according to the user's requirements. However, in some cases such as the investigated case2 and case3 shows that only *SI* proposed in chapter 3 is efficient. The results in Fig 4.10 and Fig 4.11 of the investigated case2 and case3 show that the decision-making point represented as point B (*SI* method), point C (*UI* method) and point D (*DI* method) are close together. Therefore in these cases only *SI* is enough for represent the decision making point in the viewpoint of robustness. Nevertheless, in some cases, such as the investigated case 1, the result in Fig 4.9 shows that the decision-making point represented by point B (*SI* method), point C (*UI* method) and point D (*DI* method) are apart together. The data in Table 4.5 for this case also show that the deviation of the decision-making point by *SI* method (point D) is rather large when compares with the deviation of the decision-making point by *UI* method (point B). Thus, in this case, the proposed methodology in this chapter is effective. These show that, in the viewpoint of robustness of uncertainty, the proposed methodology in this chapter is required to be evaluated before determining that the proposed method in this chapter is effective or not.

In this section we discuss for the conditions that the proposed methodology in this chapter is effective. The example conditions that the proposed methodology in this chapter is effective are shown in Fig.4.15 and Fig.4.16.

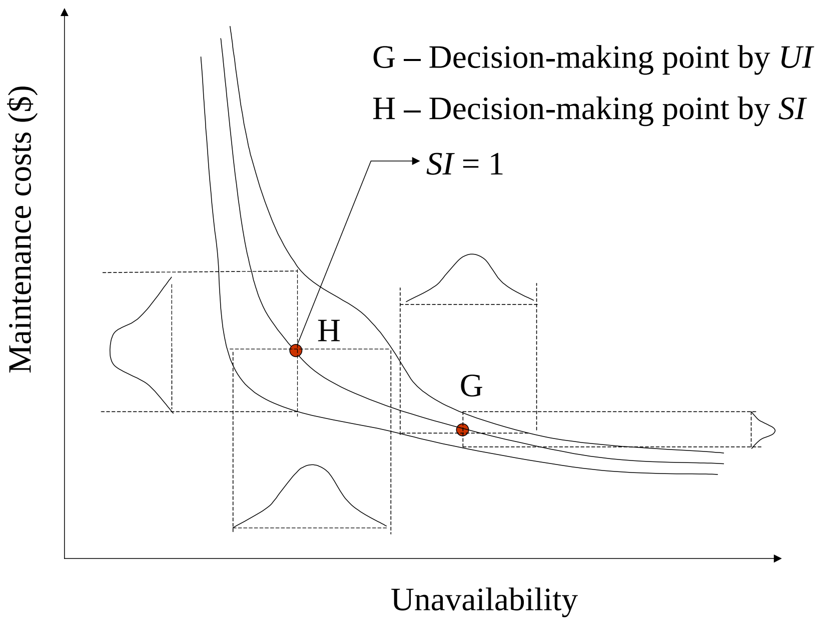

Fig. 4.15 The example condition that the proposed methodology in this chapter is effective.

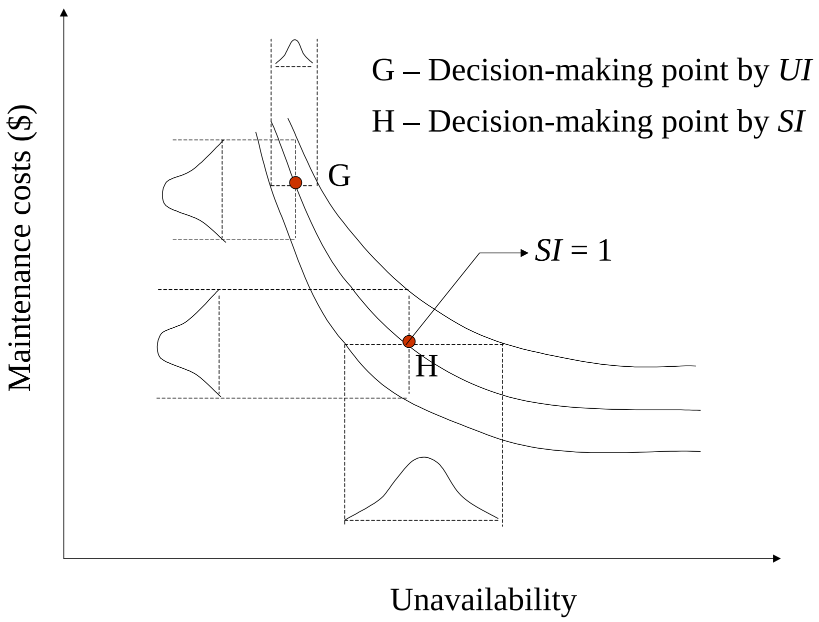

Fig. 4.16 The example condition that the proposed methodology in this chapter is effective.

For the example condition in Fig. 4.15 and Fig.4.16, point G represents the decision-making point by *UI*, and point H represents the decision-making point by *SI*. In these conditions, the decision-making point by *SI* (point H) have the large deviation of uncertainty and rather separate from the decision-making point by *UI* (point G). However, the decision-making point by *UI* (point G) is high in sensitivity. Thus, the example condition in Fig.4.15 and Fig.4.16 shows that the proposed methodology in this chapter is effective.

For the example condition in Fig.4.15, this condition may occur when the uncertainty parameters changed in some ranges. For this condition, the non-dominated sets of Pareto-optimal solutions shows the complicated shape. Therefore, results of sensitivity and the deviation of uncertainty are also complicated through the Pareto-optimal curve. Of course, the proposed methodology is required and is very effective for applying to this case.

For the example condition in Fig.4.16, this condition may occur when uncertainty parameters in one objective have the very smaller in deviation than the other. And those uncertainty parameters, which are very small in deviation, have not a large effect to the Pareto-optimal solutions (this means that those parameters do not make the large scatter in the Pareto-optimal solutions).

However, the investigated case 2 is also determined at uncertainty parameters in one objective have the very smaller in deviation than the other. The investigated case 2 is determined at %COV of unavailability parameters are larger to 10% and %COV of maintenance parameters are only 1%. But the maintenance cost parameters do make the large scatter in the Pareto-optimal solutions because the point F in Fig.4.10-a shows the rather large in scattering of maintenance cost values although its %COV is only 1%. Therefore, the proposed methodology may not be effective so much when it is applied to the investigated case 2.

The investigated case 1 in Table4.1 confirms that the proposed methodology in this chapter is effective with the reason of the example condition in Fig.4.16. The investigated case 1 is determined at %COV of unavailability parameters are only 1% and %COV of maintenance parameters are large to 10%. Moreover, the unavailability parameters do not make the large scatter in the Pareto-optimal solutions because the point A in Fig.4.9-a shows the very little in scattering of uncertainty values. Therefore, the proposed methodology is effective when it is applied to the investigated case 1.

The discussions in this section 4.7 show that, in order to obtain the decision making point in the viewpoint of robustness, the proposed methodology in this chapter is required. Because without applying the proposed methodology, we cannot know in advance that only the sensitivity index, which is proposed in chapter 3, is sufficient when the robustness of uncertainty is also required.

4.8 Conclusion remarks

In this chapter, the multi-optimization method has been performed to optimize maintenance activities in a nuclear power plant's HPIS in order to solve the trade-off problem between unavailability and maintenance costs. Nevertheless, maintenance activities typically involve significant uncertainties such as those involving downtime and costs of maintenance. Thus, in this chapter the new methodology for determining the most promising solution from a multi-objective optimization framework under uncertainties was proposed according to the user's requirements.

The promising solution obtained using the proposed methodology was compared with that obtained by the conventional method, and it was confirmed that the proposed methodology defines an optimal solution with low sensitivity at adequate robustness.

Chapter 5

Risk-based Inservice Testing Policy using the Multi-Objective Optimization with Robustness

5.1 Introduction

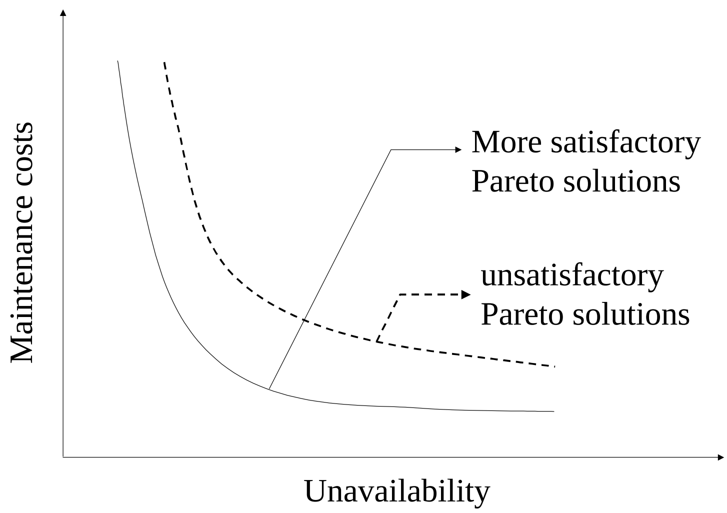

Fig.5.1 Example case shows an unsatisfactory Pareto-solution.

The multi-objective optimization is usually performed in order to solve the conflicting objective in the maintenance activities. From chapter 3 and chapter 4, in order to attain the robust solution in surveillance test, the multi-objective optimization is considered with the robust solution using the decision-making based on robustness. In addition to the application of the multi-objective optimization with robustness, the management of surveillance test interval groups is also significant for achieving the more satisfactory Pareto-optimal solutions in the risk management point of view, for example as illustrated in Fig.5.1. The following subsection shows why the management of surveillance test interval groups is important for improving the Pareto-optimal solutions.

5.1.1 Significance of RBM for improving the Pareto-optimal solution.

One of the important parameters for the surveillance test is the surveillance test interval (STI), which is adopted as the decision variable for the optimization process. In the surveillance test, the system components have been grouped into different test strategies. All components in the same group are determined as the same surveillance test interval. Therefore, the management of the surveillance test interval groups is also significant for improving the maintenance activities. In order to manage the most satisfactorily surveillance test interval groups in the viewpoint of risk, the optimization including prioritization of maintenance should be treated.

The risk-based maintenance (RBM) is the method for determining the priority of the maintenance using components risk. The RBM can be applied for managing the surveillance test interval groups. For components in the standby system, such as pumps and valves, risk-based maintenance for testing is called as risk-based inservice testing [3]. However, the methodology for updating multi-objective optimization by risk-based inservice testing has not been reported, although both of the multi-objective optimization and RBM are important.

In chapter 3 and chapter 4, the surveillance test interval groups are fixed by did not manage the prioritization for testing. In this chapter, we consider the prioritization for surveillance test as shown in Table.5.1. The surveillance test interval T^1, T^2, T^3 are considered as the decision variables in the optimal process. T^1 represents the shortest test interval, T^2 represents the medium one and T^3 represents the longest one. Then, the high-risk components should be tested more frequently than medium and low risk components.

Table. 5.1 The prioritization of test interval groups for surveillance test.

T^1	High risk components
T^2	Medium risk components
T^3	low risk components

Though, ASME has already developed the guideline of risk-based inservice testing [9], the following subsection shows how this ASME method is not sufficient in determining the most optimal test interval groups based on risk and robust consideration.

5.1.2 Problem in the risk-based inservice testing by ASME method

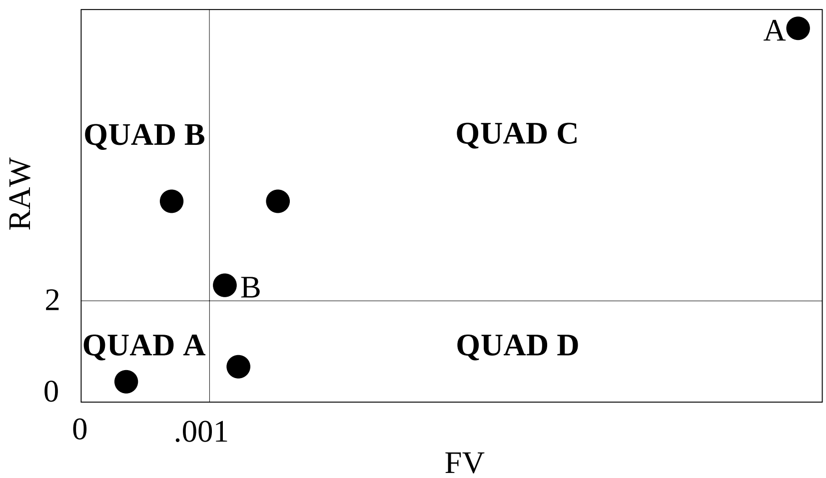

Fig.5.2 RAW/FV Quadrant graph of risk by ASME method [9].

As describe in chapter 2, the main idea of component important ranking by ASME is determined by using the combination of importance measure. That is the Fussel-Vesley (FV)[35] and Risk Achievement Worth (RAW)[35] matrix. The ranking is divided at the fixed value of FV and RAW into four quadrants as shown in Fig.5.2. The fix values of FV and RAW defined by ASME for dividing quadrant of matrix are 0.001 and 2 respectively.

From Fig.5.2, components in quadrant **A** may be candidates for no or relaxed testing. Components in quadrant **C** should have focused and effective testing. While, infrequent test are considered for components in quadrant **B** and **D**.

Nevertheless, by fixing the values of FV and RAW is not flexible enough. For example as the component A and B in the case of FV-RAW matrix in Fig.5.2, the risk significance of the components may be located in the same risk significance of test interval group because their FV and RAW values are larger than the fixed values, although there are extreme differences in their values. Moreover, the ASME method has not clearly presented the method to revise risk-ranking process. Therefore, the ASME method may not clearly give the most optimal surveillance test interval groups for the surveillance test based on risk consideration.

In addition, the method by ASME does not consider about the multi-objective optimization and robustness. Thus, the obtained test interval groups by ASME may not be appropriate in the viewpoint of robustness.

The purpose of this paper is to propose a methodology for determining the robust surveillance test with the most optimal surveillance test interval based on risk based inservice testing. The methodology for applying a multi-objective optimization to risk-based inservice testing is proposed in the following section to determine the most optimal test interval based on risk consideration. In order to obtain the robust solution, the decision-making for the multi-objective optimization solution based on robustness proposed in chapter 3 and chapter 4 is preferred depending on user's requirement.

In this chapter, the solution obtained by the proposed methodology is also compared with that by the risk-based inservice testing method of ASME and also compared with that by the typical surveillance test by the U.S. nuclear regulatory commission (USNRC) [58]. It is confirmed that the obtained optimal solution shows satisfactory solution based on risk consideration with adequate robustness.

5.2 The proposed methodology

The proposed methodology for applying the multi-objective optimization to risk-based inservice testing is illustrated in Fig. 5.3. The methodology starts with defining the considered standby system. The inventory of the system is then performed to determine the unavailability parameters, cost parameters of each component and the initial surveillance test interval groups of components. The multi-objective optimization is then performed at the initial surveillance test interval groups of components.

Because the Pareto-optimal solutions consist of a number of solutions, the most appropriate solution from the Pareto-optimal solutions with lowest sensitivity is then selected to be the representative of the Pareto-optimal solutions. We already proposed in the chapter 3 that this point can be easily identified as the point of sensitivity index (*SI*) $SI = 1$. The selected solution is then used to construct the proposed risk matrix that assist in categorizing the risk significance of the components into first approximate test interval groups. Thereafter, the revision of risk ranking is performed in order to update the multi-objective optimization result. The revising risk ranking and the multi-objective optimization process are repeated to improve the multi-objective optimization results until the test interval groups converges. By this updating process, the optimal surveillance test interval groups based on risk consideration are obtained and then provide the satisfactorily Pareto-optimal solutions in the view point of risk management. Finally, in order to obtain the surveillance test planning that is appropriate for robustness in maintenance activities, the decision-making based on robustness proposed in chapter 3 and chapter 4 is used based on user's requirement.

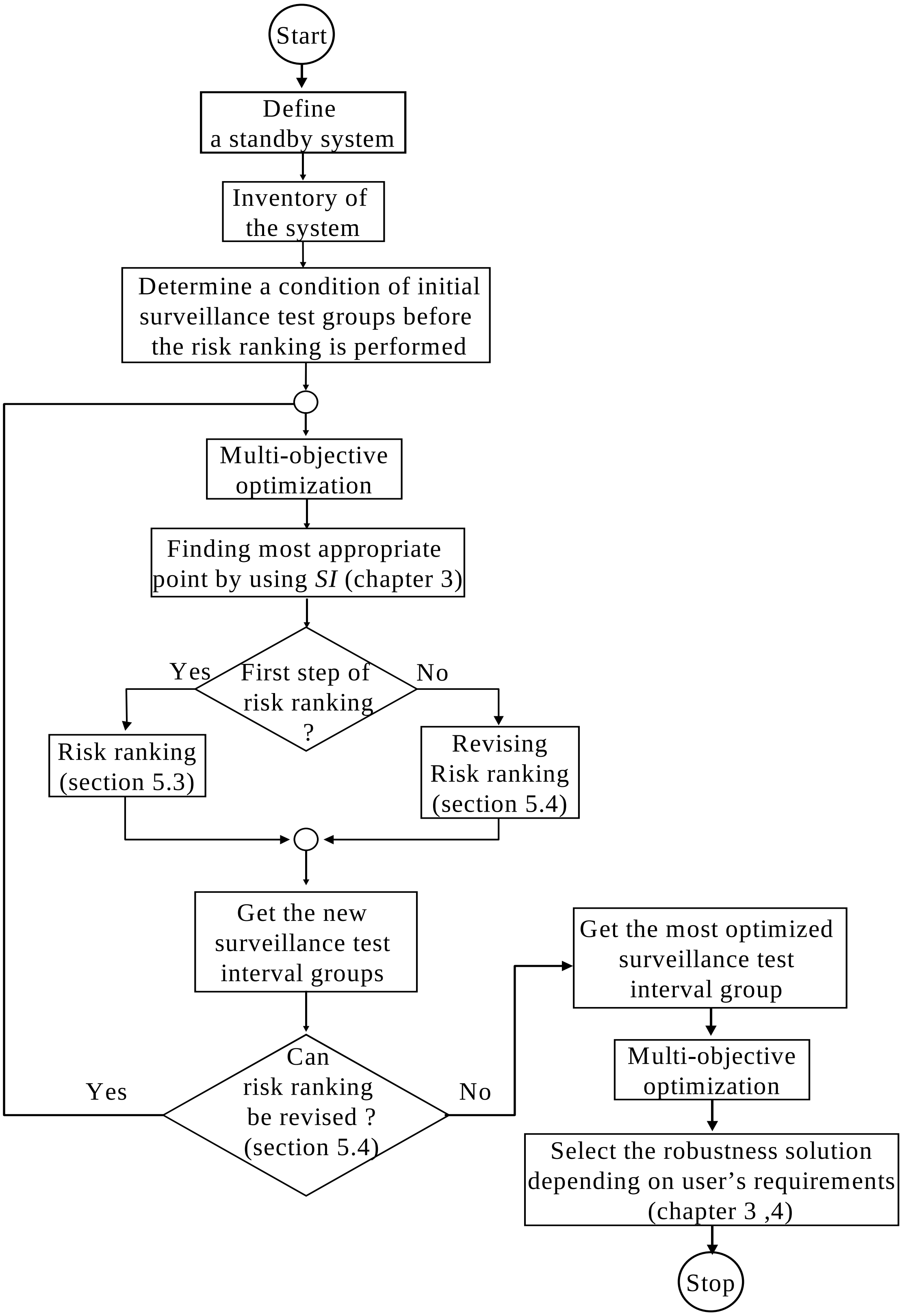

Fig. 5.3. Process of the methodology for risk-based inservice testing policy using the multi-objective optimization with robustness.

5.3 The proposed risk matrix

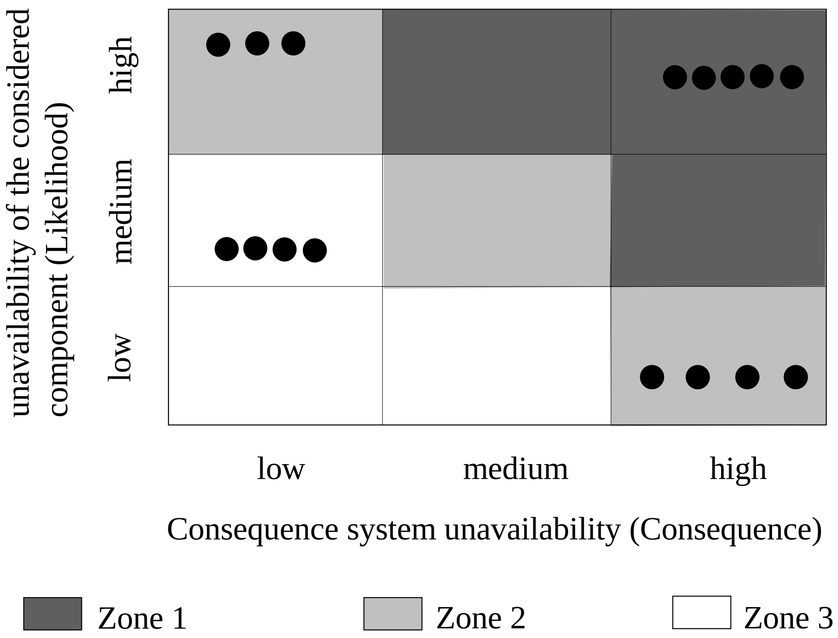

Fig. 5.4. The proposed risk matrix.

The concept of risk usually consists of the likelihood of the failure and the consequence of the failure for the interested part. In the standby system, the unavailability is a very important parameter. Therefore, this research corresponds the likelihood of the failure to the unavailability of each component.

In addition, the consequence of a component's failure to the system unavailability is defined in reference of the concept of importance measure of the Risk Achievement Worth (RAW)[35]. As described in section 2.4.4 of chapter 2, the RAW is defined as the following equation.

$$\text{RAW} = \frac{U(U_i = 1)}{U(base)} \tag{5.1}$$

where $U(U_i = 1)$ is the increased system unavailability level when the considered component i is assumed to fail or unavailability of that component equals 1.0.

$U(base)$ is the present system unavailability level.

In this research, in order to make the parameters used in the proposed risk matrix easy to assist in examining how the risk level is improved quantitatively, we correspond the consequence of a component's failure to the system unavailability as $U(U_i = 1)$.

Both the consequence of each component to the system and the present unavailability of each component are considered on the risk matrix simultaneously.

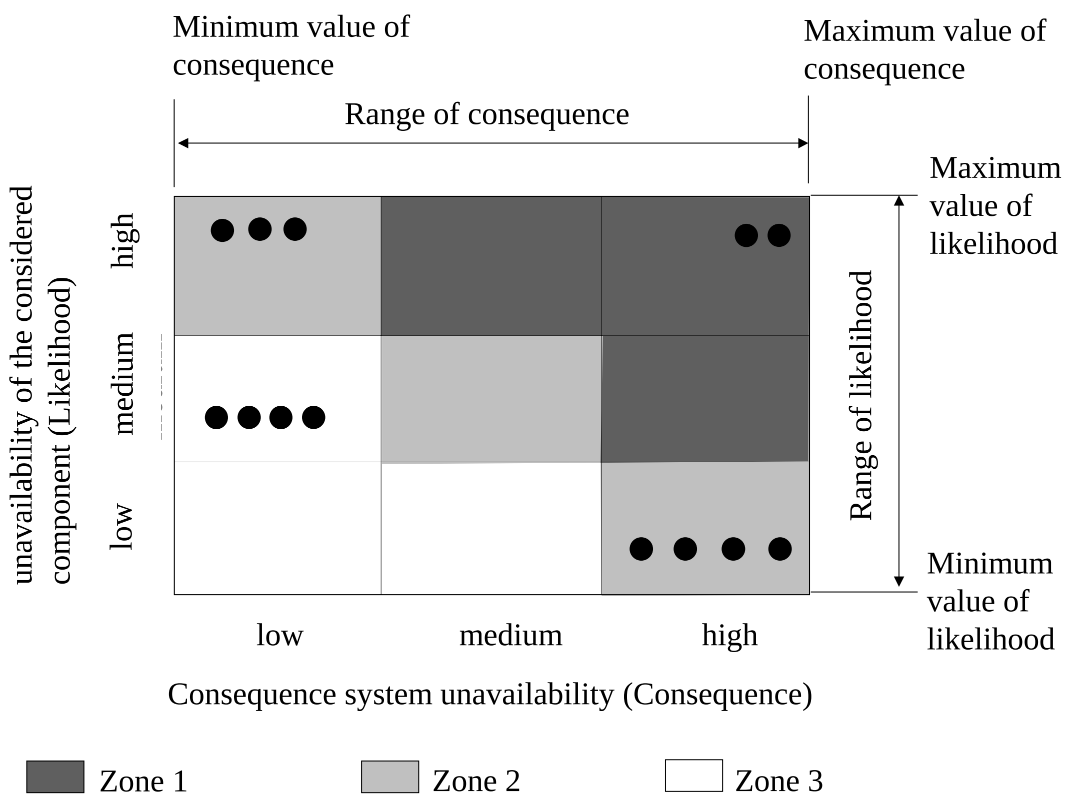

Fig.5.5 The definition of the qualitative low-medium-high category of each axis.

The likelihood and the consequence are then plotted on the risk matrix as shown in Fig.5.4. In order to define the qualitative low-medium-high category for each axis of the proposed risk matrix, the maximum and minimum values of the likelihood and consequence from all components are used to be the upper and lower bound of the ranges for creating the risk matrix. Each axis is then divided into 3 equally category of low, medium and high category for each axis of risk matrix as illustrated in Fig.5.5. Thereafter, the risk significance for surveillance test is considered as shown in Fig.5.4.

In Fig.5.4, the risk significance is divided into 3 zones of surveillance test interval T^1, T^2, T^3. The T^1, T^2, T^3 are considered as the decision variables in the optimal process. T^1 represents the shortest test interval, T^2 represents the medium one and T^3 represents the longest one. The risk significance for each divided zone is considered as follows:

1) Zone 1: The level of risk significance for the components that locate in this zone 1 is the highest risk significance components when compared with the others. Therefore, the components located in this zone should be tested most frequently. The surveillance test interval for the components in this zone 1 is then the shortest one allocated to T^1 in this research. This zone 1 is considered as an unacceptable zone for the operation.

2) Zone 2: The level of risk significance for the components that locate in this zone 2 is the medium risk significance components when compared with the others. The surveillance test interval for the components in this zone 2 is the medium test interval allocated to T^2 in this research. This zone 2 is considered as an acceptable zone for the operation.

3) Zone 3: The level of risk significance for the components that locate in this zone 3 is the lowest risk significance components when compared with the others. The surveillance test interval for the components in this zone 3 is the longest one allocated to T^3 in this research. This zone 3 is considered as an acceptable zone for the operation.

5.4 Revision of the risk matrix

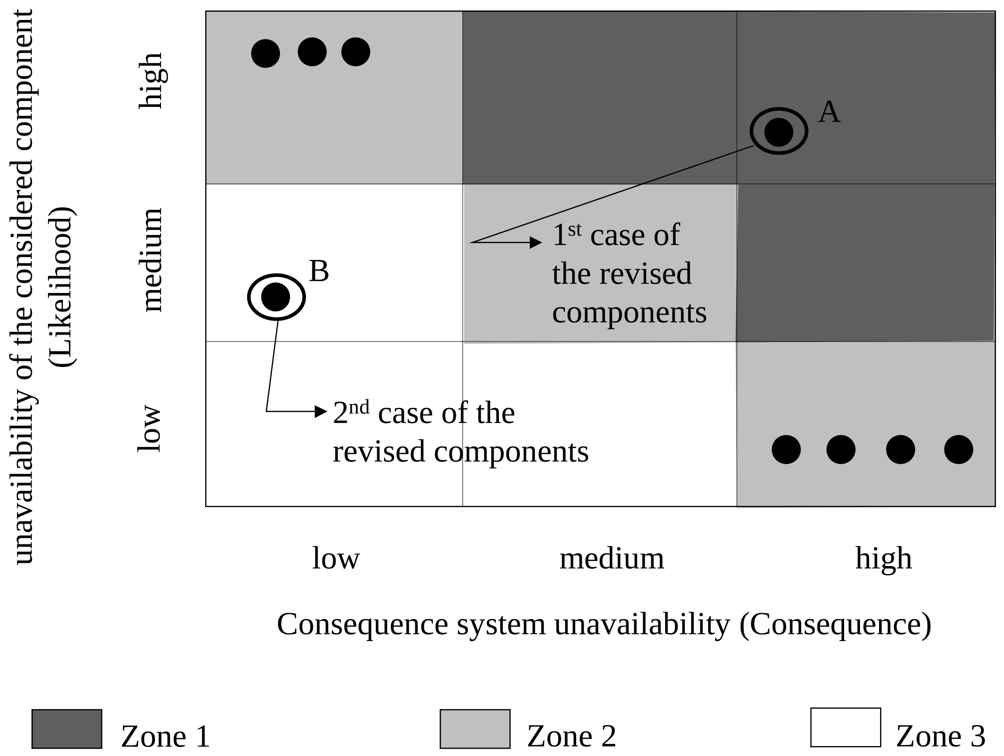

Fig.5.6 The proposed revising risk matrix

Since only one of risk ranking process is not sufficient to find the most optimal groups for surveillance test intervals, the revision of the risk matrix is then required.

In order to revise the risk ranking, the risk matrix (for the solution of the latest obtained test interval groups) is created again. After that, the interested components to be revised in the test interval groups are treated according to the following 2 cases:

1) 1st case of the revised components:

The components, which are still located in zone 1 even after the treatment, are considered as the highest risk significant components. An example of the components to be revised as this case is shown as the component A in Fig.5.6 These components will be revised by shortening the test interval.

2) 2nd case of the revised components:

The components, which are still located in zone 3, are considered as components that can be further disregarded in the maintenance activities. An example of the components to be revised as this case is shown as the component B in Fig.5.6. These components will be revised by extending the test interval.

The objective of revising the risk ranking is to improve the risk significance of components until they are converged at the optimal test interval groups based on risk consideration, whose risk significances should fall into the medium risk significance finally. The medium risk significance that is shown in zone 2 is not too conservative and not too risks significance.

5.5 Decision making for the multi-objective optimization

Because the Pareto-optimal solutions consist of a number of solutions, there must be some decision-making for the multi-objective optimization in order to select the point to be improved in the proposed methodology. In order to achieve robustness of the solution, the proposed indexes and methodologies in chapter 3 and chapter 4 are preferred to be the decision-making in the proposed methodology in this chapter.

5.5.1 Decision-making or Pareto-optimal solutions in the risk ranking and revising risk ranking step

The decision-making point for the multi-objective optimization is important because in some initial cases there are some points in the Pareto-optimal solutions may not be appropriate to be selected for improvement.

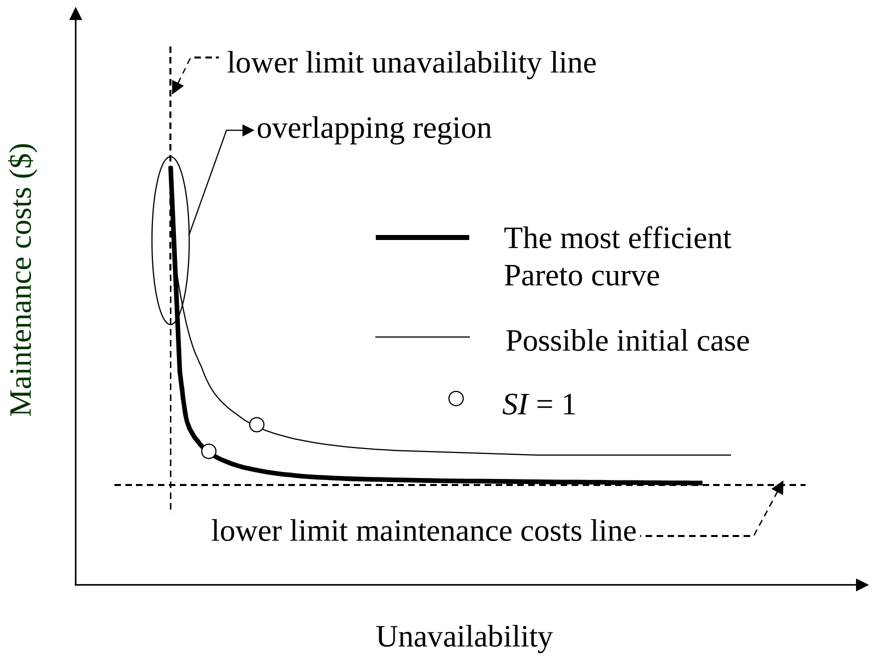

Fig. 5.7. Example of an initial case whose area overlap with the most efficient Pareto-optimal solutions.

In some initial cases, it is possible that some regions in the initial Pareto-optimal solutions overlap with the most efficient Pareto-optimal curve for example as shown in Fig.5.7. If the point in these regions is selected for improving, the obtained test interval groups may not be the most optimal test interval groups for the entire Pareto-optimal solutions because the points in these regions cannot be further improved. Nevertheless, it is impossible to know the most efficient Pareto-optimal solutions from the first stage of the simulation. Therefore, some decision making index is required in order to assist in selecting the point that is located in the non-overlapping regions.

For the multi-objective optimization of maintenance activities, there is the lower limit line of each objective function represented as dot lines in Fig. 5.7. The more Pareto curve is improved, the more Pareto curve approach to these limited lines. However, the results that approach to these limited lines are high sensitivity of one objective value in relation to another objective value. Then, the most efficient Pareto-optimal curve should have the extensive areas that are high in sensitivity.

Therefore, the suggest point, which should be selected, is the point that has the lowest sensitivity, because there is the most highly probability that this point will not overlap with the most efficient Pareto-optimal curve. Then, the sensitivity index has been proposed in the chapter 3 is appropriate because it can assist in determining the lowest sensitivity solution in the Pareto-optimal curve.

5.5.2 Decision-making for the obtained final result of Pareto-optimal solutions

In order to obtain the surveillance test planning with robustness, the selection of the final result of Pareto-optimal solution should be paid attention on the robustness of the determining solution. Therefore, the proposed indexes and methodology of decision-making for the multi-objective optimization solutions in the viewpoint of robustness in chapter 3 and chapter 4 are preferred as following case.

1) When the robustness of sensitivity is considered important, the sensitivity index (*SI*) and methodology in chapter 3 is preferred.

2) When the robustness of uncertainty is considered important or there are high uncertainty in the operating system, the proposed uncertainty index (*UI*) and proposed methodologies in chapter 4 is preferred.

3) When not only the robustness of sensitivity, but also the robustness of uncertainty is considered important, the proposed decision index (*DI*) and proposed methodologies in chapter 4 is preferred.

5.6 Results and Discussions

In order to assure the effectiveness of the proposed methodology in this chapter, the case study of HPIS explained in section 3.4 of chapter 3 is applied. The HPIS is shown again here as the Fig. 5.8 for the sake of simplicity.

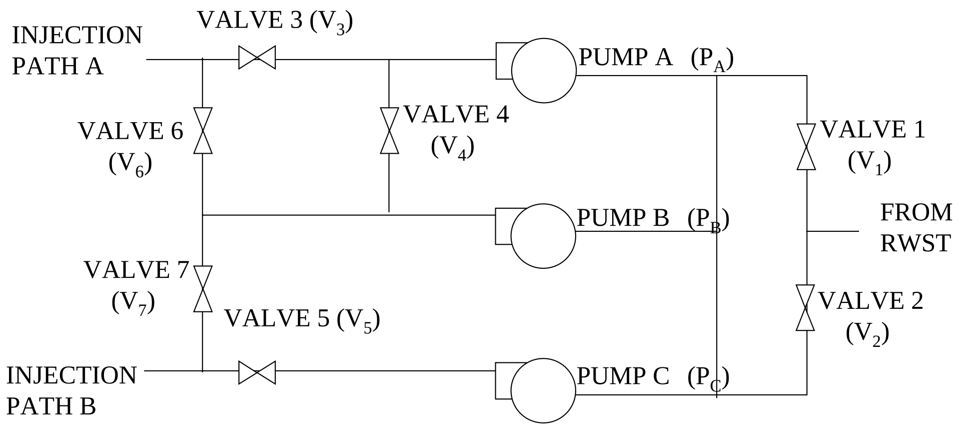

Fig. 5.8 HPIS system [33].

Table 5.2. The initial surveillance test interval groups conditions of investigated cases before performing the risk-based inservice testing.

Case	T^1	T^2	T^3
1	All components	-	-
2	V_1, V_2, P_A, P_B, P_C	V_3, V_4, V_5, V_6, V_7	-
3	V_2	V_1, P_A, P_B, P_C	V_3, V_4, V_5, V_6, V_7
4	V_1, V_2, V_3, V_4, V_5, V_6, V_7	P_A, P_B, P_C	-

In order to investigate the effectiveness of the proposed methodology, four investigated cases of the initial surveillance test interval groups before performing the risk-based inservice testing to the HPIS in Fig.5.8 are shown in Table 5.2. The symbols using in Table 5.2 are shown in Fig.5.8.

While variables T^1, T^2, T^3 in Table 5.2 are the surveillance test interval groups as described in section 5.3. The T^1, T^2, T^3 are considered as the decision variables constrained as follows,

$T^1 \leq 8760\ h$

$T^2 = k_1 \cdot T^1 \quad while \quad 1 \leq k_1 \leq 10$

$T^3 = k_2 \cdot T^2 \quad while \quad 1 \leq k_2 \leq 10$

Consequently, the maintenance activities optimization of this system has decision variables set, x, as shown in Eq.(5.2)

$$x = \{T^1, k_1, k_2\} \qquad (5.2)$$

The results of risk ranking and revising risk ranking of the processes in the proposed methodology for the investigated case 1 – case 4 in Table 5.2 are shown in Fig. 5.9 – Fig 5.12 respectively.

For investigated case 1:

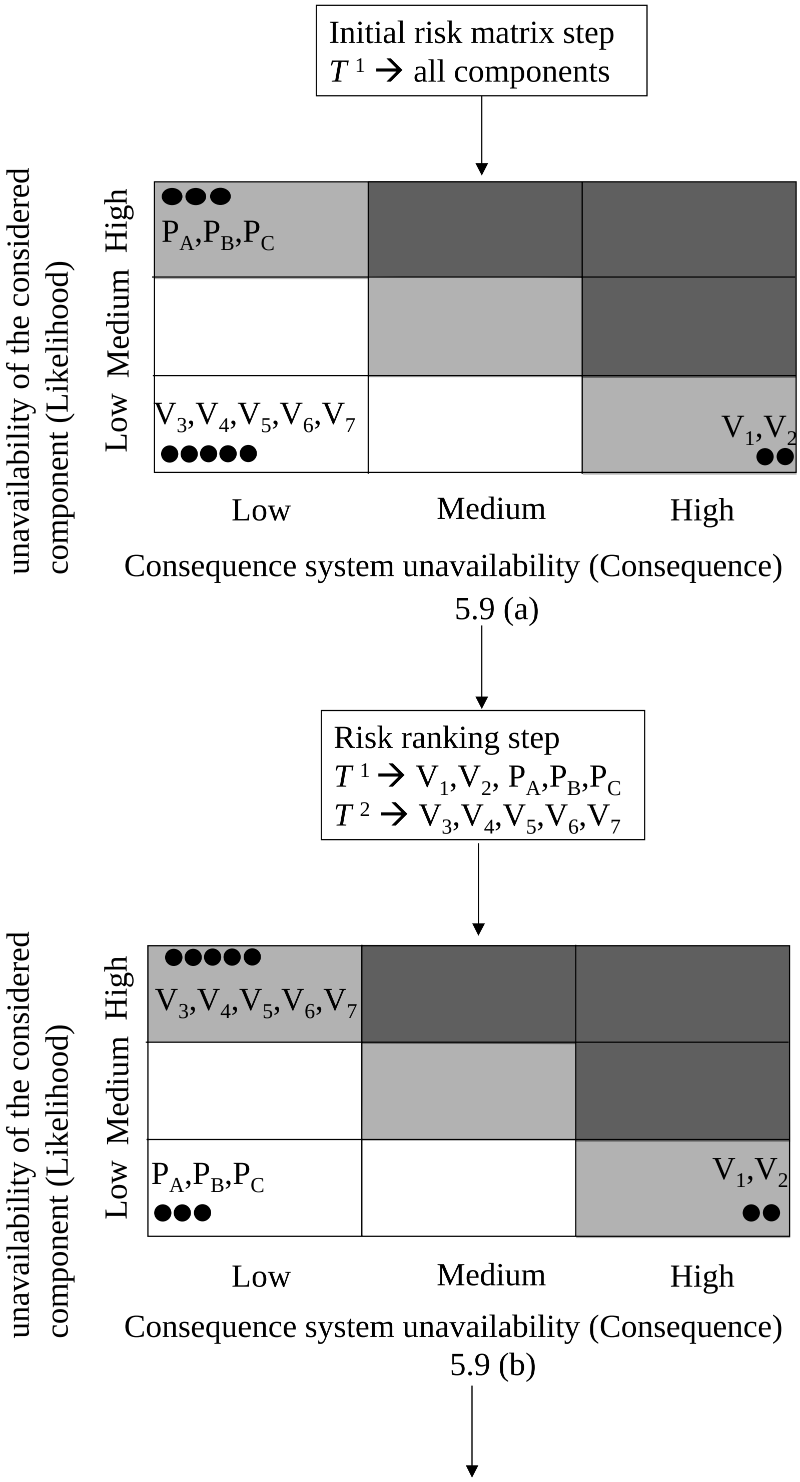

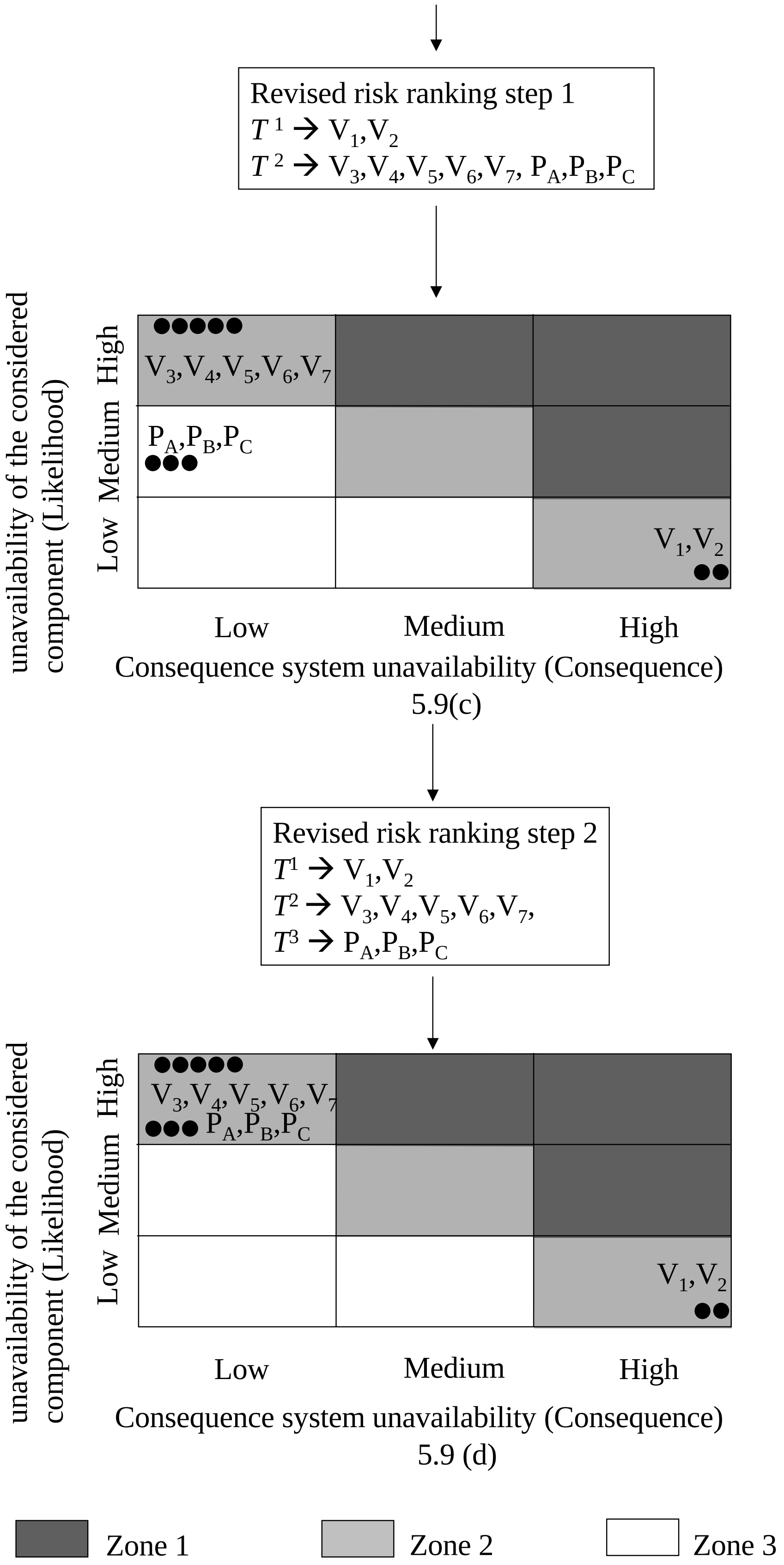

Fig. 5.9. Risk matrix and revising risk matrix for investigated case 1.

For investigated case 2:

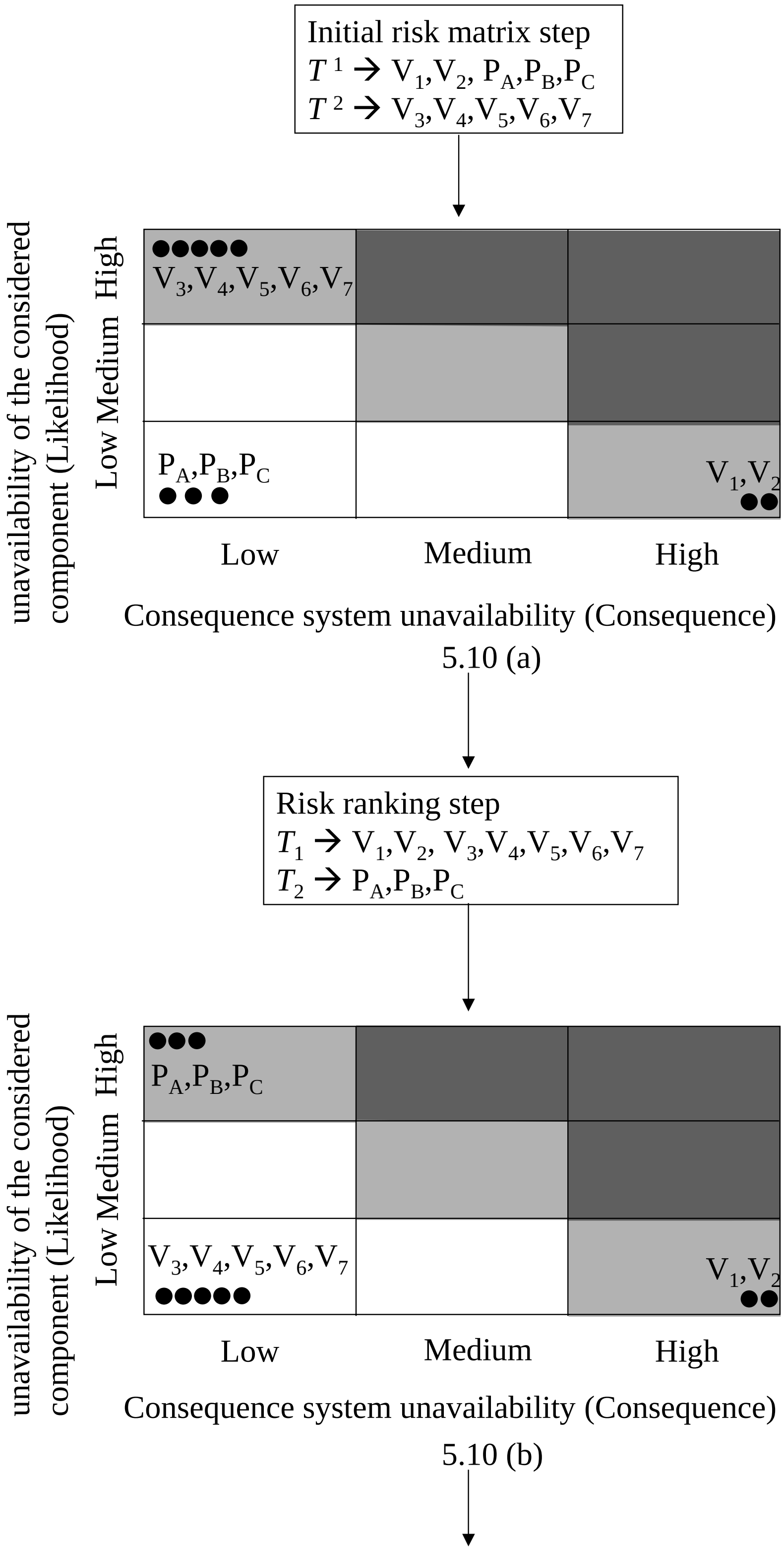

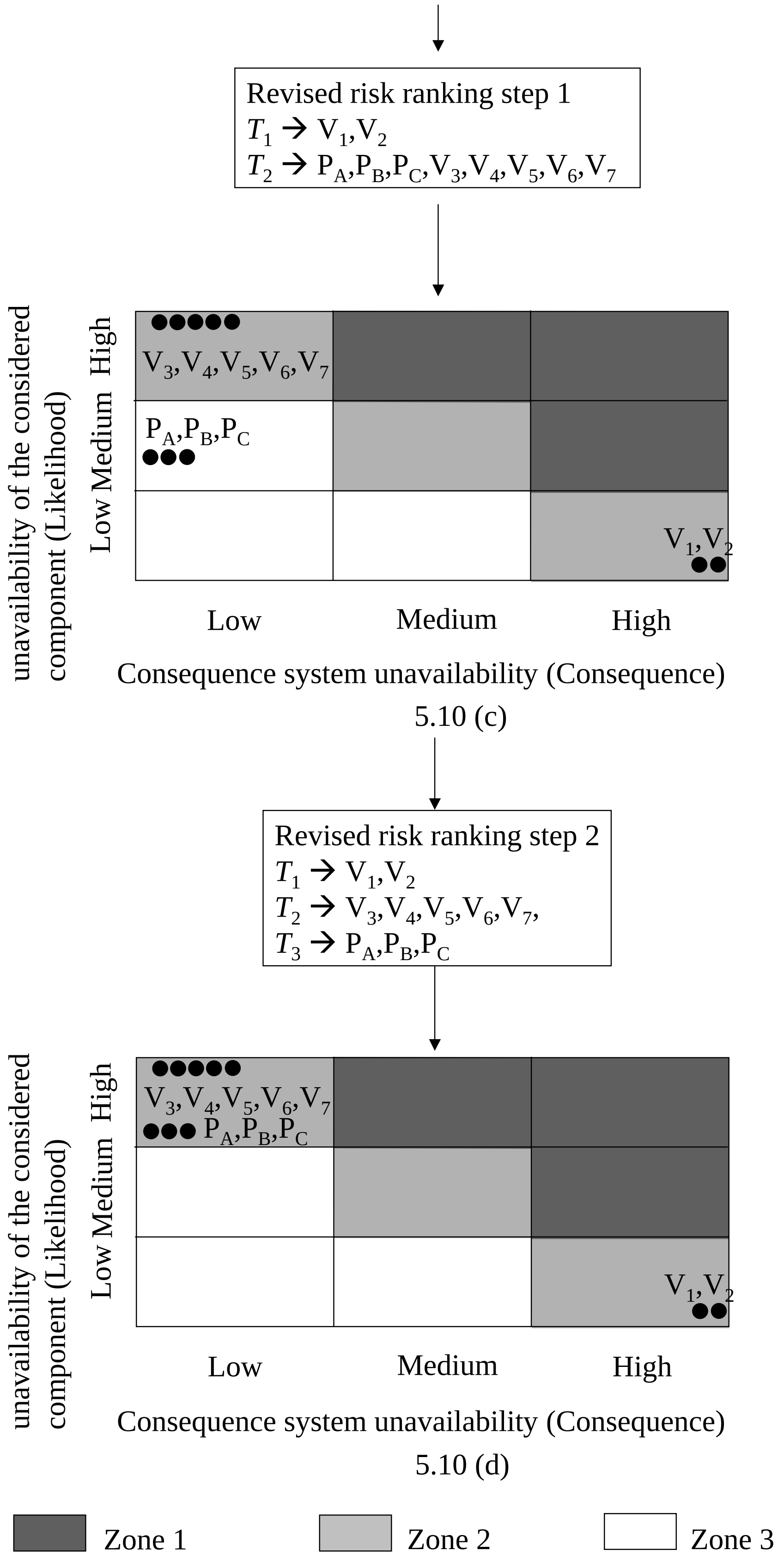

Fig. 5.10. Risk matrix and revising risk matrix for investigated case 2.

For investigated case 3:

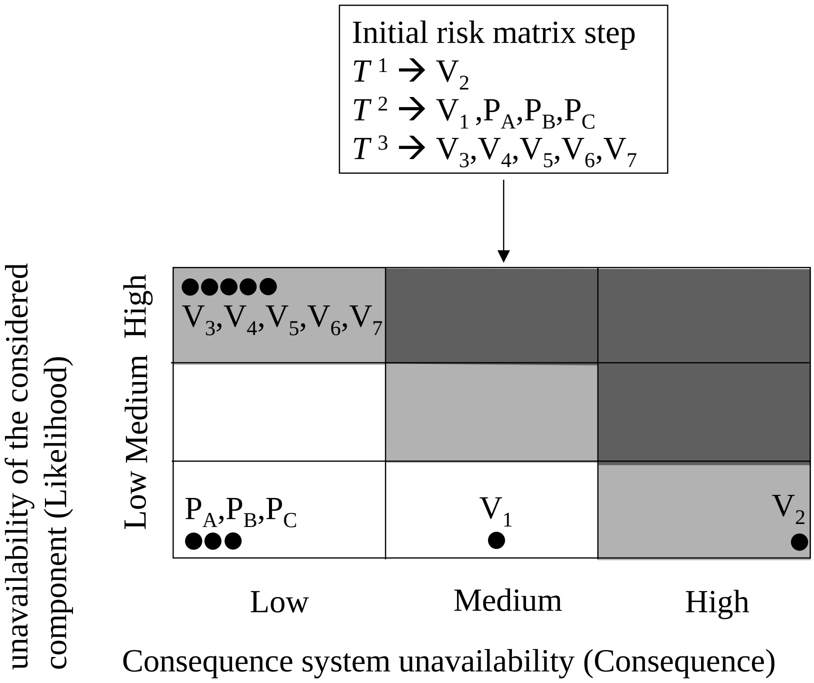

5.11 (a)

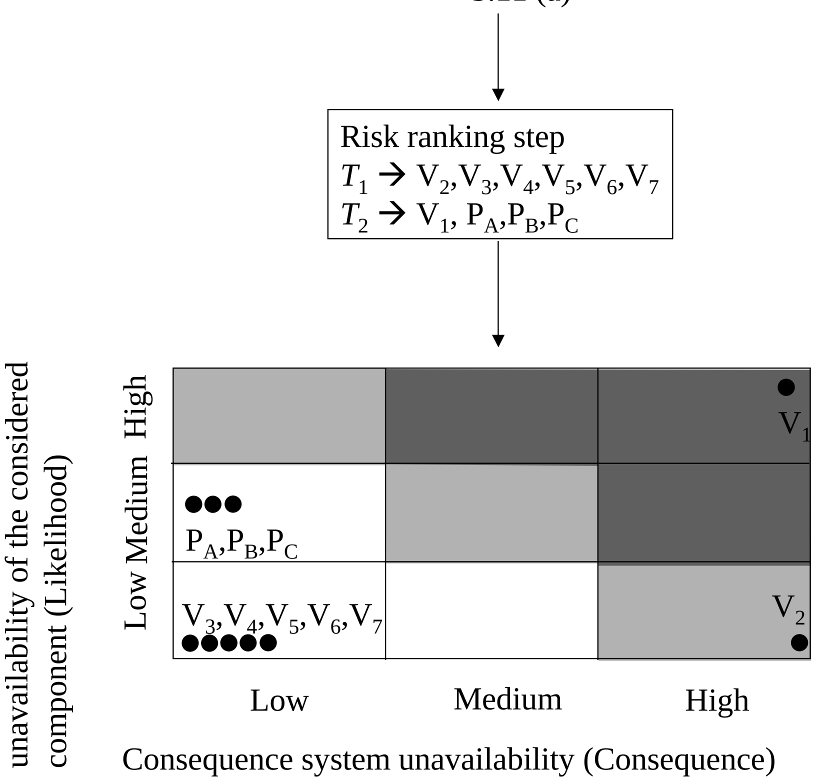

5.11(b)

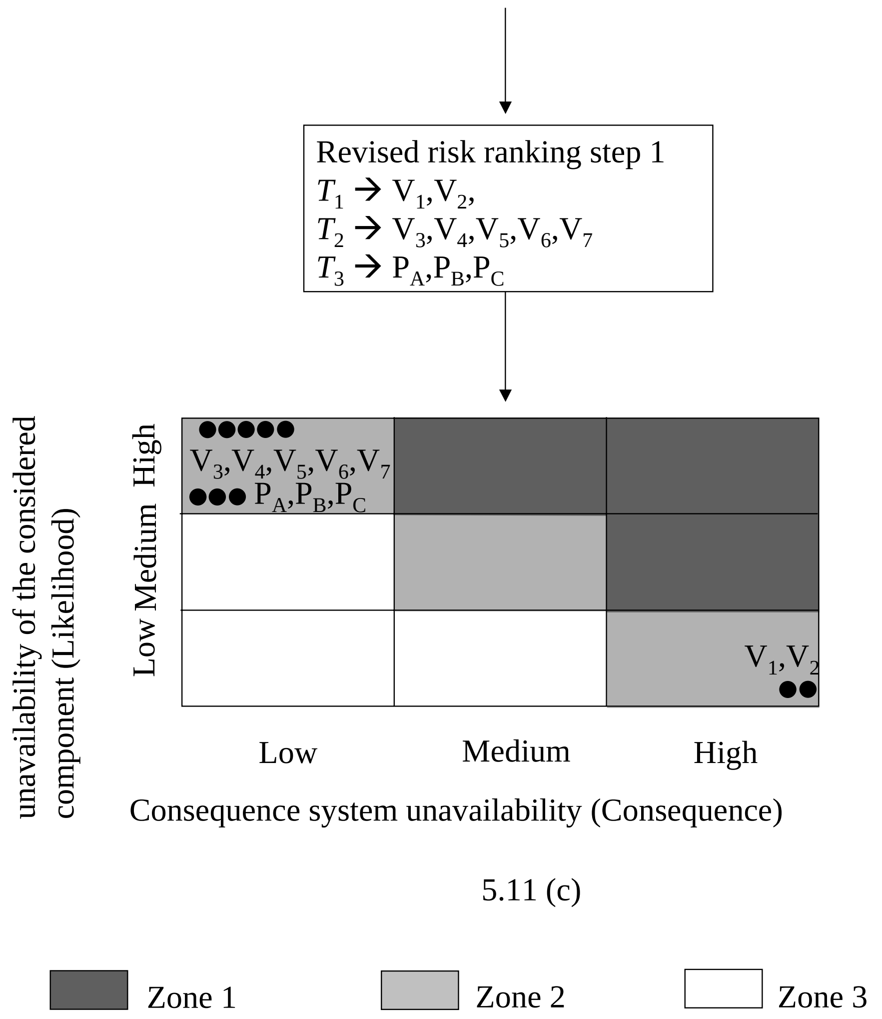

Fig. 5.11. Risk matrix and revising risk matrix for investigated case 3.

For investigated case 4:

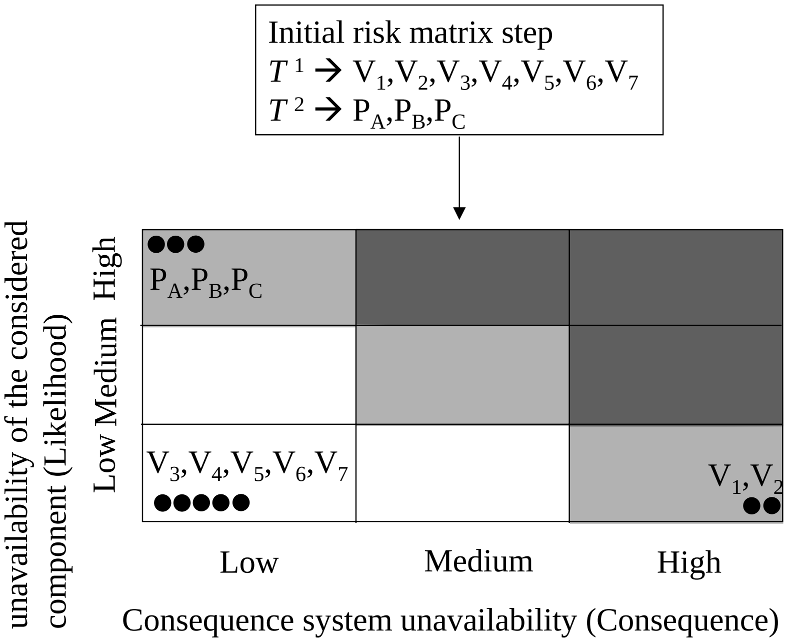

5.12 (a)

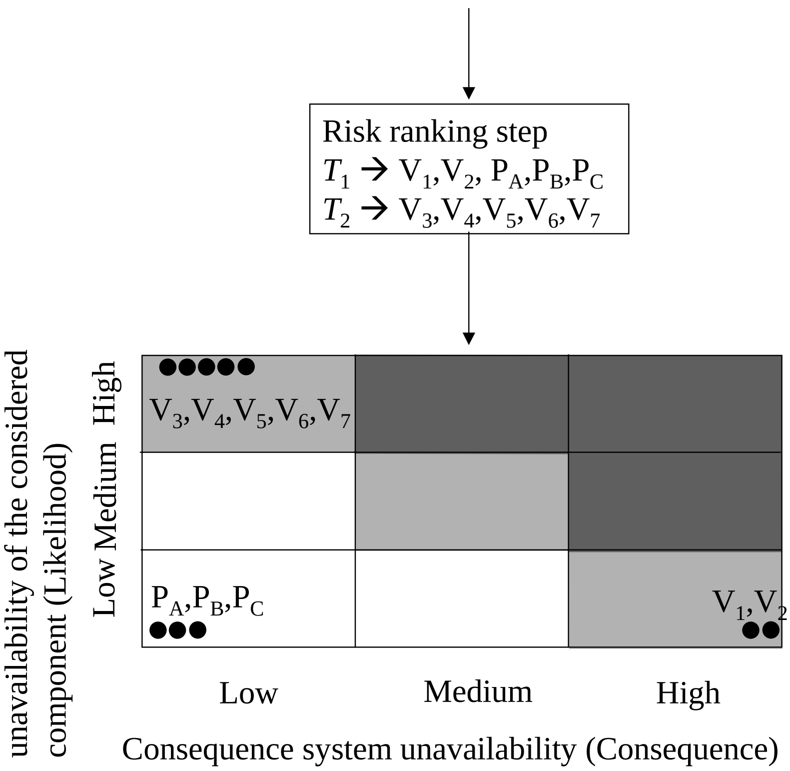

5.12 (b)

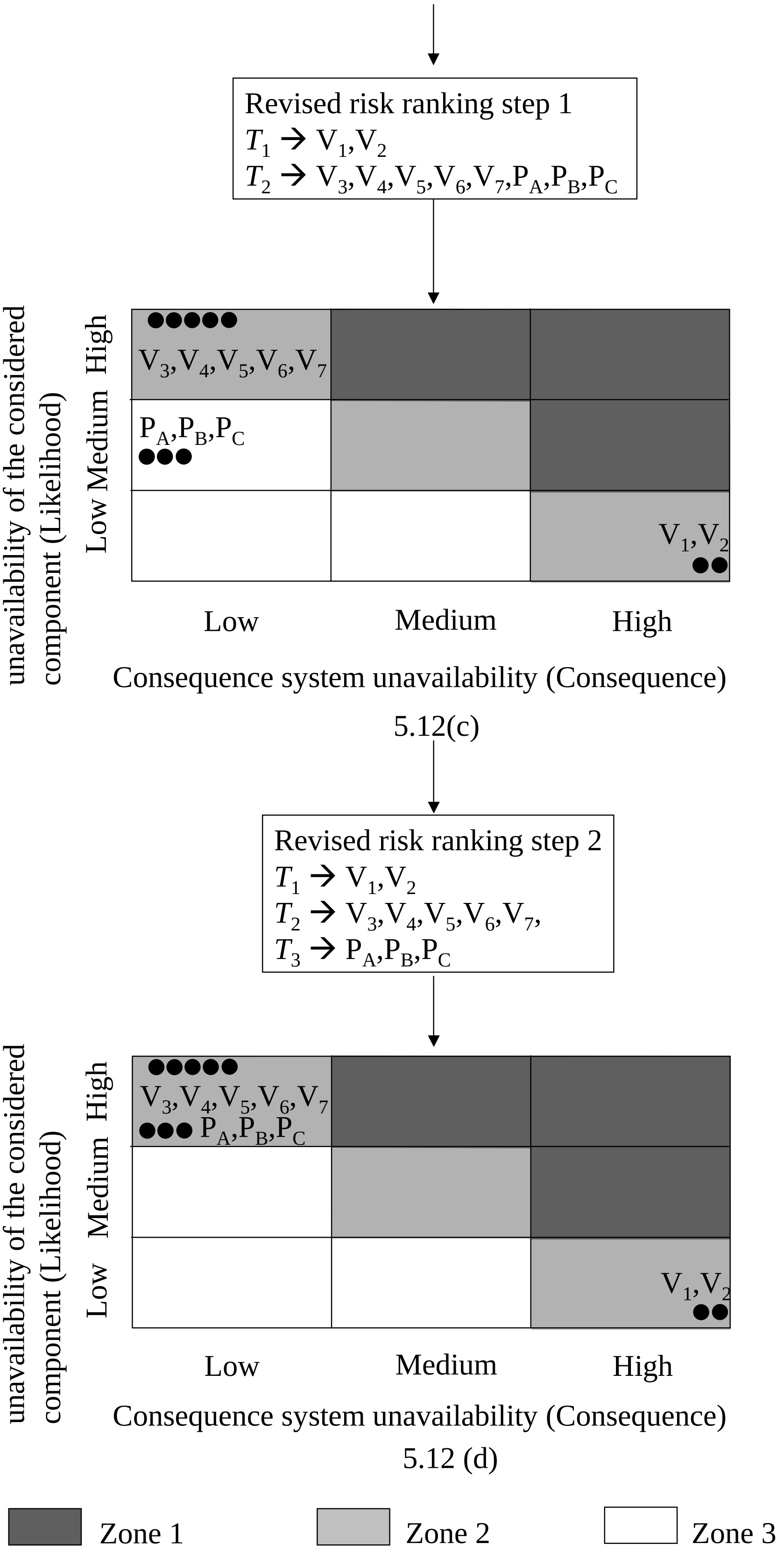

Fig.5.12. Risk matrix and revising risk matrix for investigated case 4.

The proposed methodology started with defining the standby system, which is the HPIS shown in Fig. 5.8. The HPIS has the unavailability parameters and cost parameters of each component as shown in Table 3.1 in chapter 3. After that, the multi-objective optimization is performed for the initial surveillance interval test groups of components.

Thereafter, the Pareto-optimal solutions are obtained and the lowest sensitivity solution at $SI = 1$ is selected to create the risk matrix. The result of risk matrix for each case is shown in Fig. 5.9 (a) - Fig. 5.12 (a), respectively. For the sake of simplifying the understanding in the proposed methodology, the results of investigated case 1 are explained in detail. For the investigated case 1, the result of test interval groups obtained from the risk matrix in Fig 6(a) is that the components allocated for T^1 are V_1, V_2, P_a, P_b, P_c and the components allocated for T^2 are V_3, V_4, V_5, V_6, V_7.

Thereafter, the multi-objective optimization is performed again for the latest obtained test interval groups and solution at $SI = 1$ is selected to create the risk matrix as the result shown for each case in Fig. 5.9 (b) - Fig. 5.12 (b), respectively. From this risk matrix, the components that should be revised are selected and the revised risk ranking matrix step 1 for each case is created and shown in Fig. 5.9 (c) - Fig. 5.12 (c), respectively. For the investigated case 1 of Fig. 5.9(b), P_a, P_b, P_c, are specified as the 2nd case of the revised components (described in section 5.4) that should be revised by extending the test interval. Therefore, test interval for P_a, P_b, P_c, is revised from T^1 to T^2. The result of test interval groups obtained from the revised risk ranking step1 in Fig.5.9(b) is that the components allocated for T^1 are V_1, V_2 and the components allocated for T^2 are V_3, V_4, V_5, V_6, V_7, P_a, P_b, P_c.

The process of multi-objective optimization and revising risk ranking are repeated until the test interval groups are converged like the last step in Fig. 5.9 (d), Fig. 5.10 (d), Fig. 5.11 (c), and Fig. 5.12(d). These figures in the last step show that the risk significance of all components falls into the medium risk significance (zone 2). The results are then shown to be the most optimal test interval groups based on risk.

The results for each step in the proposed methodology of all investigated cases are summarized again as shown in Table 5.4. As shown in Table 5.4, the converged results for all investigated cases (after applying the proposed methodology) are completely same regardless of the initial conditions. This shows the appropriateness of the methodology. The obtained result of the optimal surveillance test interval groups based on risk consideration for all investigated cases is shown in Table 5.3.

Table 5.3 The most efficient test interval groups based on risk consideration by the proposed methodology.

Components	Test interval group
V_1, V_2	T^1
V_3, V_4, V_5, V_6, V_7	T^2
P_A, P_B, P_C	T^3

Table 5.4. Test interval groups for each step in the processes of the proposed methodology.

Case	Shown In Fig.	Risk ranking step	Test interval groups			Values at *SI* = 1	
			T^1	T^2	T^3	Unavail-ability	Cost ($)
1	Fig. 5.9(a)	Initial risk matrix step	All components	-	-	3.75E-5	2477
	Fig. 5.9(b)	Risk ranking step	V_1,V_2, P_A,P_B,P_C	V_3,V_4,V_5,V_6, V_7	-	3.79E-5	2082
	Fig. 5.9(c)	Revised risk ranking step 1	V_1,V_2	V_3,V_4,V_5,V_6, V_7, P_A,P_B,P_C	-	3.20E-5	845
	Fig. 5.9(d)	Revised risk ranking step 2	V_1,V_2	V3,V4,V5,V6, V7	P_A,P_B,P_C	3.18E-5	851
2	Fig. 5.10(a)	Initial risk matrix step	V_1,V_2, P_A,P_B,P_C	V_3,V_4,V_5,V_6, V_7	-	3.79E-5	2082
	Fig. 5.10(b)	Risk ranking step	V_1,V_2,V_3,V_4, V_5,V_6,V_7	P_A,P_B,P_C	-	3.36E-5	1317
	Fig. 5.10(c)	Revised risk ranking step 1	V_1,V_2	V_3,V_4,V_5,V_6, V_7, P_A,P_B,P_C	-	3.20E-5	845
	Fig. 5.10(d)	Revised risk ranking step 2	V_1,V_2	V_3,V_4,V_5,V_6, V_7	P_A,P_B,P_C	3.18E-5	851
3	Fig. 5.11(a)	Initial risk matrix step	V_2	V_1, P_A,P_B,P_C	V_3,V_4,V_5, V_6,V_7	4.83E-5	1238
	Fig. 5.11(b)	Risk ranking step	V2, V_3,V_4,V_5, V_6,V_7	V1, P_A,P_B,P_C	-	3.89E-5	2234
	Fig. 5.11(c)	Revised risk ranking step 1	V_1,V_2	V_3,V_4,V_5,V_6, V_7	P_A,P_B,P_C	3.18E-5	851
4	Fig. 5.12(a)	Initial risk matrix step	V_1,V_2,V_3,V_4, V_5,V_6,V_7	P_A,P_B,P_C	-	3.36E-5	1317
	Fig. 5.12(b)	Risk ranking step	V_1,V_2, P_A,P_B,P_C	V_3,V_4,V_5,V_6, V_7	-	3.79E-5	2082
	Fig. 5.12(c)	Revised risk ranking step 1	V_1,V_2	V_3,V_4,V_5,V_6, V_7, P_A,P_B,P_C	-	3.20E-5	845
	Fig. 5.12(d)	Revised risk ranking step 2	V_1,V_2	V_3,V_4,V_5,V_6, V_7	P_A,P_B,P_C	3.18E-5	851

From risk matrix and revising risk matrix in Fig.5.9 – Fig5.12 and Table 5.4 are shown that only the initial risk-ranking step may not provide the improved solutions because this step is only the step of approximate ranking. The revising risk ranking step that is proposed in section 5.4 of this chapter is required to improve the results. The result of system unavailability of the last step of Table 5.4 provide the minimize value comparing with other steps, therefore these results confirm that the converge surveillance test interval groups in the last step for all investigated case is the most optimal surveillance test interval groups based on risk consideration for this system.

In order to confirm the proposed methodology is capable of finding the most optimal surveillance test interval groups based on risk consideration, the Pareto-optimal solutions of initial surveillance test interval groups before performing the proposed methodology are compared with the Pareto-optimal solutions of the optimal test interval groups obtained by the proposed methodology. The results are shown in Fig. 5.13.

As shown in the Fig.5.13, the objective function values SI = 1from the Pareto-optimal solutions obtained from four initial cases, which operated with the non-suitable test interval groups, are not sufficiently appropriate. Therefore, risk management is required together with the optimization and the proposed methodology is required. After comparing all of the Pareto-optimal solutions in Fig. 5.13, the Pareto-optimal solutions obtained after performing the proposed methodology provides the most satisfactory result. Therefore it is confirmed from the results from Fig.5.13 that the proposed methodology is capable of determining the most optimal surveillance test interval groups based on risk consideration that provide the most satisfactory result of the Pareto-optimal solutions

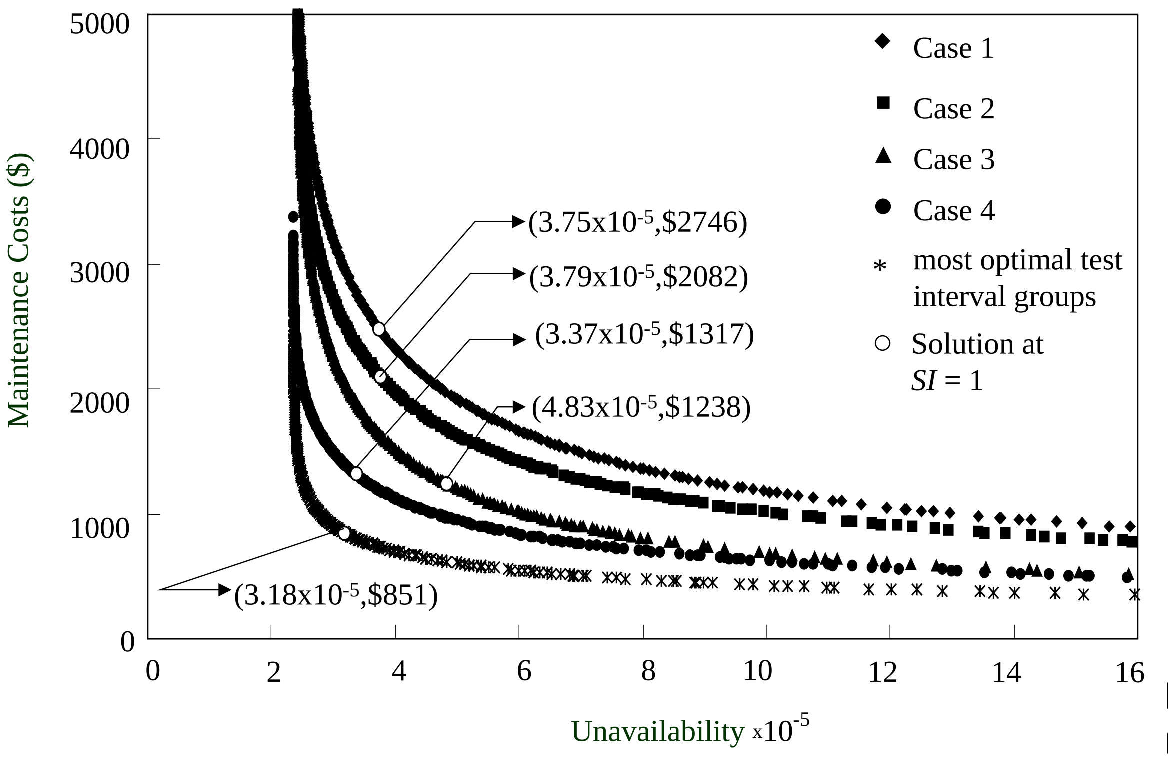

Fig. 5.13. The comparison of the Pareto-optimal solutions before performing the proposed methodology and the Pareto-optimal solutions obtained by the proposed methodology.

In addition, Fig.5.13 also shows that there is the region of the initial Pareto-optimal solutions of the investigated case 4 overlap with the most efficient Pareto-optimal solutions. In order to proof that a point in this zone is not appropriate to be selected as the representative solution for being improved. The point at the fixed value in this overlapping region of the investigated case 4 is then selected to process the risk ranking and the revising risk ranking, and the obtained results of the optimal test interval groups are not converged to the most optimal test interval groups based on risk consideration as shown in Table 5.3. However, the other point, which does not locate in the overlapped region, provide the same results as shown in Table 5.3 after performing the proposed methodology. It is then confirmed that selecting the point in this overlapping region is not appropriate. Therefore, the suggest SI = 1 point in the proposed methodology is more reasonable because selecting the point at SI = 1 to be improved in the proposed methodology for all investigated cases provide the convergent to the same result as shown in Table 5.3. for this HPIS system.

Moreover, the risk-based inservice testing by ASME is also applied to improve the surveillance test of the HPIS in Fig.5.8. Then the obtained surveillance test interval groups by ASME method are also compared with those obtained using the proposed methodology. As described in section 2.4.4 of chapter 2, the risk-based inservice testing of ASME categorize the risk significant of the components by the FV-RAW matrix. ASME method does not define the revision of risk ranking. The FV-RAW matrix for all investigated cases in Table 5.2 are then plotted and shown in Fig.5.14-5.17 respectively.

For investigated case 1:

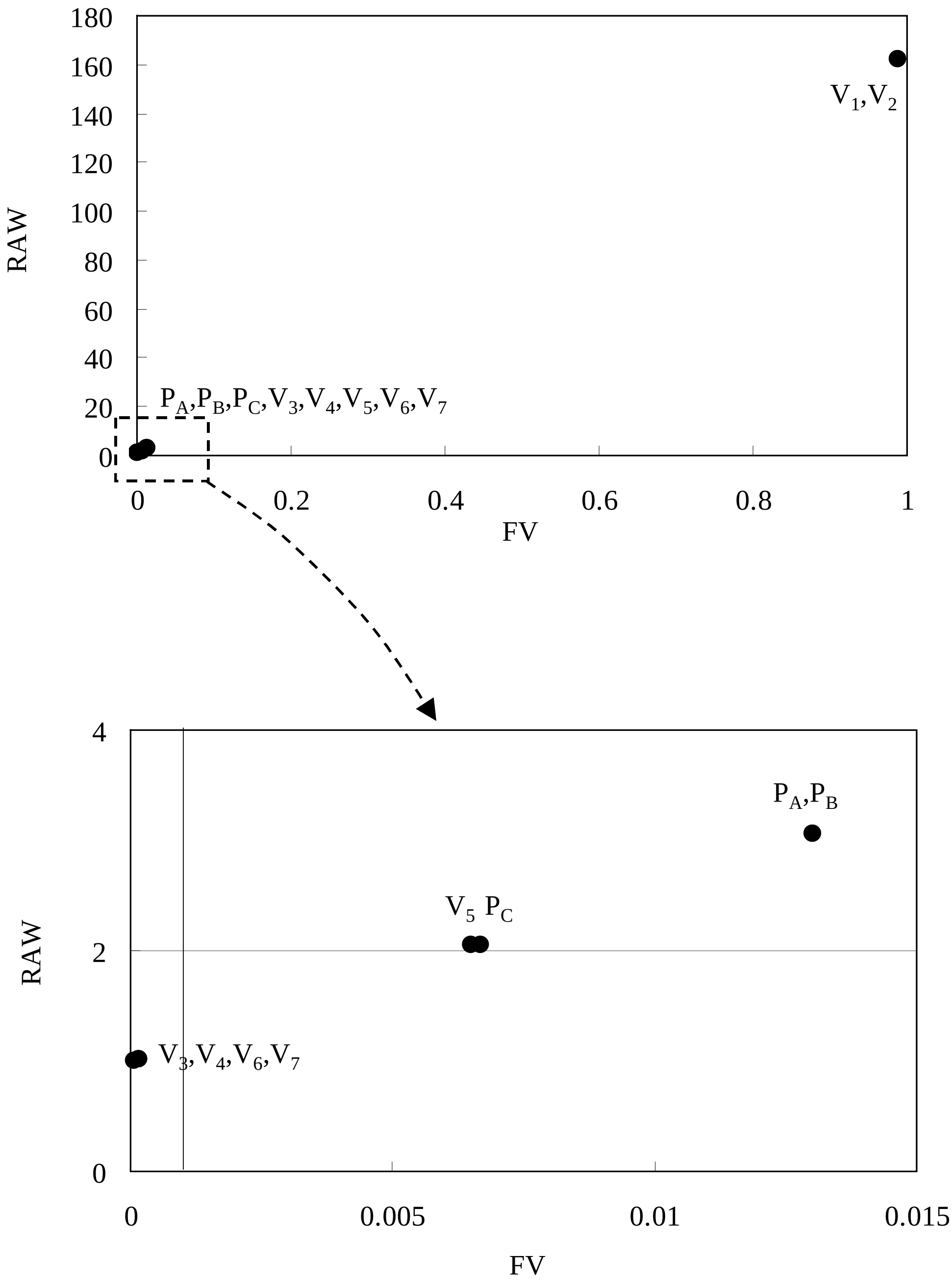

Fig.5.14 RAW/FV Quadrant graph of risk by ASME method for investigated case 1.

For investigated case 2:

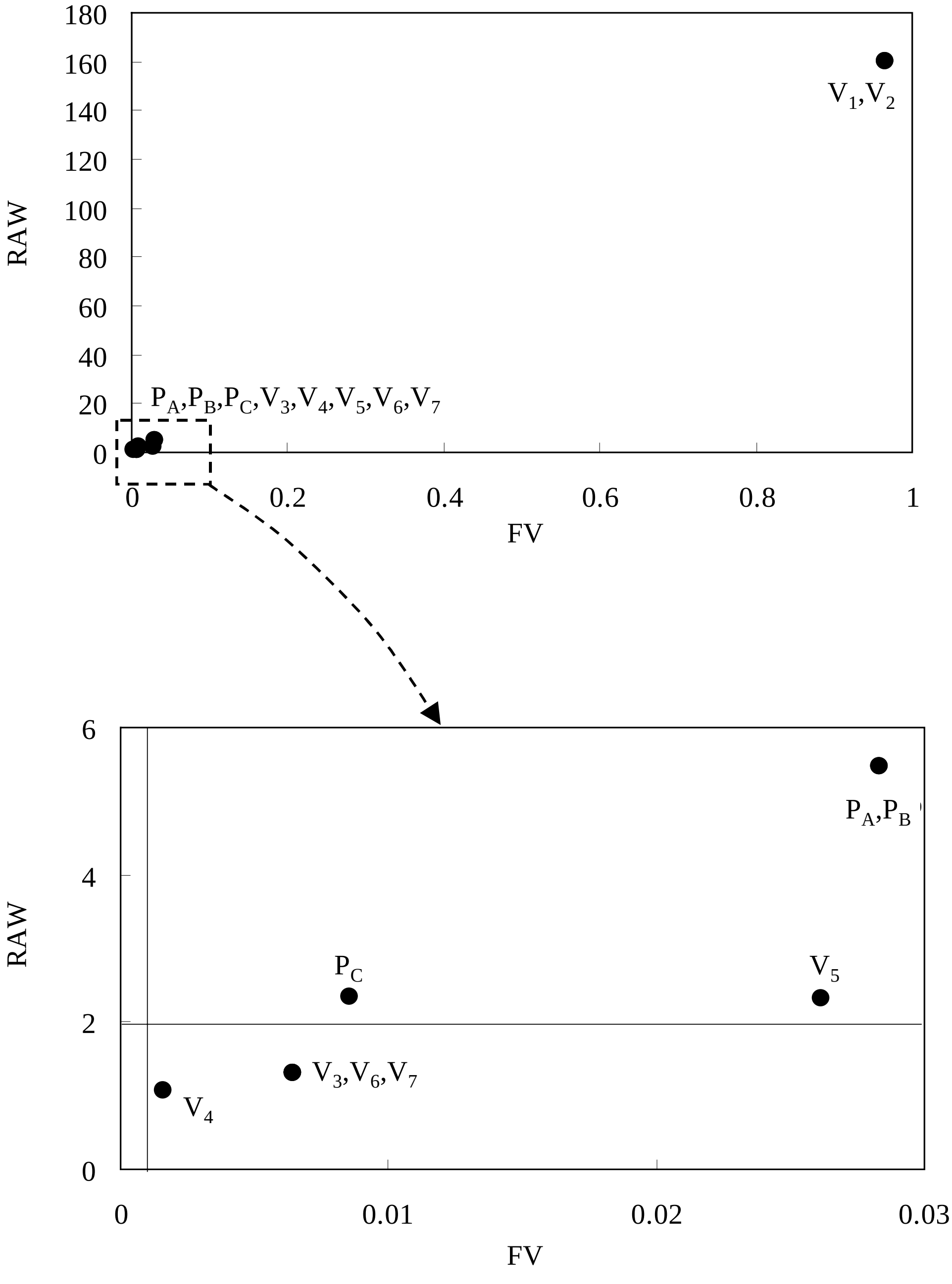

Fig.5.15 RAW/FV Quadrant graph of risk by ASME method for investigated case 2.

For investigated case 3:

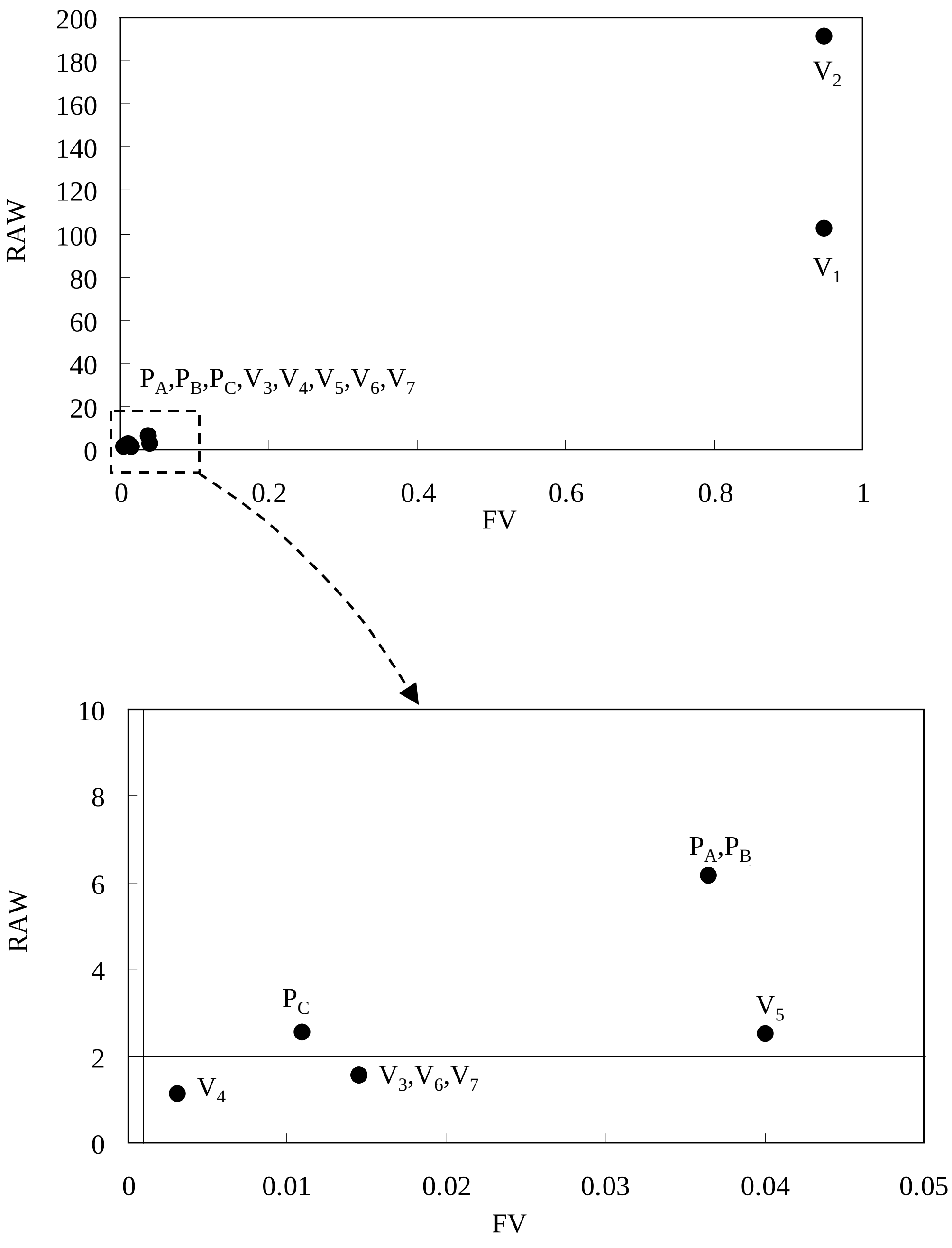

Fig.5.16 RAW/FV Quadrant graph of risk by ASME method for investigated case 3.

For investigated case 4:

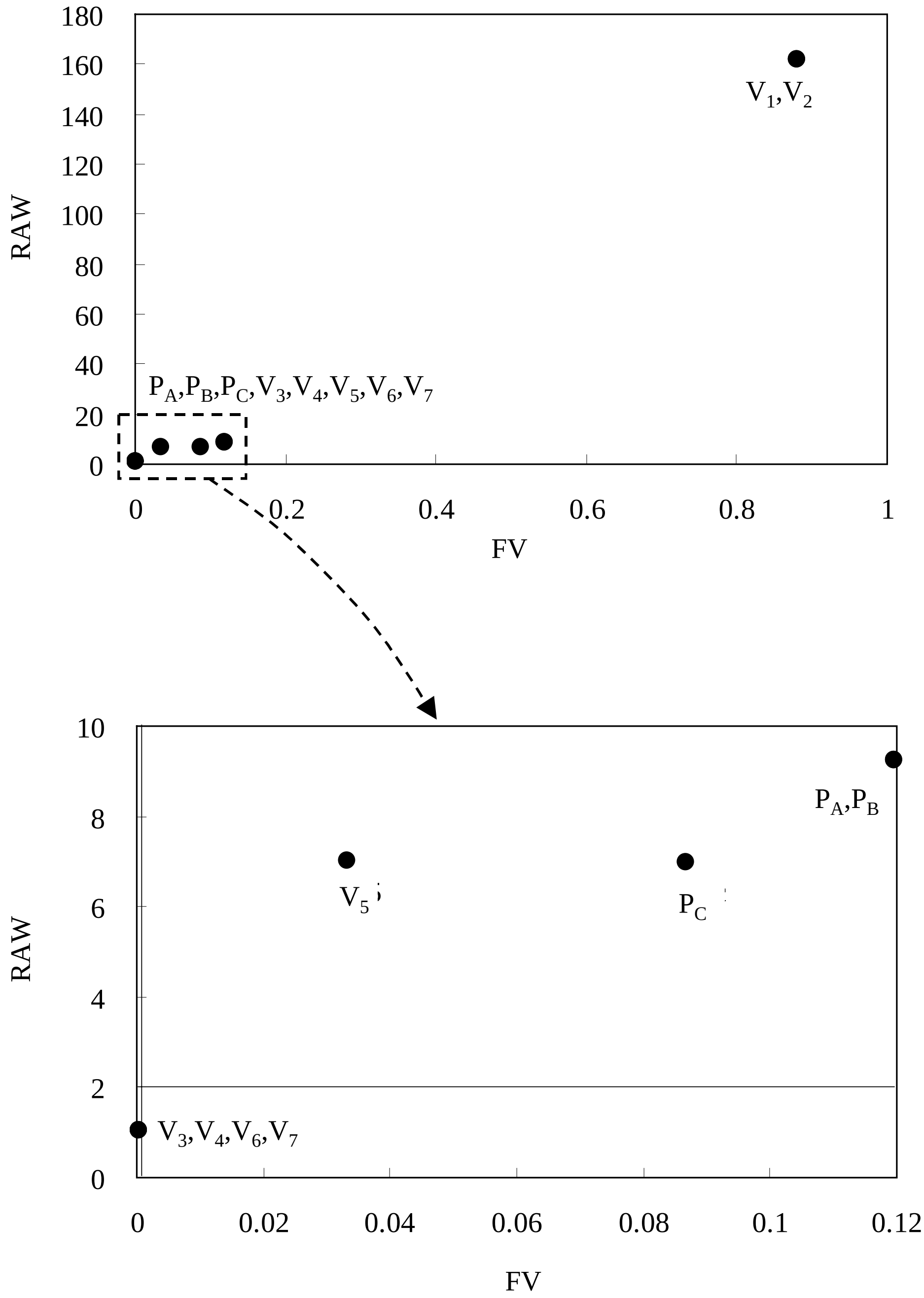

Fig.5.17 RAW/FV Quadrant graph of risk by ASME method for investigated case 4.

The surveillance test interval groups obtained by the ASME method for all 4 investigated cased are shown in Table 5.5

Table 5.5 Test interval groups obtained by ASME method

Components	Test interval group
V_1, V_2 ,V_5, P_A, P_B, P_C	T^1
V_3, V_4, V_6, V_7	T^2

For the FV-RAW matrix of the risk-based inservice testing by ASME for investigated cases as shown in Fig. 5.14 - Fig. 5.17, the value of FV and RAW of each component is very different. Nevertheless, the fix values of FV and RAW for dividing the risk significant in the FV-RAW matrix make the too high risk significant component fall in the same group of the extremely lower risk significant component. For example, V_1 and V_2 are very high in risk significant but fall in the same group of V_5, P_A, P_B, P_C. Therefore, the optimal result from test interval groups obtained by ASME method may not sufficiently satisfy. Figure 5.18 shows the comparison of the Pareto-optimal solutions obtained by the proposed methodology and that obtained by the ASME method.

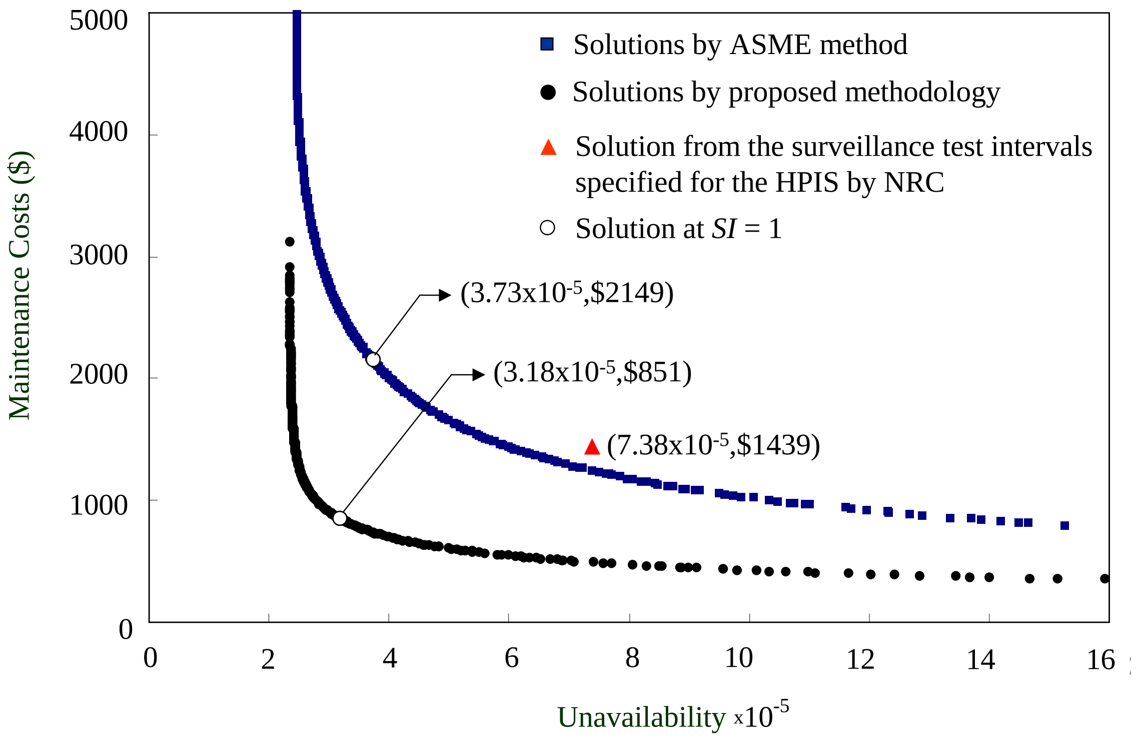

Fig. 5.18 The comparison of the Pareto-optimal solutions obtained by the ASME method and the Pareto-optimal solutions obtained by the proposed methodology and the solution from the surveillance test interval specified for the HPIS by NRC.

The results from Fig.5.18 show that the proposed methodology provides more satisfactory solutions than the solutions obtained by the ASME method. Moreover, if trying to change the selecting point in the Pareto-optimal solutions of the initial surveillance test interval groups for performing the risk ranking, the obtained test interval groups by the ASME method does not provide the same result although the select solution does not overlapped with the updated Pareto-optimal curve. Therefore, only the concept of risk-based inservice testing in the ASME method may not be appropriate for applying with the multi-objective optimization.

In addition, Table 5.6 shows typical surveillance test interval requirements included into the HPIS Technical specifications (TS) by the U.S. Nuclear Regulatory Commission (NRC).

Table 5.6 Typical surveillance test interval requirements by NRC [50].

Components	Surveillance test interval (h)
Pump (P)	2184
Valve (V)	2184

The result of unavailability and maintenance cost for the typical surveillance test interval are also shown in Fig.5.18. The results in Fig. 5.18 are also shown that after performing the optimization and risk-based inservice testing, the objective values are improved. Moreover, the obtained result by the proposed methodology provides the most satisfactory solutions when compared with both that obtained by ASME method and typical requirement by NRC.

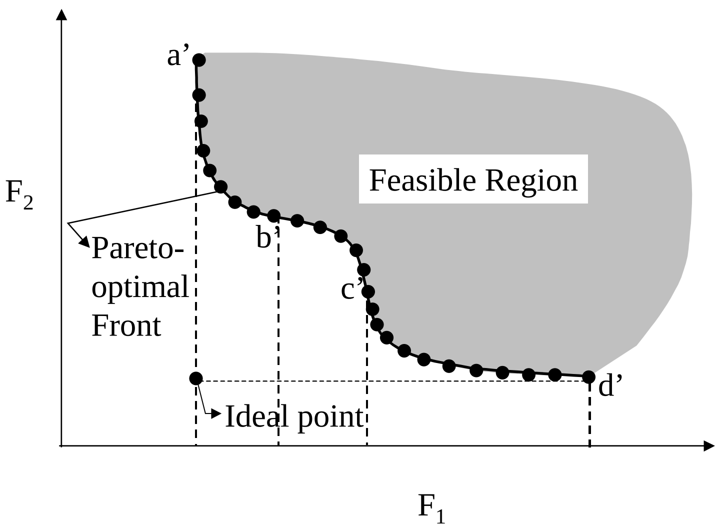

Fig.5.19 Example of complicated shape of the Pareto-optimal curve.

The proposed methodology was verified by the simply case of the Pareto-optimal curve, which is uncomplicated shape. However, in the case of applying the proposed methodology to the complicated shape of the Pareto-optimal curve, such as the concave curve in Fig.5.19, the following idea is proposed.

First, the inflection points of the Pareto-optimal solution such as point a’, b’, c’ and d’ in Fig. 5.19 are determined. The range between the adjacent inflection points is simply in the shape of the Pareto-optimal curve. Because the proposed methodology was verified that it is efficient for applying to the simply shape of the Pareto-optimal curve, therefore, the proposed methodology can also apply to each range of simple shape of the Pareto-optimal curve. After apply the proposed methodology to each range, a number of lowest sensitivity points with SI = 1are obtained. The decision-making point is the point with SI = 1 point that is closest to the ideal point, which is the optimal point from the consideration of both robustness and closeness to the ideal solution.

5.7 Concluding remarks

In this chapter, the new methodology for risk-based inservice testing policy using the multi-objective optimization with robustness was proposed in order to improve the maintenance activities to be the most satisfactorily result together with considering of the robustness.

The result obtained by the proposed methodology is also compared with that obtained by the risk-based inservice testing of ASME method and typical surveillance test interval requirement by NRC. It is confirmed that the obtained result by the proposed methodology provides the most satisfactory solutions when compared with that obtained by ASME method and that obtained typical surveillance test interval requirement by NRC.

The results from many investigated cases were confirmed that the proposed methodology provide the effective scheme to achieve the most optimal test interval groups based on risk-based consideration and also provide the robust result.

Chapter 6

Conclusions

6.1 Conclusions

This research has proposed new indexes and methodology for improving the surveillance test in the maintenance activities of a standby safety system in a nuclear power plant to be most efficient based on risk and robustness consideration. A standby system of a simplified high-pressure injection system (HPIS) in a nuclear power plant's pressurized water reactor (PWR) was conducted as the case study.

First, in order to improve the surveillance test, the optimization is required. But the single-objective, which is wildly used in the maintenance activities, may give the inappropriate solution and may inefficient because of intrinsic trade-offs in the problem. With the efficient viewpoint that can solve the conflicting objectives in the maintenance, the multi-objective optimization was carried out. The considered simultaneous objective functions in this paper are the unavailability and maintenance costs.

After the multi-objective optimization results were obtained, the idea and new methodologies for the development in this research was proposed as follows.

6.1.1 Propose the new decision making from the robustness point of view.

After the multi-objective optimization results were obtained, they showed that there are some regions in the Pareto-optimal solutions were not appropriated for decision making in the viewpoint of robustness. From the robustness viewpoint, the new decision making for determining the most promising solution from the multi-objective optimization solutions are proposed according to the user's requirement.

We have proposed the sensitivity index, *SI* for the decision-making in the viewpoint of sensitivity and then proposed the uncertainty index, *UI* for the decision making in the viewpoint of uncertainty. The decision index, *DI* was then proposed to simultaneously to achieve a good compromise between sensitivity and uncertainty.

The results were shown that each index is appropriate according to the user's requirement. The sensitivity index is appropriate for expressing the degree of robustness of the solution in the viewpoint of sensitivity. The uncertainty index is appropriate for expressing the degree of uncertainty of the solution in the viewpoint of uncertainty and the decision index is appropriated for good compromising between sensitivity and uncertainty.

6.1.2 Proposed the new methodology for applying the multi-objective optimization to risk-based inservice testing.

In order to make the maintenance activities being most efficient based on risk and robustness, the new methodology for applying the multi-objective optimization to risk-based inservice testing was proposed. This methodology was proposed in order to improve the maintenance activities to be most satisfactorily based on risk and robustness together with considering of the trade-off between the objectives.

The results from many investigated cases were shown that if the maintenance activities were operated with the non-suitable test interval groups, the obtained objective function values would not be sufficiently appropriate although the optimization was performed. Conclusively, the proposed methodology was confirmed that it is capable of determining the most optimal surveillance test interval groups that is suitable and provides the most satisfactory Pareto-optimal solutions.

Moreover, because this proposed methodology used the proposed decision making index that considers of the robustness, therefore the final obtained result was most efficient at the most robustness.

6.2 Suggestions for future work

The objectives that have been proposed in this research were approved being accomplished with the proposed methodologies. However, the future works as summarized below are suggested for more extensive idea.

6.2.1 About the objective functions for the multi-objective optimizations

This research introduced the application of the multi-objective optimization to improve the efficient of the surveillance test. By applying the multi-objective optimization, the trade-offs that is intrinsic in the problems can be solved. The most important conflicting objectives of the unavailability and maintenance cost are considered in this research. However, for the future work, another objectives should be considered as the objective functions for this maintenance activities problem, such as an effect to human, an effect to environment.

6.2.1.1 Ideas for decision-making with robustness, when the number of objective functions is more than two

In this research, we have considered two objectives and the performance of the proposed methodologies have been confirmed. When the number of objective functions is more than two, the following ideas are proposed for the decision-making in the viewpoint of robustness. After determined the decision-making with robustness, the proposed methodology in chapter 5 (Risk-based Inservice Testing Policy using the Multi-Objective Optimization with Robustness) can be applied directly.

(1) For the decision-making in the viewpoint of sensitivity (*SI*, in chapter 3).

First, plot all $\binom{M}{2} = \frac{M(M-1)}{2}$ pairs among *M* objective functions. The determined Pareto-optimal curve plot of each pair is the projection of the most optimal curve (best solutions) to that pair of objectives space plot. Thereafter, the lowest sensitivity solution of *SI* = 1 for all pairs are determined. Fig.6.1-a, Fig.6.1-b and Fig.6.1-c show example of all pairs among 3 objective functions. SI_{12}, SI_{13}, SI_{23} are the corresponding *SI* = 1 points in the F_1-F_2, F_1-F_3, F_2-F_3 pair plotted respectively.

However, *SI* = 1 point in one pair plotted may not equal to 1.0 in the other pair plotted. For example, SI_{13} and SI_{23} in F1-F2 plotted may not be 1.0 as shown in Fig.6.1-a. The ideal point for robustness is the point of (SI_{12}, SI_{13}, SI_{23}) = (1,1,1) in all pairs plotted. Therefore, the decision-making is the point among these SI_{12}, SI_{13}, SI_{23} that have the closest distance from the ideal point for robustness. For each pair plotted, the distance from the ideal point for robustness can be determined from the following equation.

$$\text{Distance from the ideal point for robustness} = \left[\Sigma(SI_{ij} - 1)^2 \right]^{1/2}; \quad i,j = 1,2,..,M \quad (6.1)$$

While i and j are the index of the pair i^{th} and j^{th} objective functions in each space plot. *M* is the number of objective functions.

After evaluate the distance in Eq.(6.1) for each pair plotted, the decision making point is the *SI* = 1 point in the pair plotted that has the lowest distance evaluated from Eq.(6.1).

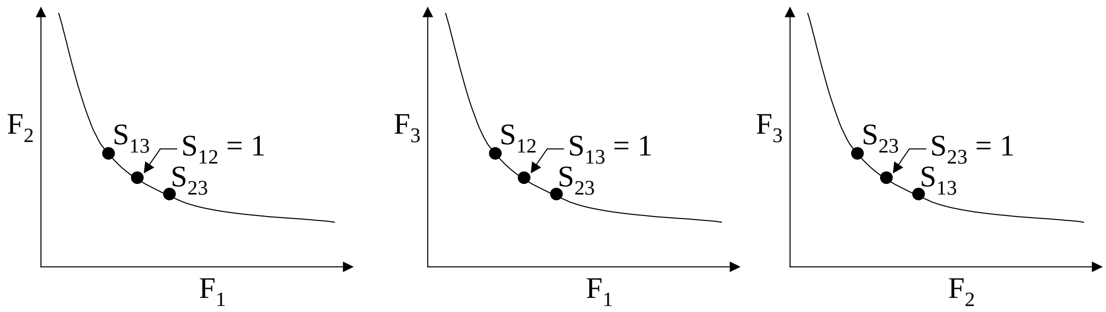

Fig.6.1-a Fig.6.1-b Fig.6.1-c

Fig. 6.1. The example of all pairs among 3 objective functions.

(2) For the decision-making in the viewpoint of uncertainty (*UI*, in chapter 4).

The uncertainty index (*UI*) is defined by the Eq.(4.1) in section 4.3.1 of chapter 4 is modified for the decision making in the viewpoint of uncertainty when the number of objective functions is more than two. The modified uncertainty index (*UI*) is shown in the following equation.

$$UI = [\ \Sigma(\%COV \text{ of } F_i)^2\ ]^{1/2}; \quad i,j = 1,2,..,M \tag{6.2}$$

Where F_i is the i^{th} of the objective function. *M* is the number of objective functions.

The minimum value of *UI* gives the decision-making solution with the lowest uncertainty for all objectives.

6.2.2 About the formulation of objective function

The unavailability function that is formulated in this research, which is reference from ref. [33], has some suggestion for being improved as follows

1) The surveillance test may have adverse effect. These adverse effects are due to unnecessary starting of the component for the surveillance test. The possible risk associated with these adverse effects are such as, unnecessary wear-out or equipment degradation and unnecessary radiation exposure to plant personnel etc. However, the unavailability function that is formulated in this research, which is reference from ref.[33], is assumption on no adverse affect that are due to surveillance test. In order to make the objective function model being more realistic, for the future work, the adverse affect due to the surveillance test should be considered.

2) The unavailability function that is formulated in this paper was assumed to be average unavailability over period of surveillance test interval. In order to make the analytical being more precisely, in the future work, the unavailability formulation should be modeled as time-dependent unavailability.

References

[1] A. J. Balkema , H. A. Preisig , R. Otterpohl b, Fred J.D. Lambert, Indicators for the sustainability assessment of wastewater treatment systems, Urban Water **4**, 153-161 (2002)

[2] American Petroleum Institute, “Risk-Based Inspection”, API Recommendeded Practice API PD580, 2002

[3] American Petroleum Institute, “Risk-Based Inspection Base Resource Document”, API Pubilcation 581, 2000

[4] A. Munoz, S. Martorell, V. Serradell, Genetic algorithms in optimizing surveillance and maintenance of components, Rel. Engng and System Safety **57**, 107-120 (1997)

[5] An ASME Research Report, Risk-based Inspection - Development of Guidelines: Volume1, General Document, The American Society of Mechanical Engineer (ASME), CTRD-Vol-20-1, 1991

[6] An ASME Research Report, Risk-based Inspection - Development of Guidelines: Volume2, Part1, Light Water Reactor (LWR) Nuclear Power Plant Components, The American Society of Mechanical Engineer (ASME), CTRD-Vol-20-2, 1992

[7] An ASME Research Report, Risk-based Inspection - Development of Guidelines: Volume2, Part2, Recommended Inspection program for LWR Nuclear Power Plant Components for ASME Cose Section XI Consideration, The American Society of Mechanical Engineer (ASME), CTRD-Vol-20-4, 1998

[8] An ASME Research Report, Risk-based Inspection - Development of Guidelines: Volume3, Fossil Fuel-Fired Electric Power Generating Stations Applications, The American Society of Mechanical Engineer (ASME), CTRD-Vol-20-3, 1994

[9] An ASME Research Report, Risk Based Inservice Testing, Development of Guidelines: Light Water Reactor (Lwr) Nuclear Power Plant Components, ASME International, CTRD-Vol. 40-2,1996.

[10] ASME Research Members on Risk-Based Inservice Inspection (ISI) and Testing (IST) and Supporting Industry Representatives, Response to reservations on "ASME risk-based inservuce inspection and testing: An outlook to the future", Risk Analysis **18**, 427-431 (1998)

[11] A. Toffolo, A. Lazzaretto, Evolutionary algorithms for multi-objective energetic and economic optimization in thermal system design, Energy **27**, 549–567 (2002)

[12] B. Alexander, G. Barton, J. Petrie, J. Romagnoli, Process synthesis and optimization tools for environmental design: methodology and structure, Computers & Chemical Engineering **24**, 1195-1200 (2000)

[13] B. John Garrick, Robert F. Christie, Probabilistic risk assessment practices in the USA for nuclear power plants, **40**, 177-201 (2002)

[14] Celso M.F. Lapa, Claudio M.N.A. Pereira, Antonio Carlos de A. Mol, Maimization of a nuclear system availability through maintenance scheduling optimization using a genetic algorithm, Nuclear Engeering and Design **196**, 219-231 (2000)

[15] Charles E. Ebeling, An introduction to reliability and maintainability engineering, McGRAW-HILL, 1997

[16] C. Hillermeier, Nonlinear Multiobjective Optimization: A Generalized Homotopy Approach, Birkhauser Verlag, 2001

[17] C. H. Park, W. H. Lee, W. S. Han, A. Vautrin, Weight minimization of composite laminated plates with multiple constraints, Composites Science and Technology **63,** 1015-1026 (2003)

[18] Faisal I. Khan and Mahmoud M. Haddara, Risk-based maintenance (RBM): a quantitative approach for maintenance/inspection scheduling and planning, Journal of Loss Prevention in the Process Industries **16**, 561-573 (2003)

[19] F. Nilsson, Risk-based approach to plant life management, Nuclear Engineering and Design **221**, 293-300 (2003)

[20] Henley J., Kumamoto H., Reliabiliry engineering and risk assessment, Englewood Cliffs, NJ: Prentice-Hall, 1961

[21] Ibrahim Khadam and Jagath J. Kaluarachchi Applicability of risk-based management and the need for risk-based economic decision analysis at hazardous waste contaminated sites, Environment International 29, 503-519 (2003)

[22] Inn Seock Kim, Improving technical specifications from a risk perspective, Reliability Engineering and System Safety **54**, 83-87 (1996)

[23] J. Branke, T. Kauler and H. Schmeck, Guidance in evolutionary multi-objective optimization, Advances in Engineering Software **32**, 499-507(2001)

[24] J. K. Vaurio, Optimization of test and maintenance intervals based on risk and cost, Rel. Engng and System Safety **49**, 23-36 (1995)

[25] John C. Duthie, Michael I. Robertson, Alan M. Clayton and David P. G. Lidbury, Risk-based approaches to ageing and maintenance management, Nuclear Engineering and Design **184**, 27-38 (1998)

[26] Joon-Eon Yang, Mee-Jung Hwang, Tae-Young Sung, Youngho Jin, Appication of genetic algorithm for reliability allocation in nuclear power plants, Reliability Engineering and System Safety **65**, 229-238 (1999)

[27] K. Deb, Multi-objective optimization using evolutionary algorithms, John Wiley & Sons, 2001

[28] K. Wang, D. Kelly and S. Dutton, Multi-objective optimisation of composite aerospace structures, Composite Structures 57, 141-148(2000)

[29] K. Falconer, Ian Hodge, Pesticide taxation and multi-objective policy-making: farm modelling to evaluate profit:environment trade-offs, Ecological Economics **36**, 263–279 (2001)

[30] Kenneth R. Balkey, Raymond J. Art, Robert J. Bosnak, ASME Risk-Based Inservice Inspection and Testing: An Outlook to the Future, Risk Analysis **18**, 407-421 (1998)

[31] L. Zadeh, Optimality and non-scalar-valued performance criteria, IEEE Transactions on Automatic Control **8**, 59-60(1963)

[32] Leemis L., Reliability, probabilistic models and statistical methods, Englewood Cliffs, NJ: Prentice-Hall, 1995

[33] M. Harunuzzaman, T. Aldemir, Optimization of standby safety system maintenance schedules in nuclear power plants, Nuclear Technology **113**, 354-367 (1995)

[34] M. Marseguerra, E. Zio, M. Cipollone, Designing optimal degradation tests via multi-objective genetic algorithms, Rel. Engng and System Safety **79**, 87-94 (2003).

[35] M. Van der Borst, H. Schoonakker, An overview of PSA importance measures, Rel. Engng and System Safety **72**, 241-245 (2001).

[36] Mark G. Stewart and Robert E. Melchers, Probabilistic risk assessment of engineering systems, Chapman & Hall, 1997

[37] Michael C. Cheock, Gareth W. Parry, Richard R. Sherry, Use of importance measures in risk-informed regulatory applications, Rel. Engng and System Safety **60**, 213-216 (1998).

[38] Michael D. Vose, The simple genetic algorithm : foundations and theory, MIT Press, 1999

[39] Michael E. Mayfield, Deborah A. Jackson, Jack Guttman, Mark Cunningham, Risk-informed inservice inspection program, Nuclear Engineering and Design 195, 211-215 (2000)

[40] N.H. Roberts, Fault Tree Handbook**,** Government Printing Office, 1992

[41] Nuclear Power Engineering Corporation(NUPEC) - リスクベースマネジメントの国内プラントへの適用性検討に関する報告書，1999

[42] O. Ditlevsen, H. O. Madsen, Structural reliability methods, Johnson Wiley & Sons, 1996

[43] Raplph R. Fullwood and Robert E. Hall, Probabilistic risk assessment in the nuclear power industry, Pergamon Press, 1988

[44] Raplph R. Fullwood, Probabilistic safety assessment in the chemical and nuclear industries, Butterworth-Heinemann, 2000

[45] R. Bowerman, B. Hall, P. Calamai, A multi-objective optimization approach to urban school bus routing:formulation and solution method, Transpn. Res.-A. **29A**, 107-123 (1995)

[46] Risk-Based Evaluation of Technical Specifications, EPRI NP-4317, Electric Power Research Institute (1985)

[47] Robert W. Youngblood, Applying risk models to formulation of safety cases, Risk analysis **18**, 433-444, 1998

[48] S. Martorell, A. Sanchez, S Carlos, V. Serradell, Simultaneous and multi-criteria optimization of TS requirements and maintenance at NPPs, Annuals of Nuclear Energy 29, 147-168 (2002)

[49] S. Marglin, Public investment criteria, MIT Press, Cambridge, Massachusetts,

1967

[50] S. Martorell, S Carlos, A. Sanchez, V. Serradell, Constrained optimization of test intervals using steady-state genetic algorithm, Rel. Engng and System Safety **67**, 215-232 (2000)

[51] The U.S. Nuclear Regulatory Commission (NRC), Available: http://www.nrc.gov

[52] The U.S. Nuclear Regulatory Commission (NRC), Importance measure derived from probabilistic risk assessments, 2000, Available: http://www.nrc.gov/reading-rm/doc-collections/acrs/letters/2000/4691872.html

[53] Thomas A. Cruse, Reliability-based mechanical design, Marcel Dekker, 1997

[54] Thomas Back, Evolutionary algorithms in theory and practice : evolution strategies, evolutionary programming, genetic algorithms, Oxford University Press, 1996

[55] Tim Bedford and Roger Cooke, Probabilistic risk analysis: foundations and methods, Cambridge, 2001

[56] Title 10 of the Code of Federal Regulations, Energy Part 50 (10CFR50): Domestic licensing of production and utilization facilities, Available: http://www.nrc.gov/reading-rm/doc-collections/cfr/part050

[57] U.S. Atomic Energy Commission, Reactor Safety Study, An Assessment of Accident Risks in U.S. Commercial Nuclear Power Plants, WASH-1400 (NUREG-75/014), October 1975

[58] USNRC, Regulatory Guide 1.177 - An Approach for Plant-Specific, Risk-Informed Decision making: Technical Specifications, 1998

[59] W.E.Vesely, Reservations on ASME Risk-Based Inservice Inspection and Testing: An Outlook to the Future, Risk Analysis **18**, 423-425 (1998)

[60] Yu, P.L, A class of solutions for group decision problems, Management Science

19, 936-946 (1973)

[61] Zeleny, M. Compromise programming. In J. L. Cochrane and M. Zeleny (Eds), Multiple Criteria Decision Making, Columbia: SC: University of South Carolina Press, 262-301 (1973).

[62] 石川島播磨重工業（株），富士彰夫，弥富正享，江口晴樹，福岡千枝，木原重光，AEA Technology, David Worswick, 設備保全一火力発電用ボイラにおけるリスクベースメンテナンス（RBM）法の適用，圧力技術誌，第 39 巻　第 1 号，2001

[63] 木原重光, 富士彰夫, RBI/RBM 入門, 日本プラントメンテナンス協会, 2002

A list of author's work

Reviewed Papers

1. ウイルンシー・ジャックサニー，酒井信介，泉聡志，ロバストネス指標に基づく多目的適化手法とその原子力発電プラント保守計画策定問題への適用，日本材料学会誌，信頼性(小)，第 53 巻　第 1 号，(2004)

2. J. VIRULSRI, S. SAKAI, S. IZUMI, Parameter sensitivity study and uncertainty analysis of the multi-objective optimization in nuclear power plant maintenance, The 5th Japan Conference on Structural Safety and Reliability, Japan (JCOSSAR), (2003).

Conferences Proceedings

1. J. VIRULSRI, S. SAKAI, S. IZUMI, Multi-objective optimization approach to maintenance of Nuclear power plant，第 19 回材料・構造信頼性シンポジウム，日本材料学会，(2002)

2. J. VIRULSRI, S. IZUMI, S. SAKAI, Effect of parameters uncertainties on the multi-objective optimization approach to nuclear power plant maintenance, 第 52 回 理論応用力学講演会，日本機械学会，(2003)

3. J. VIRULSRI, S. SAKAI, S. IZUMI, Effect of parameters uncertainties on the multi-objective optimization approach to nuclear power plant maintenance, 平成 15 年度春季講演会，日本高圧力技術協会，(2003)

4. J. VIRULSRI, S. SAKAI, S. IZUMI, Atsushi IWASAKI, Application of a multi-objective optimization to risk-based inservice testing, 2004 ASME/JSME Pressure Vessels and Piping Conference, California, USA. (2004).

5. J. VIRULSRI, S. SAKAI, S. IZUMI, Decision-making in the multi-objective optimization approach based on robustness and its application to maintenance of nuclear power plants, The 33rd International Conference on Computers and Industrial Engineering, Korea. (2004).

Acknowledgement

I would like to express my deep appreciation to my thesis advisor, Prof. Shinsuke Sakai, for giving me the chance for studying in his laboratory and for his kindly suggestion throughout the course of this work. I am so grateful that I have learned the valuable knowledge not only about the work but also the way of thoughts in many things from Professor Sakai.

I would like to express my sincere thankful to Prof. Satoshi Izumi for his advice and his assisting of many research facility that support me in studying too much.

I would like to express my sincere thankful to Prof. Katsuhiko Watanabe, Prof. Tsuyoshi Takada and Prof. Nobuhiro Yoshikawa for their kindly giving me the suggestion that make me extend the ideas of my research.

Thank you for the kindly of Dr. Atsushi Iwasaki for assisting in correcting my papers. And I also would like to thank all members in Sakai・Izumi laboratory for giving me the kindly friendship that support me to research my work.

Finally I wish to express my gratitude my family my father, my mother and my sister for their love and encouragement that are everything for me.